

DOE/BC/14958-8
(DE95000113)

GREEN RIVER FORMATION WATER FLOOD
DEMONSTRATION PROJECT

Report for the Period
October 1992 to March 1994

By
Bill I. Pennington
John D. Lomax
Dennis L. Neilson
Milind D. Deo

December 1994

Performed Under Contract No. DE-FC22-93BC14958

Lomax Exploration Company
Salt Lake City, Utah



**Bartlesville Project Office
U. S. DEPARTMENT OF ENERGY
Bartlesville, Oklahoma**

FOURTH FLOOR

DISCLAIMER

This report was prepared as an account of work sponsored by an agency of the United States Government. Neither the United States Government nor any agency thereof, nor any of their employees, makes any warranty, expressed or implied, or assumes any legal liability or responsibility for the accuracy, completeness, or usefulness of any information, apparatus, product, or process disclosed, or represents that its use would not infringe privately owned rights. Reference herein to any specific commercial product, process, or service by trade name, trademark, manufacturer, or otherwise does not necessarily constitute or imply its endorsement, recommendation, or favoring by the United States Government or any agency thereof. The views and opinions of authors expressed herein do not necessarily state or reflect those of the United States Government or any agency thereof.

This report has been reproduced directly from the best available copy.

Available to DOE and DOE contractors from the Office of Scientific and Technical Information, P.O. Box 62, Oak Ridge, TN 37831; prices available from (615) 576-8401.

Available to the public from the National Technical Information Service, U.S. Department of Commerce, 5285 Port Royal Rd., Springfield VA 22161

GREEN RIVER FORMATION WATER FLOOD
DEMONSTRATION PROJECT

Report for the Period
October 1, 1992 to March 31, 1994

By
Bill I. Pennington, Lomax Exploration
John D. Lomax, Lomax Exploration
Dennis L. Neilson, University of Utah Research Institute
Milind D. Deo, University of Utah, Chemical & Fuels Engineering

Work Performed Under Contract No. DE-FC22-93BC14958

Prepared for
U.S. Department of Energy
Assistant Secretary for Fossil Energy

Edith Allison, Project Manager
Bartlesville Project Office
P.O. Box 1398
Bartlesville, OK 74005

Prepared by
Lomax Exploration Company
Salt Lake City, Utah 84101

Contents

Abstract	ix
Executive Summary	x
1 Introduction	1
2 Field Activities	7
3 Geologic Characterization	10
3.1 Logging Methods	10
3.2 Travis Unit	11
3.3 Monument Butte Unit	12
3.3.1 B Sandstone	12
3.3.2 C Sandstone	13
3.3.3 D Sandstone	13
3.4 References	13
4 Compositions of Oils	19
4.1 Synopsis	19
4.2 Introduction	19
4.3 Experimental Equipment	20
4.3.1 GC Apparatus	20
4.3.2 C ₅ - C ₄₄ Analyses	21
4.3.3 C ₂₀ - C ₉₀ Analyses	21
4.3.4 Crude Oil Samples	21
4.4 Computations	22
4.5 Results and Discussion	23
4.6 Conclusions	23
4.7 References	24
4.8 Appendix - Mathematical Basis of Equations	24
5 Volumetric Calculations	31
5.1 Monument Butte Unit	31
5.2 Travis Unit	32
5.3 Nomenclature	33

6	Monument Butte Unit: Case Study	34
6.1	Introduction	34
6.2	Geologic Description	35
6.3	Reservoir Fluid Properties	35
6.3.1	Compositional Analyses	36
6.3.2	Measurement of Bulk Properties	37
6.3.3	Prediction of Thermodynamic Properties	37
6.3.4	Measurement of Thermodynamic Properties	38
6.3.5	Rock-fluid Properties	39
6.4	Simulation Results	39
6.4.1	Extended Predictions	41
6.5	References	42
7	Travis Case Study	67
7.1	Reservoir Description	67
7.2	Reservoir Fluid Properties	68
7.3	Simulation Results	68
7.4	References	69
8	Near Wellbore Effects	74
8.1	Synopsis	74
8.2	Technical Discussion	74
8.2.1	The Wellbore Model	77
8.3	Results and Discussion	77
8.4	Summary	78
8.5	References	78
8.6	Nomenclature	80

List of Figures

1.1	A Unit map of the Monument Butte Unit.	4
1.2	A Unit map of the Travis Unit.	5
1.3	A Unit map of the Boundary Unit.	6
3.1	Log for the well 13-35 showing major stratigraphic units in the Monument Butte Unit (GR, Gamma Ray; NPHI, Neutron Porosity; DPPI, Density porosity).	15
3.2	An isopach map of B-sandstone, Monument Butte Unit.	16
3.3	An isopach map of D1-sandstone, Monument Butte Unit.	17
3.4	An isopach map of D2-sandstone, Monument Butte Unit.	18
4.1	Chromatogram of Polywax 655 on Supelco EX-2887, 5 meter \times 0.53 mm glass capillary column with 0.1 micron film thickness.	28
4.2	Chromatogram of the crude oil sample from well 10-35 in the Monument Butte Unit. The sample was analyzed on J & W Scientific DB-1, 30 meter \times 0.25 mm O.D., glass capillary column, with a 0.25 micron film thickness.	28
4.3	Chromatogram of the crude oil (from well 10-35 in the Monument Butte Unit) plus internal standard, obtained on J & W Scientific DB-1, 30 meter \times 0.25 mm O.D., glass capillary column, with a 0.25 micron film thickness.	29
4.4	A schematic illustrating the areas of chromatograms used in the simulated distillation calculations.	29
4.5	Carbon number distributions of the oil from well 10-35 (Monument Butte Unit); both the long and the short column analyses have been shown.	30
4.6	Carbon number distributions of the oil from well 12-35 (Monument Butte Unit); both the long and the short column analyses have been shown.	30
6.1	Carbon number distributions of oils from three wells in the Monument Butte Unit.	46
6.2	Predictions of bubble point versus gas-oil-ratio (GOR) for a 35° API oil at different gas gravities.	47
6.3	Predictions of oil formation volume factor versus gas-oil-ratio (GOR) for a 35° API oil at different gas gravities.	48
6.4	Schematic of the pressure-volume-temperature apparatus used for the measurement of thermodynamic properties of reservoir fluids.	49

6.5	Experimental pressure versus volume measurements for the Monument Butte crude with a gas-oil-ratio (GOR) of 418 SCF/STB; the inflection point in the curve at 2120 psia indicates the bubble point.	50
6.6	Relative permeability curves employed in this simulation study to obtain a satisfactory match with the field results	51
6.7	Pressure contours in D-sands at the end of primary production (August 1987).	52
6.8	Saturation contours in D-sands at the end of primary production (August 1987).	53
6.9	Cumulative oil production from Monument Butte well 5-35; comparison of field production with the simulation results.	54
6.10	Cumulative oil production from Monument Butte well 4-35; comparison of field production with the simulation results.	55
6.11	Cumulative oil production from Monument Butte well 3-35; comparison of field production with the simulation results.	56
6.12	Cumulative oil production from Monument Butte well 2-35; comparison of field production with the simulation results.	57
6.13	Cumulative water injection profile used in the simulation results.	58
6.14	Oil saturation contours in D-sands at the end of the simulation period (December 1992).	59
6.15	Cumulative oil production from Monument Butte well 10-35; comparison of field production with the simulation results.	60
6.16	Cumulative oil production from Monument Butte well 12-35; comparison of field production with the simulation results.	61
6.17	Cumulative oil production from Monument Butte well 6-35; comparison of field production with the simulation results.	62
6.18	Cumulative oil production from Monument Butte well 1-34; comparison of field production with the simulation results.	63
6.19	Cumulative oil production from the entire Monument Butte Unit; comparison of field production with the simulation results.	64
6.20	Comparison of the field production GOR values with those predicted by simulations.	65
6.21	Cumulative gas production from the entire Monument Butte Unit; comparison of field production with the simulation results.	66
7.1	Cumulative oil production from the Travis Unit; comparison of field production with the simulation results.	72
7.2	Cumulative gas production from the Travis Unit; comparison of field production with the simulation results.	73
8.1	Chromatogram of an oil sample from the Monument Butte Unit showing the significant presence of high-molecular weight paraffins.	82
8.2	Typical injection profile for an injection well in the Monument Butte unit (well 2-35).	83
8.3	Schematic of the wellbore showing the sequence of resistances which are considered in the wellbore heat loss calculations.	84

8.4	Temperatures of injected fluid as a function of depth for a typical Monument Butte injector.	85
8.5	Effect of injection rates on bottom hole temperatures of injected fluids for the Monument Butte injectors.	86
8.6	Effect of surface injection temperatures on bottom hole temperatures of injected fluids for the Monument Butte injectors.	87
8.7	Surface temperatures required to keep the bottom hole injection temperatures above the oil cloud point for Monument Butte injectors as a function of injection rate.	88
8.8	Temperatures of injected fluid as a function of depth for a well 15-28 in Travis.	89

List of Tables

6.1	Results of Gas Analyses	43
6.2	Viscosities of Monument Butte Oils	43
6.3	Bulk Properties of Monument Butte Fluids	43
6.4	Reservoir Fluid Thermodynamic Properties Monument Butte Unit	44
6.5	Extended Simulation Predictions	45
7.1	Reservoir Description of the Travis Unit Employed for Reservoir Simulations	70
7.2	Bulk Properties of Travis Fluids	70
7.3	Reservoir Fluid Properties for the Travis Unit	71
8.1	Parameters used in Calculating the Temperature Profiles in Injection Wells .	81

Abstract

Fluvial deltaic reservoirs contain a significant portion of the known world oil resources. Due to the sinuous nature of the sands, it is difficult to implement improved oil recovery projects in these reservoirs. The current project targeted three fluvial deltaic reservoirs in the Uinta Basin, Utah. Water flood has been in progress in the Monument Butte unit for the last six years and has been highly successful. In primary recovery, the reservoir performance of the Monument Butte unit was typical of an undersaturated reservoir whose initial pressure was close to the bubble point pressure. The Unit had produced about 5% of the oil in place at the end of primary production and was producing at a rate of 40 stb/day, when the water flood was initiated. The water flood design was novel and was engineered to maximize water injectivity into the reservoir. The response to the water flood was extraordinary and the unit has been producing at more than 300 stb/day for the past four years. About 10% of OOIP has been recovered to date. The reservoir characteristics of Monument Butte were established in the geologic characterization study. The reservoir fluid properties were measured in the engineering study of the unit. Results of a comprehensive reservoir simulation study using these characteristics provided excellent match with the field production data. Extended predictions using the model showed that it would be possible to recover a total of 20-25% of the oil in place. Wellbore temperature profile calculations showed that there is a strong possibility of paraffin (wax) deposition and injectivity reduction in the vicinity of the wellbore. The two wells drilled in the unit clearly illustrated the nature of the ongoing water flood. Well 10-34 behaved in a manner similar to a partially depleted well in primary production, while 9-34 responded as a well repressurized from the water flood. In the Travis unit, logs from the newly drilled 14a-28 showed extensively fractured zones. A new reservoir was discovered and developed on the basis of the information provided by the formation micro imaging logs. This reservoir also behaved in a manner similar to undersaturated reservoirs with initial reservoir pressures close to the reservoir fluid bubble point. The water flood activity was enhanced in the Travis unit. Even though the reservoir continued to be gradually pressurized, the water flood in the Travis unit appeared to be significantly affected by existing or created fractures. A dual-porosity, dual permeability reservoir model provided a good match with the primary production history. The well drilled in the Boundary unit did not intersect any producible zones, once again illustrating the unique challenges to developing fluvial deltaic reservoirs. Technology transfer has been an extremely successful aspect of this project. Based on the results of the project, paper presentations have been made at technical meetings. Two large water floods have been initiated in the Uinta Basin based on the experience gained in this project and several others are being planned.

Executive Summary

The objectives of this project were to understand and demonstrate improved oil recovery techniques in fluvial deltaic reservoirs. Three distinct units were targeted in this study; the Monument Butte unit, the Travis unit and the Boundary unit. All the three units are located in the Uinta Basin in east-central Utah. The wells in these units typically intersect 10-20 hydrocarbon bearing sands; however, oil is usually produced from about 1-4 commercial sands.

Monument Butte unit is the most developed of the three units and currently has 22 wells, eight injectors and the rest producers. The unit contains about 9 MMstb of original oil in place (OOIP) primarily in two sand layers, the 'D' and the 'B'. The primary production performance of the Monument Butte unit was typical of an undersaturated oil reservoir close to its bubble point. About 4.5% of the OOIP had been recovered by primary production, when the water flood was initiated in late 1987. The flood has been very successful and the oil recovery since the start of secondary recovery has already exceeded primary production. Since the start of this project, two wells were drilled in Monument Butte, 10-34 and 9-34. Well 10-34 drilled in late 1992, did not appear to be affected by the water flood. The production from 10-34 has resembled production from a well producing from a partially depleted undersaturated reservoir. Well 9-34 drilled in late 1993 penetrated producing sands and appeared to be producing from zones which were pressurized by the water flood. The production performances for these two wells were logical considering the distances of these wells from injection wells, 5-35 and 13-35. Formation Micro-Imaging (FMI) logs were obtained for these wells for better geologic understanding. Logs and stratigraphic sections from several wells were analyzed and a geologic model of the reservoir was constructed. As part of the comprehensive engineering study of the unit, a general purpose core flooding, pressure-volume-temperature (PVT) system capable of measuring reservoir fluid properties was designed and built. Compositions of the Monument Butte oils were measured using a novel capillary chromatographic method. All the relevant reservoir fluid properties were measured. The geologic data and the reservoir fluid property data were integrated into a detailed reservoir simulation study. The overall field production data was matched by the reservoir simulator within 10% and the individual well data were matched within 15%. This satisfactory reservoir simulation study showed that the complex mechanisms of multiphase thermodynamics and multiphase flow have been well represented by the models for the Monument Butte unit. The results of one of the simulation studies resulted in a paper SPE 27749, which will be presented at the Improved Oil Recovery Symposium in Tulsa, Oklahoma in April 1994. A thermal wellbore model was developed to examine the temperature profiles in the wellbore. The model showed that under the conditions of injection, injected water

could be reaching the perforations 50-70°F lower than the reservoir temperature. Due to the high paraffin contents of the reservoir fluids, the study concluded that there was a strong possibility of paraffin deposition in the vicinity of the wellbore.

The Travis unit had produced about 245 Mstb of oil and 1.08 MMMscf of gas in primary production. Most of the production was from the Lower Douglas Creek (LDC) sand. Injection in 15-28 at 1000 stb/d appeared to pressurize the reservoir. However, when well 14-28a was drilled in late 1992, injection in 15-28 had to be stopped due to water channeling in 14a-28. Producer 10-28, also had the water channeling problem. The new FMI logs in 14a-28 showed that LDC was extensively fractured. The fracture orientations were found to coincide with the channeling paths. The new logs in 14a-28 also revealed the existence of thin, but producible D sands. Based on this information, 14a-28 and also wells 14-28 and 10-28 were completed in the D-sand interval. The production from this zone was similar to production from an undersaturated reservoir close to the initial fluid bubble point. Once the production from 14a-28 declined, it was converted to an injector, injecting about 300 stb/d into the D-sands. Well 15-28 was started back on injection at a slower rate of about 300 stb/d, and well 3-33 was converted to an injector, injecting about 300 stb/d into LDC. The surface pressure data showed that the reservoir was being gradually pressurized. The water flooding operations in Travis appear to be dominated by natural or created fractures. An engineering study of the Travis unit, similar to the Monument Butte was conducted. The geologic data and reservoir fluid properties were integrated into a dual-porosity, dual-permeability fractured reservoir model. The model provided a good match with the primary production history and predicted increased oil production on water flooding.

Well 10-20 drilled in the Boundary unit did not intersect producing sand layers. This illustrated the risks involved in operating in fluvial deltaic environments.

The success of the water flood in the Monument Butte field and an understanding of the underlying mechanisms as a result of this project, has resulted in the initiation of two major water floods in the Uinta Basin by Equitable Resources Inc. and by Pacific Gas and Energy. The results of the project have been presented at several meetings and have been compiled into three technical papers. Thus the technology transfer aspect of the project has been highly successful.

Chapter 1

Introduction

Geologic complexity makes exploitation of fluvial deltaic reservoirs challenging. Application of improved oil recovery methods, like water flooding is also difficult for these geologic environments. However, for the commercial viability of developing these reservoirs, application of improved recovery methods is almost imperative, since primary recovery typically yields only about 5% of the oil in place. Lomax Exploration Company, in conjunction with the University of Utah Research Institute, and the University of Utah Department of Chemical and Fuels Engineering entered into a cooperative agreement with the U.S. Department of Energy as part of their Class I Reservoir Program. The objective of the project was to study the effectiveness of secondary oil recovery methods in the lacustrine environments of the Green River Formation. This Tertiary age formation is located in the Uinta Basin, in northeastern Utah, and is made up in part of productive sediments that formed deltas at the margins of an ancient lake. In addition to these deltas, oil is also produced from sands formed in fluvial channels and offshore bars. The Green River Formation has produced in excess of 200 million barrels of oil, predominantly from three large fields: Red Wash, Wonsits Valley and Walker Hollow located in the greater Red Wash area. These fields with their varied environments of deposition and their heterogeneous reservoirs did not appear to be good candidates for water flooding, but primary production of only about 5% made the application of a secondary recovery technique a necessity.

Monument Butte Unit located on the south flank of the Uinta Basin currently has 22 wells, eight injectors and the rest producers. Map of the Unit is shown in Figure 1.1¹. The reservoir has about 9 MMstb of oil in place contained in two major sand bodies and several minor sand bodies. Primary production from the Unit had yielded about 4.5% of the oil in place. The oil production from the Unit had dropped to about 40 stb/d, when water flood was initiated (September 1987). The water flood effectively pressurized the reservoir, reducing gas oil ratios and gradually increasing production to over 300 stb/d. The Unit production has been steady at this rate for the last three years. Success of this water flood prompted this investigation into the understanding of the mechanisms underway. The idea was to transfer the technology to other fields in the vicinity, particularly to the Travis and the Boundary Units operated by Lomax Exploration. The project undertaken by a team of geoscientists and engineers consisted mainly of three parts:

¹Illustrations and tables are at the end of the chapter

1. Field Activity: Drilling wells for the continued application of the improved oil recovery technologies in fluvial deltaic systems.
2. Geologic Characterization: Use of novel logging techniques for a better understanding of the underlying geology and also integration and analysis of all the data for the development of improved geologic models of the reservoirs involved.
3. Engineering Study: Development of engineering reservoir models for understanding past reservoir performance and projecting future production, wherever possible.

The field activity during this project consisted of drilling four wells, two in Monument Butte and one each in Travis and Boundary. The Units maps for Travis and Boundary are shown in Figures 1.2 and 1.3. Well 14a-28 in Travis was the first well completed in the course of this project. The main target sand body was Lower Douglas Creek (LDC) which had been subjected to water flooding at a rate of 1000 stb/day through well 15-28, located about 660 ft away. Water channeling through LDC was discovered on drilling 14a-28 and direct fractures between 14a-28 and 15-28 were suspected. New Formation Micro Imager logs obtained for well 14a-28 confirmed that LDC was significantly fractured. The water injection in 15-28 was stopped. The new logs also showed the commercial potential of D-sands in Travis. Based on this new geologic information, D-sand zones were completed, not only in 14a-28, but also in 14-28 and 10-28. Through December 1993, these wells had produced 7,953, 8,846 and 4,060 barrels of oil respectively. The water injection was resumed in 15-28 at a lower rate of about 300 stb/d. Water injections were begun in D-sands in 14a-28 and in LDC in 3-33. The reservoir appeared to be pressurizing well. However, the water flood performance in Travis appears dominated by existing and created fractures. Well 10-34 drilled in Monument Butte was not affected by the water flood. Well 9-34 drilled closer to the injection pattern was producing from zones pressurized by the injected water. Well 10-34 had produced 8,955 barrels of oil by December 31, 1993, while well 9-34 had produced 3,232 barrels of oil by January 31, 1994 at an average rate of 140 stb/d. At the time of this writing, the well was producing at about 70 stb/d. The well 10-20 drilled in Boundary did not intersect producible sands. The field activity is detailed in Chapter 2.

The geologic study of the full diameter core obtained from well 14a-28 in Travis and a field geologic model for the Monument Butte Unit are the subject of Chapter 3.

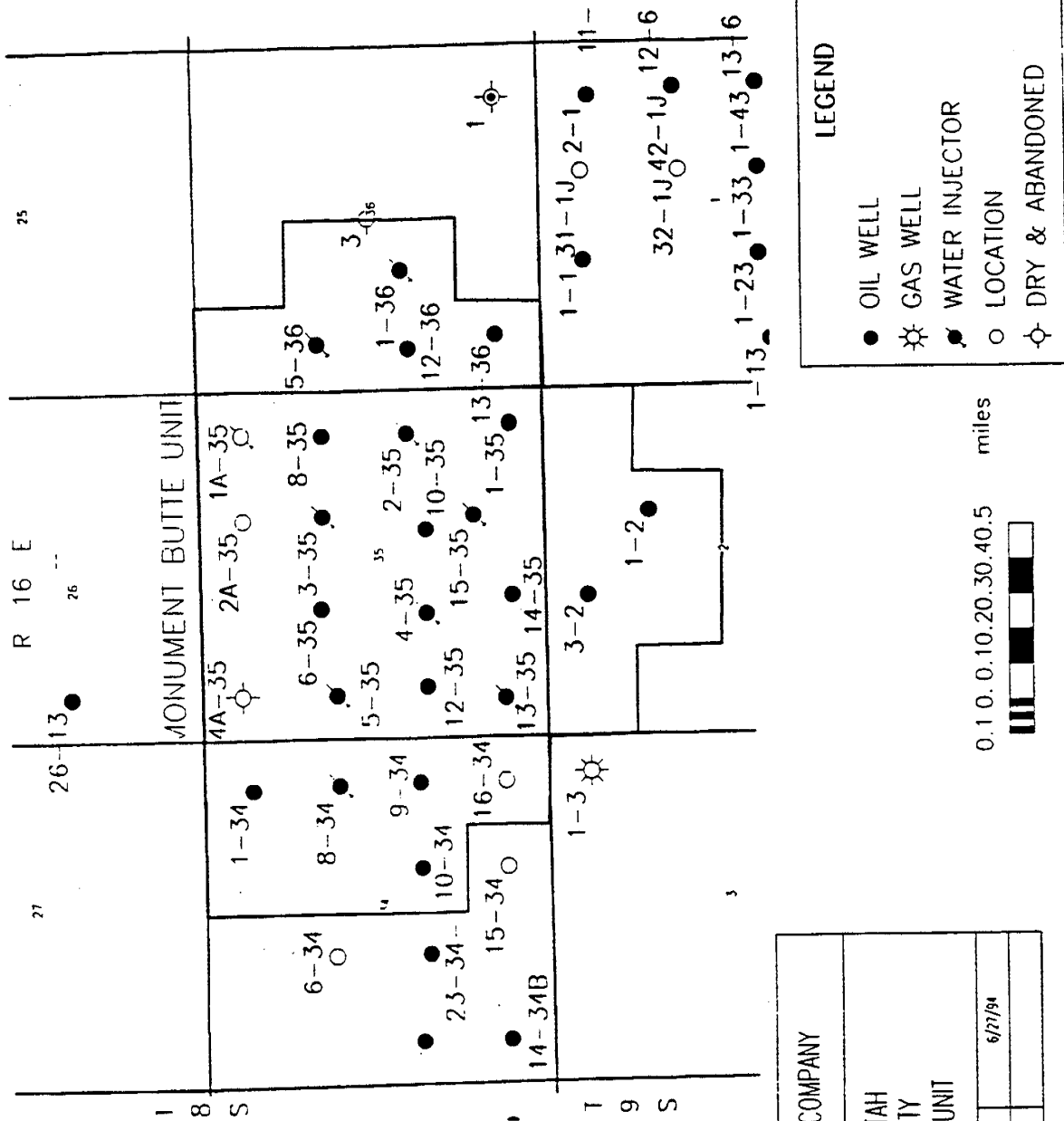
The highly paraffinic waxy crudes of the Monument Butte and Travis presented special analysis problems. A new technique using capillary gas chromatography was developed for determining the compositions of these oils. The technique and the data are presented in Chapter 4. Chapter 5 deals with the overall reservoir engineering volumetrics for Monument Butte and Travis. The production data for both these Units indicate production from undersaturated reservoirs close to their bubble points. The primary production history of Travis does not indicate presence of an extensive fracture network. The overall reservoir engineering study also points out that if by some means gas can be reinjected into these reservoirs, the primary production could possibly be doubled.

Chapter 6 is a comprehensive reservoir engineering study of the Monument Butte Unit. In this chapter design and construction of a general purpose reservoir fluid property measurement system is detailed. Data on reservoir fluid properties of Monument Butte is presented. As part of a comprehensive reservoir simulation study, several parallel reservoir models were

developed. Results of one of the successful reservoir simulation study is presented in Chapter 6. Extended predictions are also given. The reservoir simulator provided good agreement with the field production results. The comprehensive case study resulted in an SPE paper (SPE 27749). This paper was presented at the Improved Oil Recovery Symposium of the SPE-DOE in Tulsa, April 17-21, 1994.

Chapter 7 is a preliminary case study of the Travis Unit. Reservoir fluid property data for the Travis Unit is presented in this chapter. Also included are the results from a dual-porosity, dual-permeability fractured reservoir simulator. Based on the log information on 14a-28, a fractured representation was used for Travis. The reservoir simulator did an excellent job of matching the overall primary oil and gas production.

Cold water at 60°F is injected into these reservoirs. The temperature profile in the wellbore and the temperature at which the water reaches the perforations will determine the likelihood of paraffinic deposition in the vicinity of the wellbore. Paraffin problems have been studied with respect to production wells and not much attention has been paid to cold water injection and its impact on paraffin deposition. After a detailed literature review, a thermal heat transfer model has been developed in Chapter 8 in order to determine temperature effects in the injectors. This study conclusively shows the strong possibility of paraffin deposition in the vicinity of the injection wellbores and also presents surface injection temperatures required to avoid paraffin deposition in the injectors.



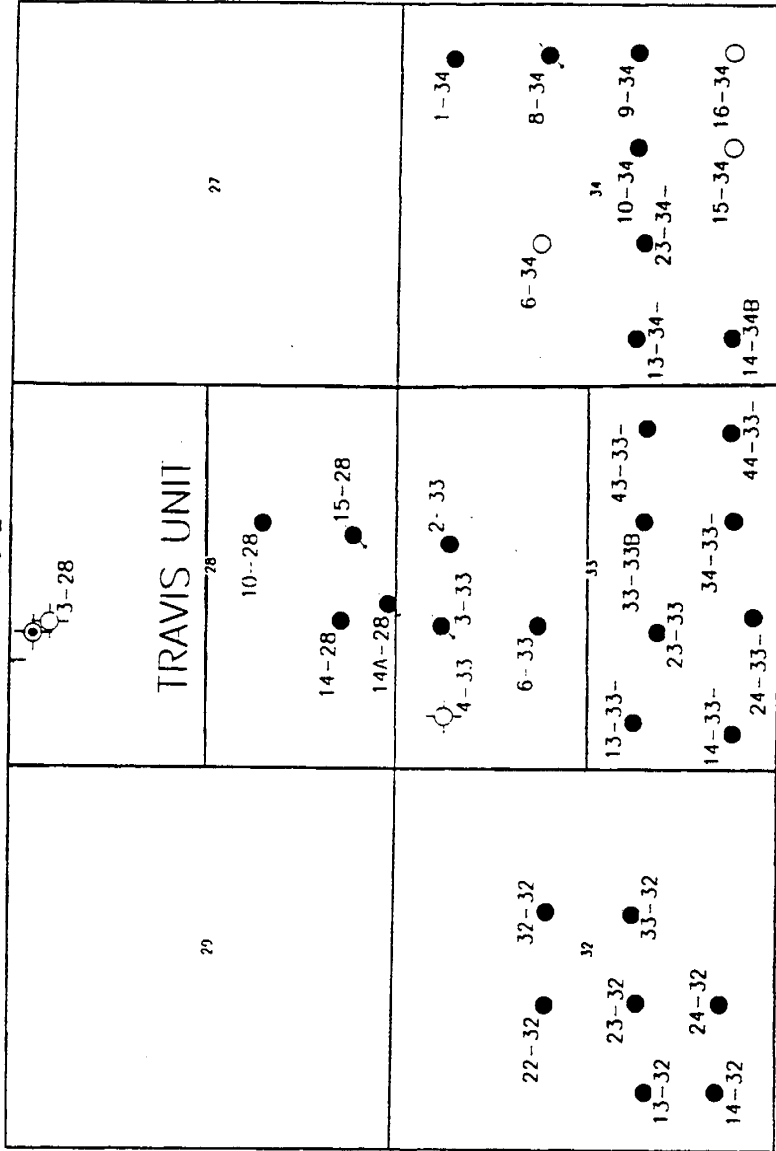
LOMAX EXPLORATION COMPANY	
UINTA BASIN, UTAH DUCHESNE COUNTY MONUMENT BUTTE UNIT	
John D. Lomer	6/27/94
060804A	Scale 1:2000



LEGEND	
●	OIL WELL
★	GAS WELL
●	WATER INJECTOR
○	LOCATION
⊗	DRY & ABANDONED

Figure 1.1: A Unit map of the Monument Butte Unit.

R 16 E



T
8
S

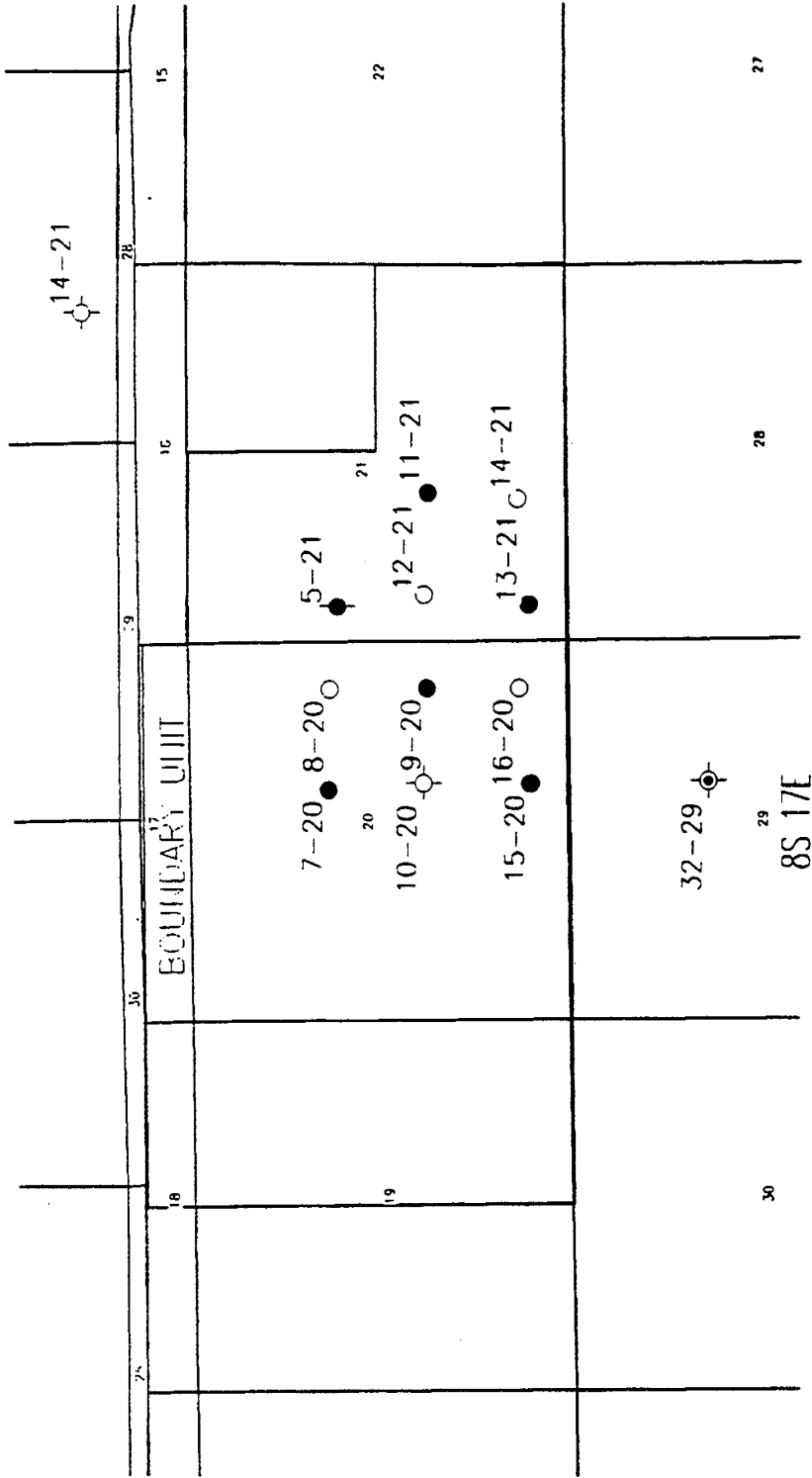
LOMAX EXPLORATION COMPANY	
UNTA BASIN, UTAH DUCHESE COUNTY TRAVIS UNIT	
John B. Long	6/17/74
REVISIONS	Scale 1:5000

0.1 0 0.1 0.2 0.3 0.4 0.5 miles



LEGEND	
●	OIL WELL
●/	WATER INJECTION WELL
○	LOCATION
⊗	DRY & ABANDONED

Figure 1.2: A Unit map of the Travis Unit.



LEGEND	
●	OIL WELL
⊗	WATER INJECTION WELL
○	LOCATION
⊕	DRY & ABANDONED

Scale 1:32000.

LOMAX EXPLORATION COMPANY	
UNIT: BASK, UNIT	
COUNTY: DOUGLAS COUNTY	
BOUNDARY UNIT	
DATE:	1/1/80
BY:	[signature]
SCALE:	1:32000

Figure 1.3: A Unit map of the Boundary Unit.

Chapter 2

Field Activities

The Monument Butte #10-34 was spud on 10/2/92. The Monument Butte #10-34 was drilled to a depth of 6400 ft. On the 38th day after the spud date, logging of the #10-34 was started. Based on the results of the logging and coring process, 5 1/2 in casing was cemented in the hole. As of 11/24/92, the #10-34 had been completed. Our objectives were to complete in the Castle Peak, Black Shale, 'A' and the 'D' intervals of the Green River Formation. All four intervals have been perforated and fractured. The Monument Butte #10-34 was completed as an oil producer. From 11/27 through 1/27/93, oil production was 3,393 barrels (54 barrels per day). Through March 31, 1993, Monument Butte 10-34 had produced 4,953 barrels of oil and 4,039 Mcf of gas. By June 30, 1993, the Monument Butte #10-34 had produced 6,277 barrels of oil and 6.5 MMcf of gas. Through September 30, 1993, the Monument Butte #10-34 had produced 7,526 barrels of oil and 7,824 Mcf of gas and by December 31, 1993, the Monument Butte #10-34 produced 8,955 barrels of oil and 9,850 Mcf of gas.

Travis #14a-28 was spud on 10/6/92. The Travis #14a-28 was drilled to a depth of 6190 ft. On the 20th day after the spud date, logging of the #14a-28 was started. Based on the results of the logging and coring process, 5 1/2 in casing was cemented in the hole. We have completed in the Lower Douglas Creek and the 'D' intervals of the Green River Formation. However, due to the fracturing of the Lower Douglas Creek, only the 'D' sand interval was put on production the first of January, 1993. From 1/1/93 through 1/28/93, the #14a-28 had produced 2,947 barrels of oil (105 barrels per day) and 1.9 Mcf of gas (107 Mcf per day) from the 'D' sand interval. Due to the success of the 'D' sand, plans were made to recomplate other Travis unit wells with 'D' sand intervals behind pipe. Further study of the Lower Douglas Creek interval will be done before an attempt to putting the interval on production due to the extensive fracturing. Travis 14A-28 (1/1/93 first production) had produced 6,187 barrels of oil and 7,829 Mcf of gas from inception through March 31, 1993. Due to fracture information provided by Formation Microimaging log and subsequent completion in the D sand in the Travis #14A-28 well, we recompleted the behind pipe D sand zones in the Travis Federal #14-28 in March of 1993 and the Travis #10-28 in May of 1993. The 14-28 had produced 2,411 barrels of oil through March 31, 1993 or 105 barrels per day. By June 30, 1993, Travis #14A-28 had produced 7,717 barrels of oil and 19.9 MMcf of gas. while, the Travis #14-28 and #10-28 had produced 6,543 barrels of oil (22.6 MMcf of gas) and 1,391 barrels of oil (763 MMcf of gas), respectively. Due to the success of the D

sand interval of the Green River Formation, water injection was begun in the third quarter of 1993 (October, 1993) in the Travis #14a-28. Travis #14A-28 (1/1/93 first production) had produced 7,953 barrels of oil and 23,045 Mcf of gas when it was converted to a water injector. Through September 30, 1993, the Travis #14-28 and #10-28 had produced 5,529 barrels of oil (31,993 Mcf of gas) and 2,907 barrels of oil (4,929 Mcf of gas), respectively. Through December 31, 1993, the Travis #14-28 and #10-28 had produced 8,846 barrels of oil (43,309 Mcf of gas) and 4,060 barrels of oil (8,943 Mcf of gas), respectively. At this time, Travis well #14A-28 operated as a water injector into the D-sands. Through 12/31/93, 10,736 barrels of water had been injected into the #14A-28 well at an average pressure of 37 psi.

Water injection was resumed in the Travis 15-28 in mid March. The average daily rate was 263 barrels per day. Lomax and the Department of Chemical and Fuels Engineering agreed to a slower injection rate in the 15-28 due to the fractures found in the logging and coring of the 14A-28 well. On March 31, 1993, the tubing pressure of the 15-28 was at 90 psi and casing pressure was at 480 psi. We continued water injection in the Travis #15-28 throughout the second quarter of 1993. The average daily water injection rate for the second quarter of 1993 was 275 barrels. On June 30, 1993, tubing pressure of the #15-28 at 363 psi. Applications were filed to secure the appropriate permits to convert the Travis #3-33 into a water injector to inject into the Lower Douglas Creek member of the Green River Formation in the third quarter of 1993. We continued water injection in the Travis #15-28 throughout the third quarter of 1993. The average daily water injection rate for the third quarter of 1993 was 275 barrels. We converted the Travis #3-33 into a water injector to inject into the Lower Douglas Creek member of the Green River Formation in October of 1993. To repressure the Lower Douglas Creek member in the Green River formation in the Travis unit, we continued to inject water throughout the fourth quarter of 1993. The average daily water injection rate for the fourth quarter of 1993 in the Travis #15-28 was 300 barrels at an average injection pressure of 756 psi. In well #3-33, the average daily water injection rate for the fourth quarter of 1993 was 270 barrels at an average injection pressure of 900 psi.

Due to weather constraints, the Boundary 10-20 location was not approved by the BLM until April of 1993. The Boundary 10-20 well was spudded in April. The 10-20 was the first of two wells committed to be drilled in the Boundary unit in 1993 as part of the water flood development. The main oil objectives in the 10-20 well are the lower Douglas Creek and the 'D' sand members of the Green River formation. We started drilling of the Boundary #10-20 in April of 1993. By the end of April, we reached a total depth of 6,560 ft. After running a Dual Laterolog (DLL) and compensated neutron density logs, no commercially productive sands were found in the Green River Formation. We decided not to complete in this well and proceeded to plug and abandon the well by April 29, 1993. The well was apparently drilled outside the channel we projected. The geologic information from this well will be utilized to drill the next Boundary unit well.

On 11/15/93, we spud the Monument Butte #9-34 well. Our initial objective was to target for completion the D and B sands of the Green River Formation. Our plan was to convert the #9-34 into a water injector. Drilling of the #9-34 started on 12/1/93 and was completed on 12/6/93 to a depth of 6,500 ft. On 12/6/93, logging of the #9-34 was started. Based on the results of the logging and coring, 5 1/2 in casing was cemented into place in two stages. The D (4992-97 ft; 5000-08 ft) and B (5334-50 ft; 5355-60 ft) sand members were

perforated and fractured. Also, due to the logging program, the Castle Peak sand member of the Green River formation was perforated (5854-68 ft; 5902-5912 ft) and fractured. All the completed sands were swabbed with bottom hole pressure tests run. At the current date, the #9-34 well has been put on oil production. From 1/9/94 to 1/31/94, the #9-34 had produced 3,232 barrels of oil (140 barrels per day). It appeared that the D and B sands have been affected by the water flood front. Well #9-34 is being monitored over the next 90-120 days to decide what future steps need to be taken to the well and water flood unit.

Chapter 3

Geologic Characterization

3.1 Logging Methods

The DOE program has allowed Lomax Exploration to utilize state-of-the-art methods to evaluate the geological processes that influence the water flood. The Schlumberger Fullbore Formation MicroImager ('FMI') and the Numar's Magnetic Resonance Imaging Log ('MRIL') were used in the evaluation of the Monument Butte #10-34 and Travis #14a-28 wells.

The Schlumberger FMI was used to evaluate the stratigraphic sequences of interest to develop a better understanding of the stratigraphy and depositional environment of potential reservoir beds. This log is also valuable in locating fractures along with determining the orientation and size of the fractures. Fractures were found in areas where they had not previously been detected. This information is critical to selecting completion intervals and designing stimulation treatments. The FMI log is also very useful for thin bed evaluation, and for locating the best places to take rotary sidewall cores.

The second advanced research log that we have used is Numar's MRIL. This log was used to evaluate the movable fluid content of the reservoir rock, and to determine the effective permeability within the reservoir. This log uses a pulsed magnetic field to realign the hydrogen atoms and the tool measures the response time for the atoms to return to normal, thereby determining the mobility of the oil and water in the reservoir. At least one zone that by sample analysis and core analysis (Monument Butte #10-34, Black Shale interval) appeared to be non-commercial, was indicated by the MRIL to have movable hydrocarbons. Subsequent completion has established commercial production.

The original logging program for the Federal 10-20 in the Boundary Unit called for utilizing the Schlumberger FMI log and the Numar MRI log. This was scheduled on the premise that the D-sand zone and the Lower Douglas Creek sand zone would be present. The purpose of running these two logs was to evaluate the lithology, the bedding characteristics and the fracturing of the reservoir. Additionally, if the fractures were found, orientation could be determined. The FMI log would also indicate the best places to take the side wall cores. The MRIL log was designed to evaluate the reservoir in relation to the fluid content and the relative mobility of water and oil found in the reservoir. At the time the well had reached total depth and the conventional logs (Compensated Neutron Density and Dual Laterolog Gamma Ray) had been run, it was determined that there was only ten feet of gross D sand with only two feet with porosity greater than ten percent. The LDC did not

develop any sand that could be considered potential reservoir. After reviewing these logs and the mud logs, it was determined that no positive reservoir data could be obtained and the FMI and MRIL logs were not run on this well.

In the Monument Butte Unit, an average well has approximately twenty sands to evaluate. Ten sands will usually be eliminated as being too discontinuous or too thin. The ten remaining sands have to be evaluated with regard to their relative permeability. The evaluation of effective permeability has been most difficult information to obtain, and yet it is critical to making a commercial completion. Early indications are that prudent use of these new logs may enhance completion practices and reduce the cost of well completions.

3.2 Travis Unit

A full diameter core was collected from 5550 ft to 5646 ft in the lower Douglas Creek interval of well 14A-28. The core was photographed and described in detail. The sandstone of the lower Douglas Creek in well 14A-28 is composed of thick packages of planar-laminated, fine-grained sandstone exhibiting various degrees of dewatering and soft-sediment deformation, that are separated by thinner disrupted or massive bedded, very fine-grained sandstone and siltstone beds. The planar-laminated sandstones occur in 15 ft thick packages with an intraclast-rich base and a dewatered top. The sandstones are interpreted as moderate to low-density turbidite channel deposits. Two deformed planar-laminated sandstone units occur, from 5632.7 ft. to 5623.5 ft. and from 5605.5 ft to 5588 ft. Both of these units are strongly oil-stained.

The most strongly oil-stained sandstones are those facies that are planar-laminated, whether or not they are disrupted or undeformed. Presumably, these laminated facies are also the best reservoir units. Moderately stained sandstones of the lower turbidite channel sequence have oil saturations that range from 49.6 to 40.5%, horizontal permeabilities in the .46 to .77 mD range and vertical permeabilities in the .50 to .99 mD range. The plug from 5638 ft had the highest vertical permeability of any of the measured samples, because the laminations are steeply inclined at this depth. Porosities in this facies range from 9 to 11.7%. Strongly oil-stained planar-laminated sandstones in the upper turbidite unit are 67 to 70.7% oil saturated. Horizontal permeabilities in this sandstone unit are much higher than those of the lower turbidite unit and range from 2.5 to 13 mD. Porosities range from 14.8 to 16.6%. The core from the lower Douglas Creek interval is moderately fractured. There is some lithologic control on the formation of fractures. In general, fractures are developed in cemented sandstone beds rather than in more ductile finer grained lithologies. In the upper portion of the core, fractures are present in carbonate-cemented sandstone beds at 5570-5572 ft, 5582 ft and at 5589-5590 ft. In these beds, the fractures are open, subvertical and planar. Fractures in the upper and lower turbidite sandstone units are more irregular. At 5608-5611 ft and 5625-5627 ft, open fractures are subvertical but tend to mimic the orientation and geometry of dewatering pipes in the laminated sandstones and are nonplanar. In general, the open, natural fractures have dips greater than 60°. The dewatering pipes exhibit similar dips and are commonly subvertical.

Activities of the University of Utah Research Institute revolved around a reevaluation of the stratigraphy and depositional controls of the Lower Douglas Creek sandstone. This

unit can have the thickest accumulations of reservoir sandstones in the Uinta Basin area. However, predictions of thicknesses in new wells have proven to be difficult. Gamma ray and density logs were re-interpreted using the FMI logs collected in the Travis #14a-28 well. These logs show the thick section of the Lower Douglas Creek sandstone has a depositional vector to the northeast trend. Analysis of the Monument Butte #10-34 well shows that the Lower Douglas Creek section may be faulted out. The new concepts developed through this ongoing study will be tested with the drilling of subsequent wells.

3.3 Monument Butte Unit

Wireline logs for the Monument Butte unit were reduced to a scale of 40 feet per inch to facilitate a re-evaluation of the distribution of reservoir rocks. Well Monument Federal 13-35 was designated the type log for the unit (Figure 3.1). One of the principal difficulties in the Uinta Basin is that the stratigraphic nomenclature is not standardized. Each operator has developed their own designations, and thus correlation of reservoir units on a regional scale is extremely imprecise. In illustrating a type log, we hope to communicate stratigraphic details that will aid other operators in the area.

The lowest marker bed shown on Figure 3.1 is the B Limestone marker. Based on correlation with wells in the Duchesne field to the west, the B Limestone is equivalent to the 'Top of the Carbonate Marker Unit' of Fouch (1981). Since the B Limestone is a clearly recognizable unit across the southern portion of the basin, we assume that it represents open lacustrine deposition.

The prominent marker above the B Limestone is termed the Bicarbonate marker. In the section between these two markers, the B Sandstones constitute important petroleum reservoirs.

The uppermost marker shown on Figure 3.1 is the Douglas Creek marker. Imaging logs through this unit suggest that it is a sandy limestone. Between the Bicarbonate and Douglas Creek markers are the D and C Sandstones. The principal reservoir units that will be discussed in this report are the D and B Sandstones that are the principal reservoirs involved in the water flood.

3.3.1 B Sandstone

This unit occurs within the stratigraphic interval between the B Limestone and the Bicarbonate markers. There appear to be at least three, and perhaps five, stratigraphically distinct sands. The important sandstones in terms of thickness and porosity are located near the base of the section, above the B Limestone. At times the sandstones are deposited directly on the B Limestone, and it is clear that there is an erosional unconformity above the B Limestone.

Figure 3.2 is an isopach map of the B2 and B3 Sandstones. It is interpreted as representing a meandering fluvial system, although more information is needed to eliminate the possibility that it does not represent the effects of a fluvial system superimposed upon a delta, where, as seen in the D1, sandstone accumulations of > 30 feet are possible. Nevertheless, it is our interpretation that the B sandstone represents a delta plain environment with fluvial

systems separated by mud flats.

The northwest trend of the thickest portions of the sandstone are notable. This trend is parallel the trends of gilsonite dikes, which are certainly younger than the channel system, but the two may have resulted from similar structural controls. From the standpoint of the water flood, the sandstones are probably well confined by shale horizons providing a good geometry for the waterflood sweep.

3.3.2 C Sandstone

Beneath the D2 sandstone is the C sandstone reservoir unit. The C sandstone is present in most wells. It is normally thin, but is over 30 feet thick in some wells. This reservoir is not involved in the waterflood at the present time.

3.3.3 D Sandstone

The D Sandstone interval has been well characterized from full-diameter core taken in the 6-35 and 12-35 wells (Davies, 1983, written communication). Davies characterizes these sandstones as deposits of a playa environment formed along the margins of a larger permanent lake. Terrigenous clastics were carried onto the playa by unchanneled sheetfloods and braided fluvial channels.

As isopach map of the D1 sandstone is shown in Figure 3.3. This shows a maximum thickness of 32 feet with a lensoid shape having a WNW-ESE orientation. Although the thicker portions of the body occur as a single unit, sections through the margins show that as the body gets thinner, it also breaks up into two or three separate sands separated by shale horizons that are generally 2 to 4 feet thick.

An FMI image through the D1 in well 10-34 shows that the bedding is oriented 230° (Figure 3.3), showing sediment transport away from the thicker portions of the body. This sections of side wall cores suggest that the D1 was deposited as a sublacustrine bar. The presence of abundant rounded micrite clasts and micrite-coated quartz and feldspar grains suggests formation of the grains in a shallow bay or lagoon and then transportation to an off-shore environment. The overall fine grain size and lack of strong grading preclude deposition as channelized sands. An isopach of the D2 sandstone is shown in Figure 3.4. In contrast to the D1, the D2 is much less continuous, probably due to its deposition in channels. The nature of the sandstone distribution suggests that the depositing streams were meandering. Due to its irregular distribution, the D2 is not a good drilling target.

3.4 References

- Fouch, T. D., 1981, Distribution of rock types, lithologic groups, and interpreted depositional environments for some lower Tertiary and Upper Cretaceous rocks from outcrops at Willow Creek Indian Canyon through the subsurface of Duchesne and Altamont oil fields, southwest to north central parts of the Uinta Basin, Utah: U.S. Geological Survey, Chart OC-81.

Davies Report, 1983, Environment of Deposition, Reservoir Quality and Fluid Sensitivity of Green River Sandstones, Monument Butte Field, Duchesne County, UT, David K. Davies and Associates, Inc., Kingwood, TX, Available for reference at the offices of Lomax Exploration Company in Salt Lake City, UT.

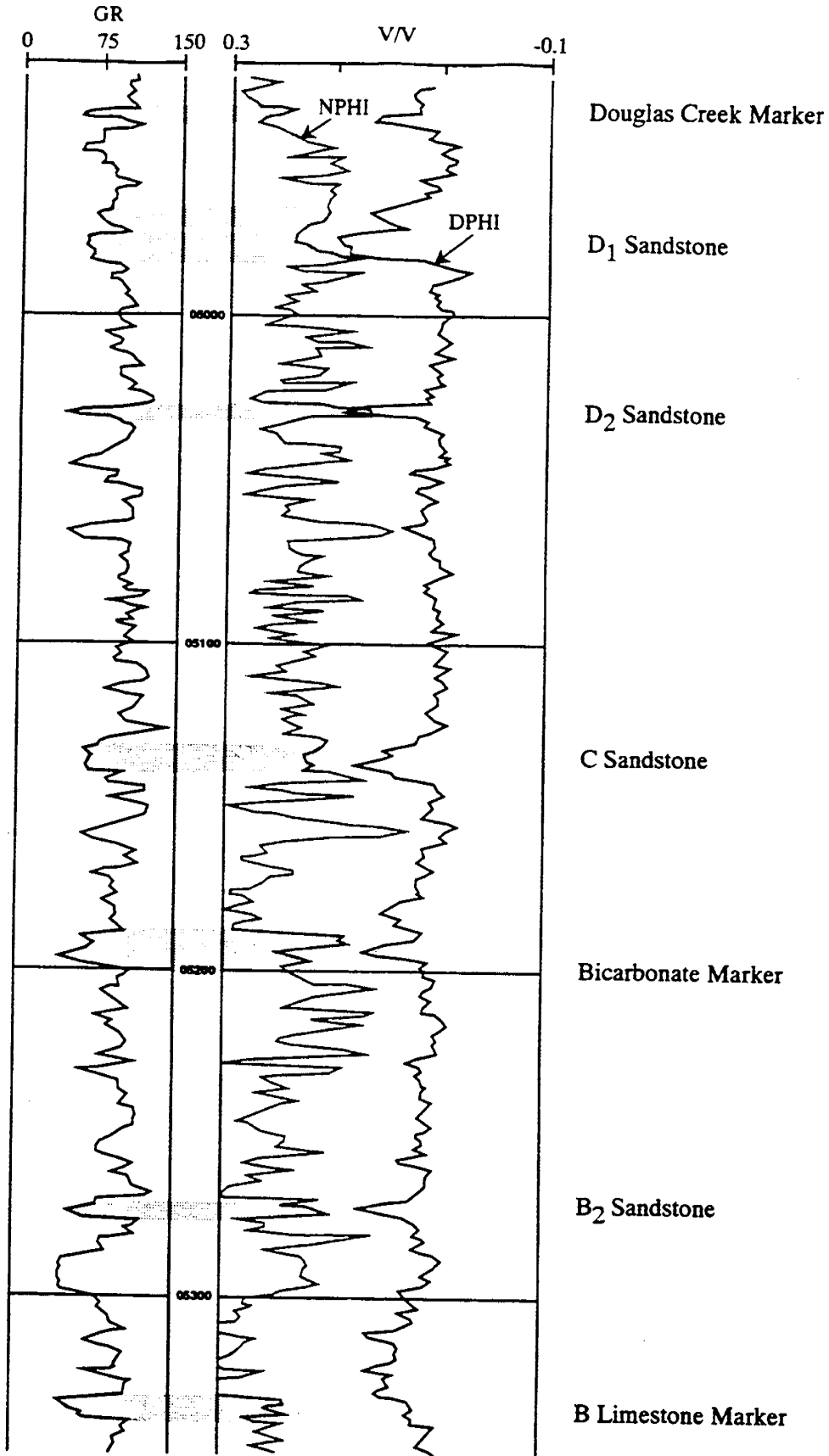


Figure 3.1: Log for the well 13-35 showing major stratigraphic units in the Monument Butte Unit (GR, Gamma Ray; NPHI, Neutron Porosity; DPHI, Density porosity).

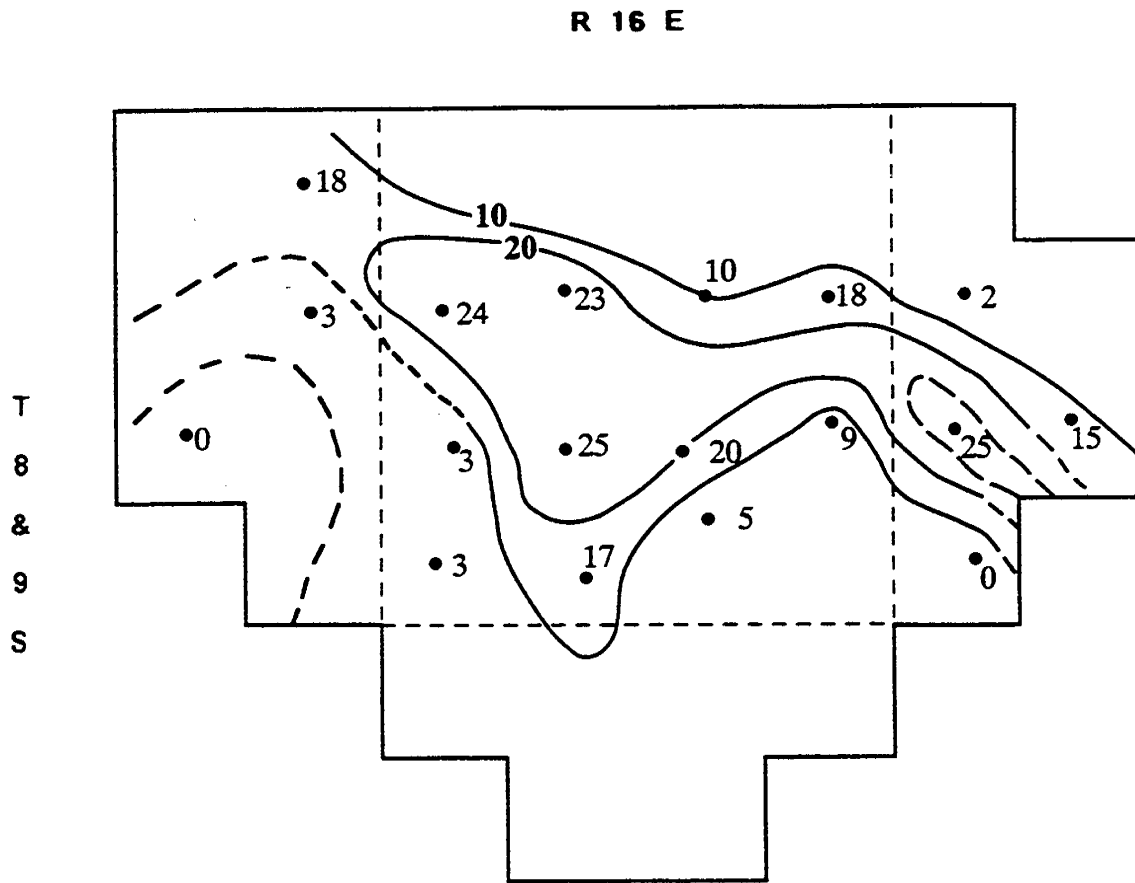


Figure 3.2: An isopach map of B-sandstone, Monument Butte Unit.

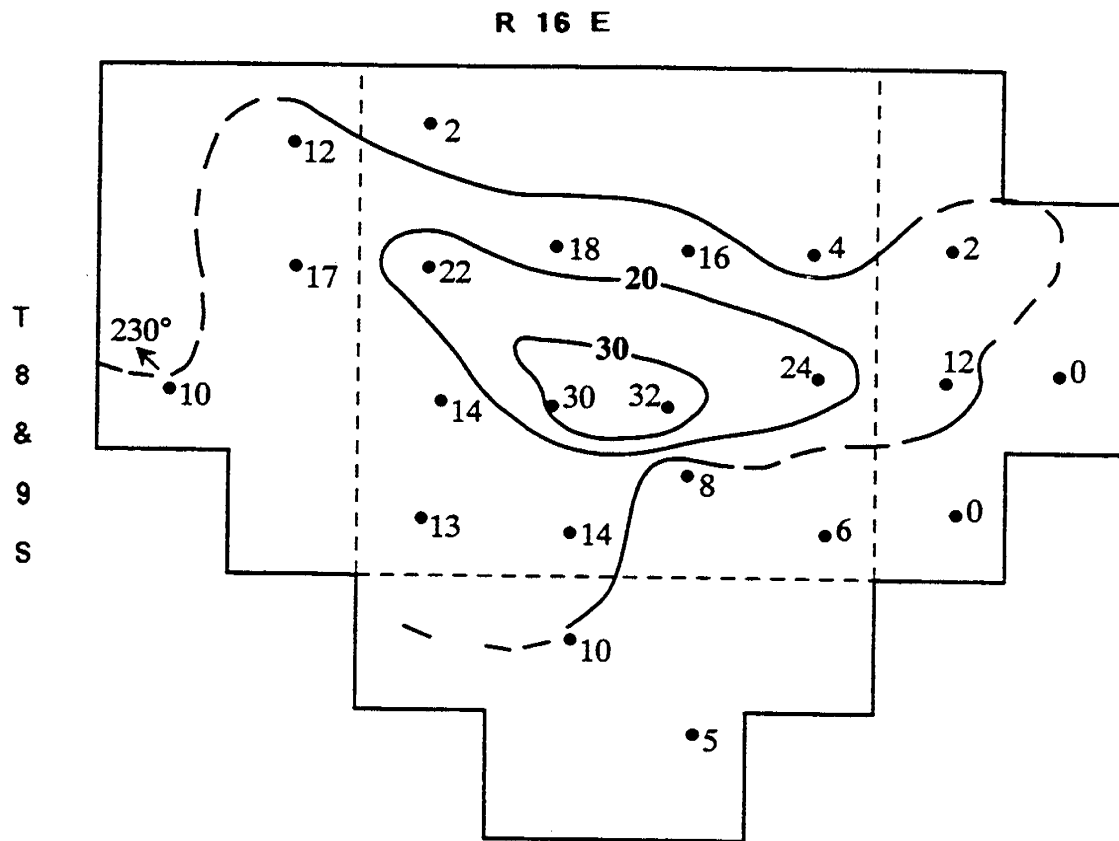


Figure 3.3: An isopach map of D1-sandstone, Monument Butte Unit.

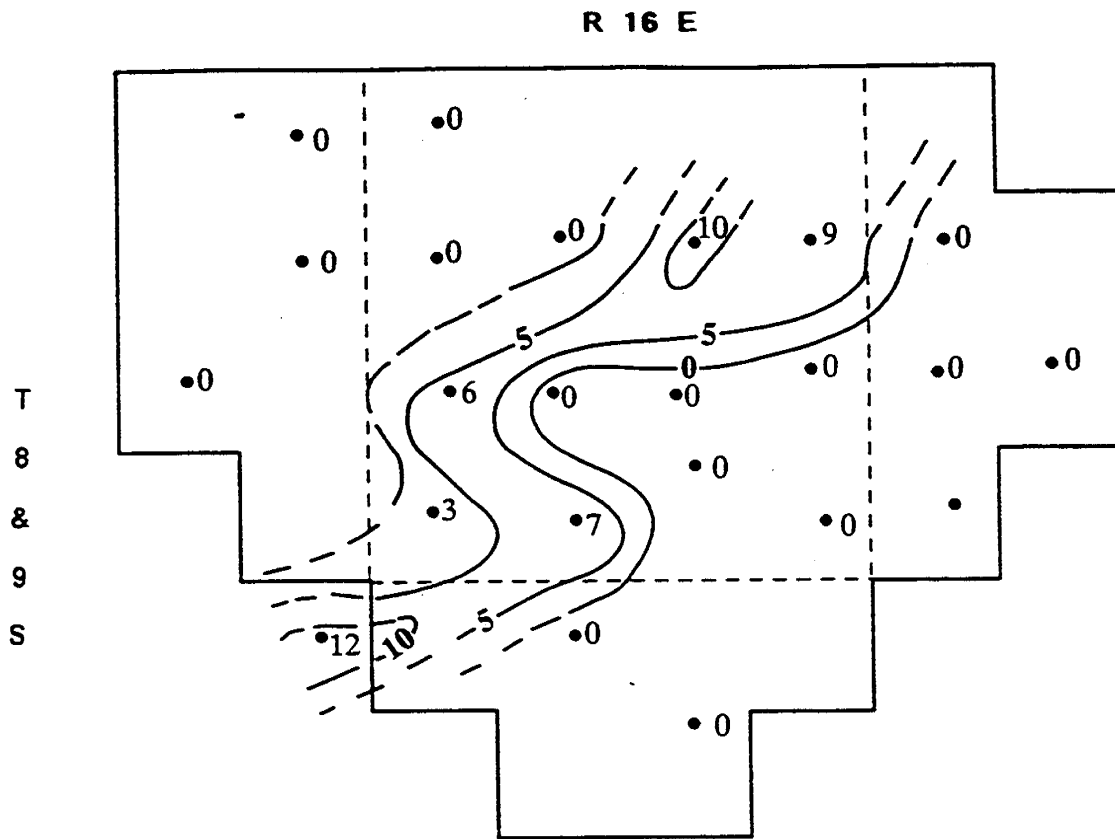


Figure 3.4: An isopach map of D2-sandstone, Monument Butte Unit.

Chapter 4

Compositions of Oils

4.1 Synopsis

Simulated Distillation (SIMDIS) using gas chromatography is an expedient technique for the determination of boiling range and thus carbon number distributions of crude oils. A procedure to calculate the uneluted fraction of the oil (from the chromatographic column) exists in the literature. Mathematical equivalence between this procedure and a more intuitive inverse lever-arm principle has been established in this Chapter. Capillary gas chromatography permits the analyses of samples containing higher boiling compounds at temperatures similar to those employed in packed column chromatography. Using a short (5 m) capillary column, samples containing compounds with carbon number up to C_{90} can be characterized. However, for accurate measurement of compositions from $C_5 - C_{44}$, a longer capillary column is required. A two-column procedure has been developed in this Chapter to obtain a 'wide' $C_5 - C_{90}$ distribution for crude oils. A longer (30 m) column is employed for compositional measurements in the range of $C_5 - C_{44}$. A short (5 m) column is used to obtain carbon number distributions from $C_{20} - C_{90}$. For the two oils analyzed as part of this study, excellent agreement is observed in the overlapping region of the two analyses. The procedure developed in this Chapter allows for a high-resolution characterization of the $C_5 - C_{90}$ fraction of the oil while limiting the uncharacterized portion of the oil to C_{90+} .

4.2 Introduction

Crude oils are composed of hundreds of components. Distillation (ASTM D2892, 1990) is a standard test to classify the crude oil into a manageable number of components. This compositional characterization of crude oils is used in the representation of the oils for subsequent phase behavior and other types of modeling, and hence is very important. Gas chromatographic techniques for simulating this distillation process were devised to significantly reduce the analysis time. The original concept (Green et al., 1964) and the ASTM standard (ASTM D2887, 1989), which is based on this concept permit the analyses of petroleum fractions with atmospheric boiling points up to 540°C . The relationship between boiling points and equivalent n-alkane carbon numbers is well known. The practical temperature limit on most packed columns is 350°C . At this temperature, nC_{44} (B.P. = 545°C) is the highest paraffin

that elutes normally on a packed column used for simulated distillation. Even if columns with higher temperature limits were available, at temperatures higher than about 375°C, thermal decomposition of the oils becomes a primary concern. Under these constraints, to determine the fraction of crude oil boiling above 540°C, Worman and Green (1965) proposed a procedure which required chromatograms of the sample and the sample mixed with an internal standard (IS). This procedure has been standardized (ASTM D5037, 1992) and also been applied to supercritical fluid chromatography (Stadler, et al., 1993). Using the intuitive, universal lever-arm rule, it is possible to derive the expression for the total area of the chromatogram, proposed by Worman and Green (1965) and adopted in ASTM D5037 (1992). This derivation has been provided in the Appendix of this Chapter.

The emergence of capillary chromatography has allowed the elution of higher boiling hydrocarbons at the same temperatures employed for packed column chromatography. Trestianu et al (1985) reported the simulated distillation of heavy petroleum fractions up to 800°C true boiling point by capillary gas chromatography. Using capillary gas chromatography with an upper column temperature limit of about 375°C, it is possible to elute normal paraffins with carbon numbers up to 90 (B.P. = 732°C). These analyses thus make it possible to characterize a greater portion of the crude oil. The uneluted portion of the oil is limited to a C₉₀₊ fraction. SIMDIS characterization of oils up to a carbon number of 90 by capillary gas chromatography requires the use of a short, typically 5 m, column. Satisfactory resolution of peaks in conventional C₅ - C₄₄ analysis requires the use of a longer capillary column. Thus, for the characterization of oils with a wide carbon number distribution, a two-step procedure was designed.

1. A conventional simulated distillation analysis, using a 30 meter capillary column to obtain a carbon number distribution from C₅ to C₄₄. This analysis provides a C₄₄₊ fraction.
2. A higher-temperature, short capillary column analysis which provides a carbon number distribution of the oil from C₂₀ to C₉₀. This analysis provides a breakdown of the C₄₄₊ portion of the sample provided by the long-column analysis, in addition to providing a C₉₀₊ fraction.

It should be noted that both the techniques involve analysis using an internal standard. There is a carbon number overlap between the short and the long column analyses. Determination of reliable compositions ranging from C₂₀ to C₉₀ would require similar results in the region of the overlap. This section demonstrates that the above two-step concept can be used effectively to obtain compositional analyses of oils up to a carbon number of C₉₀ and an estimate of the C₉₀₊ fraction.

4.3 Experimental Equipment

4.3.1 GC Apparatus

The GC used was a Hewlett-Packard (HP) (San Fernando, CA) Model 5890 Series II with on-column injection, using helium as the carrier gas. Injections were performed manually due

to the viscous nature of the samples. The injections were accomplished using a Hamilton 10 μ l syringe. The sample size was 0.5 μ l. Two analysis techniques were used as detailed below. A flame ionization detector was used to detect the material eluted from the column, with the detector signal stored on a microcomputer. Results were later analyzed via the use of two SIMDIS computer programs developed by the authors.

4.3.2 C₅ - C₄₄ Analyses

The compositional measurements for carbon numbers up to C₄₄ were obtained using a J & W Scientific (Folsom, CA) DB-1, 30 meter x 0.25 mm O.D., glass capillary column, with a 0.25 micron film thickness. This column was chosen for high-resolution peak separation. The initial oven temperature was 40°C and was held at that value for 4.50 minutes. The temperature was then increased to a maximum temperature of 350°C at a constant rate of 12°C/minute. The temperature was then held at 350°C for 20 minutes. The injector temperature was programmed to track the column temperature, while the injector pressure was held at 138 kPa. The C₅-C₄₄ SIMDIS calibration mixture was obtained from Hewlett-Packard Analytical Supplies Division (Wilmington, DE).

4.3.3 C₂₀ - C₉₀ Analyses

The compositional measurements from C₂₀ through C₉₀ were obtained using a Supelco (Bellefonte, PA) EX-2887, 5 meter x 0.53mm I.D., glass capillary column, with a 0.1 micron film thickness. This column has lower resolution than the above column, but will elute higher boiling components. The initial oven temperature was 35°C and was held at that value for 4.50 minutes. The temperature was then increased to the maximum temperature of 380°C at a constant rate of 12°C/minute. The temperature was then held at 380°C for 8.75 minutes. The injector temperature was programmed to track the column temperature, with the injector pressure kept constant at 11 kPa. This lower pressure is used because the wider bore (short) column allows gases to flow more easily, and thus requires a lower pressure drop to maintain the appropriate flow rate. The Polywax 655 calibration mixture containing C₂₀ to C₉₀ hydrocarbons was also purchased from Supelco.

4.3.4 Crude Oil Samples

Crude oils were provided by Lomax Exploration Company, Salt Lake City, Utah. The Oils were from their Monument Butte Unit, located to the south of Roosevelt, Utah. All of the oils from the unit had API gravities of about 34°API and viscosities of 14 cP at 60°C. The crudes were waxy in nature, indicating the presence of a significant fraction of high molecular weight paraffins. Analyses of two of the oils from the Monument Butte Unit have been provided. All of the analyses were performed using approximately 30 wt% internal standard.

4.4 Computations

Simulated distillation requires four chromatographic runs: the calibration mixture, the crude oil, the crude oil mixed with an internal standard, and a blank run. The area of the blank run is subtracted from the other chromatogram areas as the base line. Figure 4.1¹ shows the calibration chromatogram for the Polywax 655 standard. This chromatogram was obtained using the short 5 m column. This standard contains even numbered oligomers of polyethylene wax. Once the carbon number versus retention time calibration is established, the subsequent chromatograms are divided into carbon number distributions. Figure 4.2 is a chromatogram of one of the crude oil samples studied during this work, while the blank run is shown as the baseline on Figure 4.2. Figure 4.3 is a chromatogram of the same crude oil, with an internal standard added. The calculation of the uneluted portion of the chromatograms requires that the internal standard be completely eluted. The internal standard is a mixture of n-C₁₄, n-C₁₅, n-C₁₆, and n-C₁₇, and elutes completely under both of the analysis routines used.

The development of relevant equations based on the lever-arm rule have been provided in the Appendix. The uneluted portion of the chromatogram can be calculated as

$$U = \frac{(A_{IS} - B_{IS} R - A W)}{(A_{IS} - B_{IS} R)(1 - W)} \quad (4.1)$$

where U is the uneluted fraction of the injected material, A_{IS} is the area of the internal standard segment of the chromatogram of the crude oil plus the internal standard, B_{IS} is the area of the crude oil only chromatogram over the same time segment as A_{IS}, R is ratio of the areas of the segments not including the internal standard peaks for the chromatogram of the sample with the internal standard divided by the area of the same segments for the sample without the internal standard, A is the total eluted area of the chromatogram of the sample with the internal standard, and W is the weight fraction of the internal standard in the mixture of crude oil and internal standard. The weight fraction of each carbon number cut of the sample distribution can be determined as

$$w_n = \frac{(B_n - B_{n-1})}{M} \quad (4.2)$$

where w_n is the weight fraction of the sample that elutes between the carbon numbers n and n-1, and B_n is the total chromatogram area (less the baseline area) that elutes up to the time that n-C_n elutes. M is the total area that the chromatogram would have if all of the oil were to elute. Figure 4.4 shows these various areas.

Worman and Green (1964) proposed an expression for the total area (eluted + uneluted) of the chromatogram, which was adopted for ASTM D5037 (1992). The total area is given by:

$$M = \left(A_{IS} \frac{B - B_{IS}}{A - A_{IS}} - B_{IS} \right) \frac{1 - W}{W} \quad (4.3)$$

where B is the total eluted area of the chromatogram of the sample without the internal standard. The carbon number weight fractions are calculated using equation 2.

¹Illustrations are at the end of the Chapter

The total area of the chromatogram (equation 3) can be derived from equation 1. This derivation has been provided in the Appendix. Thus a logical explanation and a mathematical basis for the use of equation 3 has been established.

When the standard C_5 - C_{44} is used as a calibration mixture (in the long column analysis), the uneluted portion of the chromatogram corresponds to $C_{44}+$ portion of the oil. This technique is equivalent to the ASTM D5037 analysis. The use of the Polywax calibration mixture (C_{20} to C_{90}) allows for the characterization of oil up to a carbon number of 90 and the uneluted fraction of the sample chromatogram corresponds to $C_{90}+$. Equations 1 to 3 were used for the development of both the computer programs used in this study. Equations 1 and 3 are used for the determination of the uneluted fraction of the oil and the total sample area respectively, while equation 2 is employed for the computation of the carbon number distributions.

4.5 Results and Discussion

The crude oil samples were analyzed using the two-step, short and long-column analyses. Results of two of the analyses have been presented. The carbon number distributions from the long-column analyses (C_5 - C_{44} and a $C_{44}+$ fraction) and the short-column analyses (C_{20} - C_{90} and a $C_{90}+$ fraction) for these two crude oils are presented in Figures 4.5 and 4.6. These oils are from different oil-bearing sands and some compositional variation is expected. It should be observed from these figures that in the region of the overlap between the short and the long column analyses (carbon numbers C_{20} - C_{44}) there is a reasonably close agreement between the two sets of carbon number distributions. The $C_{44}+$ fractions of the crude oils presented in Figures 4.5 and 4.6 were 0.28 and 0.29 respectively. The short column analyses provide a breakdown of this $C_{44}+$ fraction into a C_{45} - C_{90} carbon number distribution and a $C_{90}+$ fraction. The $C_{90}+$ fractions of the two oils shown in Figures 4.5 and 4.6 were 0.07 and 0.08 respectively. The close agreement in the overlapping region suggests that the results of the two analyses can be combined with confidence. Thus, the two column approach produces a reliable C_5 - C_{90} carbon number distribution for the crude oils of interest and an estimate of the $C_{90}+$ fraction. Compared to the conventional C_5 - C_{44} analysis, more of the oil is characterized. In the specific case of the oils presented in Figures 4.5 and 4.6, the unknown ($C_{44}+$) fraction of the oil is reduced from 0.28 to 0.07 and from 0.29 to 0.08 respectively. Thus, the validity of using a two-column analysis approach has been demonstrated using two oils from two different fields.

4.6 Conclusions

The formula for computing the total area of an oil chromatogram was derived using the lever-arm rule. For analyses of crude oils over a wide carbon number range (C_5 - C_{90}), a two-column procedure was employed. A higher-resolution long column (30 m) provided the C_5 - C_{44} analyses and a $C_{44}+$ fraction. A more detailed breakdown of the $C_{44}+$ fraction was obtained using a short, 5 m, capillary column. The second analysis provided a carbon number distribution of C_{20} - C_{90} and a $C_{90}+$ fraction. For all of the crude oils analyzed, an excellent match was obtained in the overlapping regions of the two analyses (C_{20} - C_{44}).

Thus, a reliable procedure was developed to obtain C₅ - C₉₀ carbon number distributions of crude oils and to limit the 'unknown' portion of the crude oil to the C₉₀₊ fraction.

4.7 References

- Standard ASTM D2892-90, 1990, Test Method for Distillation of Crude Petroleum (15- Theoretical Plate Column), Annual Book of ASTM Standards, 500-530.
- L.E. Green, L.J. Schmauch, and J.C. Worman, 1964, Simulated distillation by gas chromatography, *Analytical Chemistry*, 36(8): 1512-1516.
- Standard ASTM D2887-89, 1989, Test Method for Boiling Range Distribution of Petroleum Fractions by Gas Chromatography, Annual Book of ASTM Standards, 276-283.
- J.C. Worman, and L.E. Green, 1965, Simulated distillation of high-boiling petroleum fractions, *Analytical Chemistry*, 37(12): 1620-21.
- Standard ASTM D5037-92, 1992, Test Method for Determination of Boiling Range Distribution of Crude Petroleum by Gas Chromatography. Annual Book of ASTM Standards.
- M.P. Stadler, M.D. Deo, and F.M. Orr, Jr., 1993, Crude oil characterization using gas chromatography and supercritical fluid chromatography, SPE 25191, Proc. of the Int. Symp. on Oilfield Chemistry, 413-420.
- S. Trestianu, G. Zilioli, A. Sironi, C. Saravalle, and F. Munari, 1985, Automatic simulated distillation of heavy petroleum fractions up to 800°C TBP by capillary gas chromatography - part I: possibilities and limits of the method, *J. of High Resolution Chromatography and Chromatography Communications*, 8: 771-781.

4.8 Appendix - Mathematical Basis of Equations

The lever rule describes the relationship between the mass of two phases and the partitioning of a component between those phases.

$$m_f = m_1 + m_2 \quad (\text{A} - 1)$$

and

$$m_f x_f = m_1 x_1 + m_2 x_2 \quad (\text{A} - 2)$$

where m_f equals the mass of both phases, m_1 and m_2 are the masses of the two final phases, x_f is the fraction of the component of interest in the overall system, and x_1 and x_2 are the fractions of the same component in phases 1 and 2 respectively. Equations 4 and 5 yield:

$$\frac{m_2}{m_1} = \frac{(x_1 - x_f)}{(x_f - x_2)} \quad (\text{A} - 3)$$

Defining phase 1 as the eluted fraction of the injected crude oil sample, and phase 2 as the uneluted fraction, these relationships can be used to calculate the mass fraction of the crude oil sample which does not elute. In this case,

x_f = the internal standard (IS) fraction in the injected sample = W

W = weight IS/(weight IS + weight sample)

x_1 = IS fraction in the eluted portion of the chromatogram

x_2 = IS fraction in the uneluted portion of the chromatogram = 0 (all IS elutes)

Thus the ratio of the uneluted fraction to the eluted fraction is calculated by the following equation:

$$\frac{m_2}{m_1} = \frac{x_1}{x_f} - 1 \quad (\text{A} - 4)$$

Using the above definitions for the portions of the two chromatograms,

$$x_1 = \frac{A_2}{A} \quad (\text{A} - 5)$$

where A_2 is the area of A_{IS} that is due to the presence of the internal standard. This can be calculated as the difference between A_{IS} and the area A_{IS} would have if no internal standard was present. The areas of the chromatogram excluding the internal standard areas can give this information, when combined with the measured area B_{IS} . Assuming that all of the areas in the chromatogram will increase in proportion to the amount of material eluted, the amount of crude oil present in each sample will be proportional to the area of the chromatogram excluding the internal standard area. Thus,

$$A_2 = A_{IS} - B_{IS} R \quad (\text{A} - 6)$$

where R is the ratio given by:

$$R = \frac{A - A_{IS}}{B - B_{IS}} \quad (\text{A} - 7)$$

$$x_1 = \frac{(A_{IS} - B_{IS} R)}{A} \quad (\text{A} - 8)$$

$$\frac{m_2}{m_1} = \frac{(A_{IS} - B_{IS} R)}{(A W)} \quad (\text{A} - 9)$$

Defining Z as the uneluted fraction of the crude oil and internal standard mixture,

$$\frac{m_2}{m_1} = \frac{Z}{(1 - Z)} \quad (\text{A} - 10)$$

$$Z = \frac{m_2}{(m_1 + m_2)} \quad (\text{A} - 11)$$

Where, $Z \equiv$ uneluted fraction/(uneluted + eluted + internal standard).

Defining U as

$U \equiv \text{uneluted}/(\text{eluted} + \text{uneluted})$

$$U = \frac{Z}{(1-W)} = \frac{(m_2/m_1)}{(1 + m_2/m_1)(1-W)} \quad (\text{A} - 12)$$

Substituting for m_2/m_1 and simplifying,

$$U = \frac{A_{IS} - B_{IS} R - A W}{(A_{IS} - B_{IS} R)(1-W)} \quad (\text{A} - 13)$$

Recalling that U is the uneluted fraction of the crude oil.
Noting that:

$$A = A_1 + A_{IS} + A_3 \quad (\text{A} - 14)$$

$$U = \frac{A_{IS} - B_{IS} R - (A_1 + A_{IS} + A_3) W}{(A_{IS} - B_{IS} R)(1-W)} \quad (\text{A} - 15)$$

However, $A_1 = B_1 R$ and $A_3 = B_3 R$.

Thus,

$$U = \frac{A_{IS} - B_{IS} R - (B_1 R + A_{IS} + B_3 R) W}{(A_{IS} - B_{IS} R)(1-W)} \quad (\text{A} - 16)$$

Adding and subtracting $B_{IS} R$ to the last term in the numerator,

$$U = \frac{A_{IS} - B_{IS} R - (B_{IS} R - B_{IS} R + B_1 R + A_{IS} + B_3 R) W}{(A_{IS} - B_{IS} R)(1-W)} \quad (\text{A} - 17)$$

Observing that:

$$B = B_1 + B_{IS} + B_3 \quad (\text{A} - 18)$$

$$U = \frac{A_{IS} - B_{IS} R - (B R + A_{IS} - B_{IS} R) W}{(A_{IS} - B_{IS} R)(1-W)} \quad (\text{A} - 19)$$

Rearranging the numerator:

$$U = \frac{(A_{IS} - B_{IS} R)(1-W) - B R W}{(A_{IS} - B_{IS} R)(1-W)} \quad (\text{A} - 20)$$

Further rearrangement yields:

$$U = \frac{\left(\frac{A_{IS}}{R} - B_{IS}\right) - B \left(\frac{W}{1-W}\right)}{\left(\frac{A_{IS}}{R} - B_{IS}\right)} \quad (\text{A} - 21)$$

$$U = 1 - \frac{B}{\left(\frac{A_{IS}}{R} - B_{IS}\right) \left(\frac{1-W}{W}\right)} \quad (\text{A} - 22)$$

It should be noted that:

$$R = \frac{A - A_{IS}}{B - B_{IS}}$$

The uneluted fraction of the chromatogram (U) is related to the total area of chromatogram (M) by the following relationship.

$$U = 1 - \frac{B}{M} \quad (\text{A} - 23)$$

Comparison of equations 25 and 27 implies that the total area of the chromatogram is given by:

$$M = \left(A_{IS} \frac{B - B_{IS}}{A - A_{IS}} - B_{IS} \right) \frac{1 - W}{W} \quad (\text{A} - 24)$$

This expression for the total area of the chromatogram is identical to the one published by Worman and Green (1964) and prescribed in ASTM 5037. Thus a logical explanation to the calculation of the total area of the chromatogram has been established.

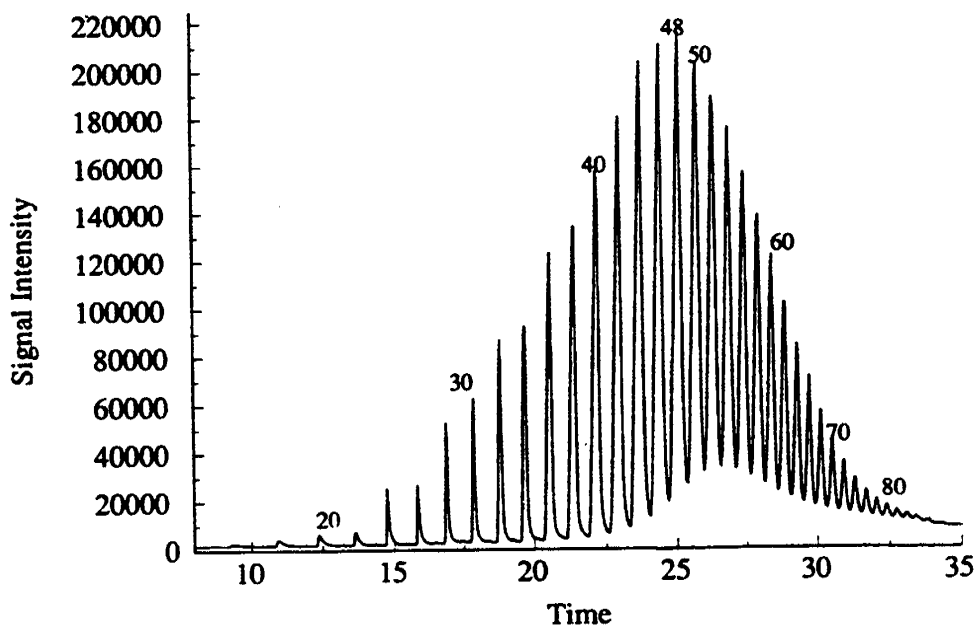


Figure 4.1: Chromatogram of Polywax 655 on Supelco EX-2887, 5 meter \times 0.53 mm glass capillary column with 0.1 micron film thickness.

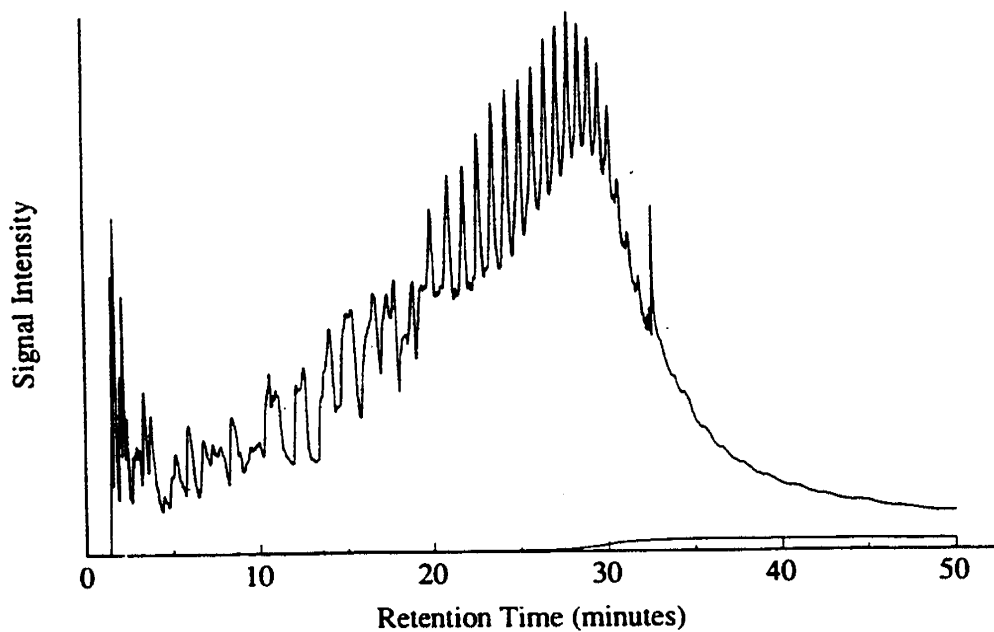


Figure 4.2: Chromatogram of the crude oil sample from well 10-35 in the Monument Butte Unit. The sample was analyzed on J & W Scientific DB-1, 30 meter \times 0.25 mm O.D., glass capillary column, with a 0.25 micron film thickness.

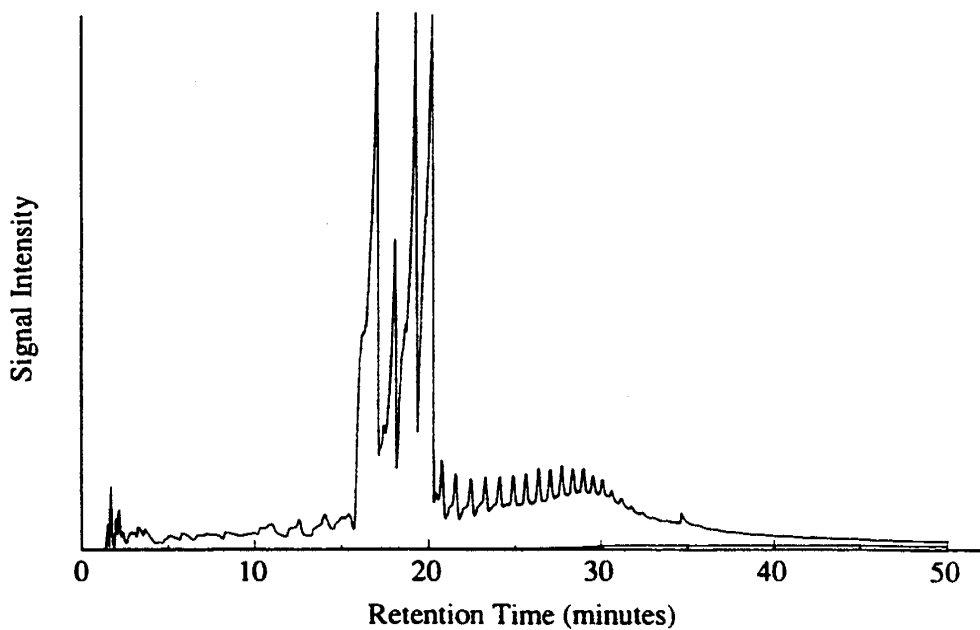


Figure 4.3: Chromatogram of the crude oil (from well 10-35 in the Monument Butte Unit) plus internal standard, obtained on J & W Scientific DB-1, 30 meter x 0.25 mm O.D., glass capillary column, with a 0.25 micron film thickness.

$$A = A_1 + A_{IS} + A_3 \quad B = B_1 + B_{IS} + B_3$$

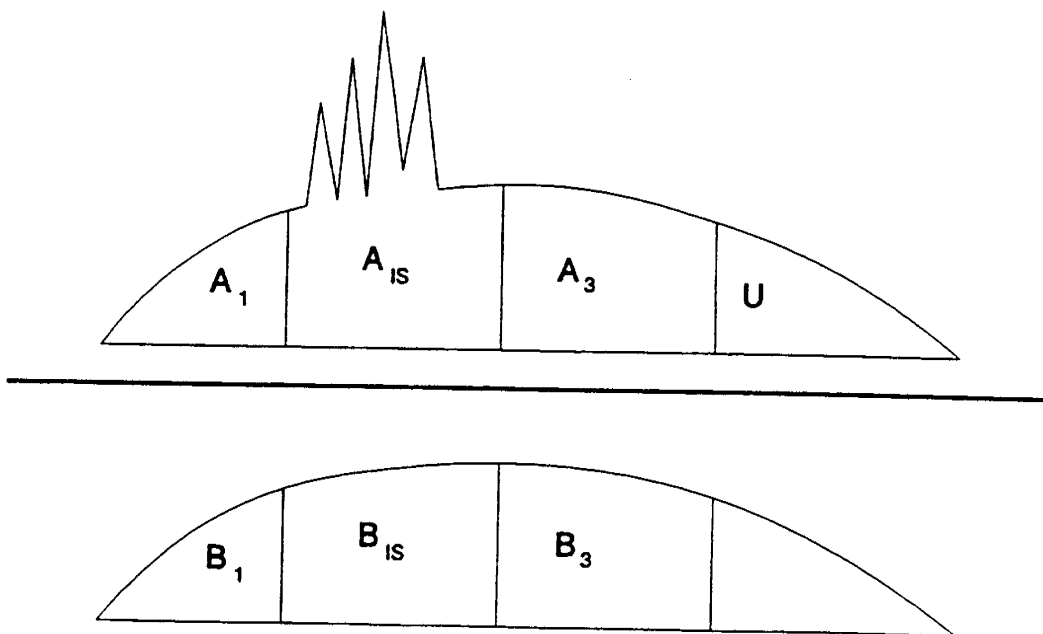


Figure 4.4: A schematic illustrating the areas of chromatograms used in the simulated distillation calculations.

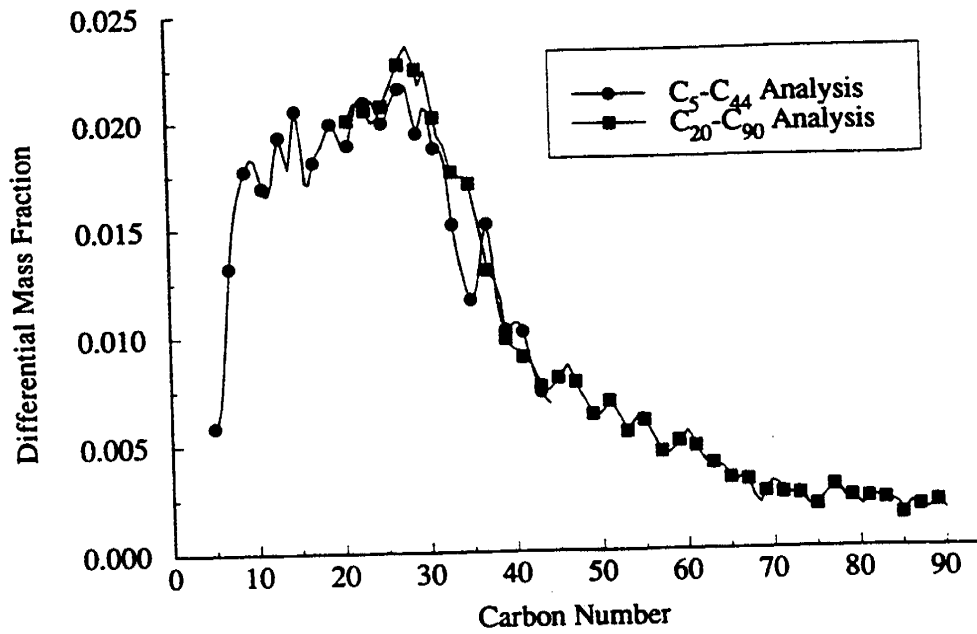


Figure 4.5: Carbon number distributions of the oil from well 10-35 (Monument Butte Unit); both the long and the short column analyses have been shown.

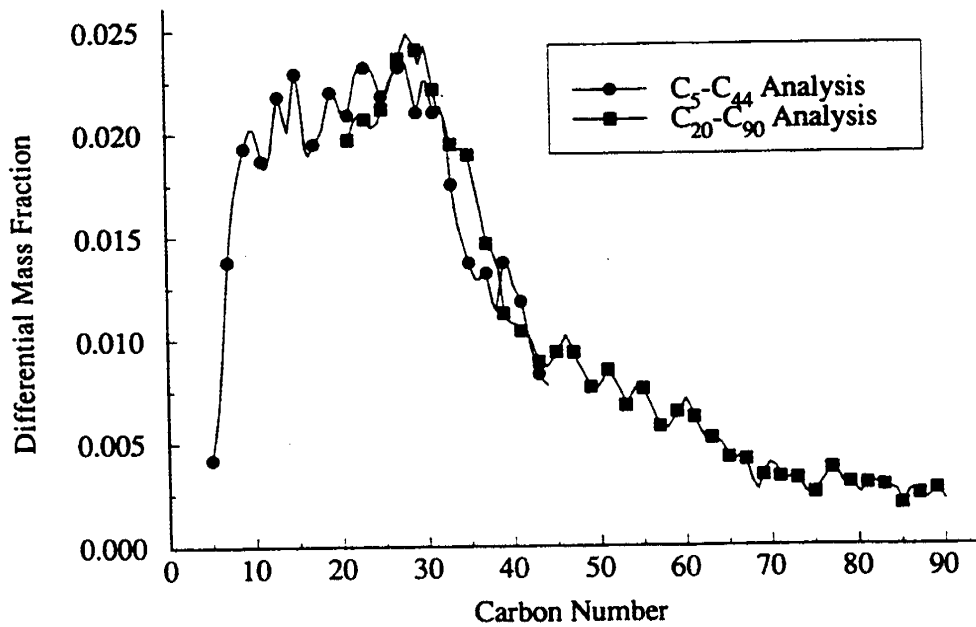


Figure 4.6: Carbon number distributions of the oil from well 12-35 (Monument Butte Unit); both the long and the short column analyses have been shown.

Chapter 5

Volumetric Calculations

5.1 Monument Butte Unit

The original oil in place (OOIP) can be projected using the available gas and oil production data if the thermodynamic properties of the oil are established. The oil produced in stock tank barrels (N_p) and the original oil in place (N) are related by the following equation if the water and formation compressibilities are neglected and if there is no initial gas cap in the reservoir. Since most of the primary depletion occurs below the fluid bubble point, it is reasonable to neglect fluid and reservoir compressibilities in this study.

$$\frac{N_p}{N} = \frac{(B_o - B_{oi}) + B_g(R_{si} - R_s)}{B_o + B_g(R_p - R_s)}$$

In the above equation, B_{oi} and B_o are the initial and final (at the end of primary production) oil formation factors respectively, R_{si} and R_s are the initial and final solution gas oil ratios (GOR) respectively and R_p the cumulative GOR. B_g is the gas formation volume factor. The initial reservoir pressure in the Monument Butte Unit was just over 2300 psia (the exact number is not known). The initial GOR was about 500 scf/stb corresponding to a measured bubble point pressure of 2275 psia. The PVT properties of the Monument Butte fluids have been measured and used in the reservoir simulation study which was reported earlier. A drawdown to about 1200 psia in primary production (end of August 1987) resulted in the production of 419 Mstb of oil and 1.612 MMMscf of gas for a cumulative GOR of 3847 scf/stb. Relevant thermodynamic properties of the Monument Butte fluids are listed below. Experimental determination of these properties is explained in detail in the Monument Butte Unit Case Study, Chapter 6.

Property	Value
Reservoir Temperature	140°F
Oil API Gravity	34°
Gas Gravity	0.78
B_{oi}	1.26 rb/stb
B_o at 1200 psia	1.15 rb/stb
R_{si}	500 scf/stb

R_s at 1200 psia	276 scf/stb
B_g at 1200 psia	0.0024 rb/scf

Use of the above equation gives an OOIP of 9.6 MMstb for the entire Monument Butte Unit. The primary production fractional recovery is thus, 4.36%. The above approach considers production of oil from all the major sand layers. Reservoir simulation results, reported in the Case Study used the isopach information for only the D and the B sands and arrived at the OOIP by completely independent means. The OOIP by the reservoir simulation approach was also 9.6 MMstb and the average reservoir pressure at the end of the primary was about 1250 psia. The fractional primary recovery determined by reservoir simulation was 4.3%, reasonably close to the recovery calculated by using the overall reservoir engineering approach.

The total free-gas volume can be calculated by using the equation:

$$G_f = NR_{si} - (N - N_p)R_s - N_p R_p$$

The free gas volume divided by the total hydrocarbon volume of the reservoir gives the average free gas saturation in the reservoir. The average free gas saturation at the end of primary was 9.9% by reservoir engineering calculations and is very close to the value of 9.7% predicted by by reservoir simulation (please see the section on Monument Butte Case Study, Chapter 6). Thus the overall reservoir engineering calculations and results of the reservoir simulation are in reasonably close agreement. The reservoir simulation is geologically and physically more sophisticated than the overall reservoir engineering volumetrics.

Monument Butte consists of multiple thin sand layers and gas reinjection may not be practical. However, if 60% of all the gas had been recompressed and reinjected during primary production, the fractional recovery would have been 8.27% or the primary oil production would have been 794 Mstb. Thus, gas reinjection should not be ruled out in managing these reservoirs.

5.2 Travis Unit

In primary (end of December 1990), the Travis Unit, producing predominantly from the Lower Douglas Creek sand, had yielded 245 Mstb of oil and 1.08 MMscf of gas at a cumulative producing GOR of 4408 scf/stb. The overall reservoir engineering calculations for the Travis Unit will depend on the initial reservoir pressure and the initial producing GOR. At the current time, there is some uncertainty concerning these two values. The relevant thermodynamic properties for the Travis fluids are listed below:

Property	Value
Reservoir Temperature	152°F
Oil API Gravity	33°
Gas Gravity	0.79
B_{oi}	1.28 rb/stb

B_o at 1250 psia	1.1 rb/stb
R_{si}	550 scf/stb
R_s at 1250 psia	270 scf/stb
B_g at 1250 psia	0.00215 rb/scf

A higher initial production GOR than the Monument Butte field (550 scf/stb compared to 500 scf/stb) with a depletion down to a pressure of 1250 psia would indicate an OOIP of 5.8 MMstb and a recovery of about 4.22% in primary production. The calculations also show free gas saturations of about 14% at the end of primary production. These values are about 40% higher than the free gas saturation values for the Monument Butte Unit. This, coupled with the presence of thicker sands in the Travis Unit may explain a slower than expected response to the water flood that has been observed to date. Once again, if half of the produced gas (0.542 Bcf) had been recompressed and reinjected into the reservoir, the primary recovery would have been 8.05% of OOIP or about 467,000 stb.

The overall reservoir engineering studies are useful in reassessing important mechanisms in reservoirs and to obtain an overall perspective on their performance. Detailed Travis Unit Case Study is Chapter 7 of this report.

5.3 Nomenclature

- B_g Gas formation volume factor (rb/scf)
- B_{oi} Initial oil formation volume factor (rb/stb)
- B_o Oil formation volume factor at any pressure (rb/stb)
- G_f Free gas volume (scf)
- N Original oil in place (stb)
- N_p Oil produced at any time (stb)
- R_{si} Initial solution gas oil ratio (scf/stb)

Chapter 6

Monument Butte Unit: Case Study

6.1 Introduction

The history of the Monument Butte field indicated that the water flood was very successful in the field. In order to match the 12-year field history and to provide reliable predictions for the future, a reasonably accurate knowledge of two basic aspects of the system was required:

1. Reservoir geology; thicknesses of the relevant pay zones, porosities, permeabilities and fluid saturations.
2. Thermodynamic properties of the reservoir fluids; bubble points, gas oil ratios (GOR), oil formation volume factors, etc. and rock-fluid properties or relative permeabilities.

The isopach data developed in the geologic characterization of the Monument Butte Unit were used as guidelines when assigning thicknesses to individual grid blocks. The thicknesses in the blocks containing wells were adjusted to reflect perforated intervals. While other relatively thin sands exist in the reservoir, only the D and the B sands were represented. Bubble points, GORs and oil formation volume factors, were predicted using correlations developed by Glaso (1980) and were also confirmed by experiment. The simulations were initially performed with measured relative permeability curves. These were later adjusted to curves with less curvature to obtain appropriate response to the water flood. A parallel planning approach proposed by Saleri (1993) was used. Initial reservoir simulations were performed with available data. As new data became available, the models were updated to reflect that information. The results presented in this report are from one of several models that were developed. Results of a slightly different model, which uses only the isopach information and relies more on local permeability adjustment than on porosity and thickness modifications is presented in **SPE 27749**, a paper on Monument Butte case study, presented at the Improved Oil Recovery Symposium of the the Society Petroleum Engineers and the U.S. Department of Energy. New models, with better resolution and with expanded boundaries are currently being developed.

The overall performance of the simulations in being able to match the field results was fairly satisfactory. The overall cumulative oil and gas production values predicted by the simulations were within 10% of the field results. The individual well production simulation predictions were within 15-20% of the actual well productions. The agreement between

the field results and the simulation predictions was considered reasonable since a number of factors applicable to the field were not considered in the simulations. The geologic model, for instance, was not tuned to incorporate local heterogeneities. The initial fractures initiated around the wellbore were not specifically considered; however their effect on increasing the overall reservoir permeability was incorporated. The frequent hot oil treatments used in this unit were not considered. The model was subsequently used to project the production in the next five years.

6.2 Geologic Description

A black oil simulator, IMEX, developed by the Computer Modeling Group (CMG), was used for all of the Monument Butte reservoir simulations. A Cartesian coordinate system was used to describe the Monument Butte unit with a $15 \times 13 \times 3$ grid to represent the reservoir. As indicated earlier, this was one of several multilayer models developed during this study. The total areal dimensions of field were $9240 \text{ ft} \times 7920 \text{ ft}$. The reservoir was modeled using a variable thickness, variable depth option with three layers present. The top layer corresponded to the D-sands, the middle layer to an impermeable zone between the D and the B sands and the third layer to the B-sands. As explained earlier, the thicknesses of the sands were assigned based on the isopach information and the perforated interval data for each well. The porosities and thicknesses were tuned to match individual well field results once the overall field results were matched. A constant reservoir wide permeability of 15 md was used in these simulations. The matrix permeability as measured from the core data is typically of the order of 1-5 md. An overall permeability of 15 md for the of the reservoir was chosen in order to account for the average effect of local fracturing around the well bores. Over the entire reservoir, a base porosity of 0.09 was used, although some of the individual blocks were assigned porosities ranging from 0.05 to 0.135. A uniform oil saturation of 0.76 was assumed for the entire field. Since there was no free gas present in the reservoir initially, the connate water saturation was 0.24. With this reservoir description, the D-sands were determined to contain 6.5 MMstb of original oil in place (OOIP) and the B-sands had 3.1 MMstb of OOIP for a total of 9.6 MMstb of OOIP in the entire Monument Butte unit (D and B sands). This estimate of the OOIP for the unit is in close agreement with the estimates developed by Lomax Exploration by independent means.

6.3 Reservoir Fluid Properties

Oil and gas samples were collected from several producing wells in the Monument Butte unit. The characterization of reservoir fluid properties consisted of the following measurements and calculations:

1. Compositional analyses of the oil and the gas samples.
2. Measurement of the bulk properties of the oils; API gravities and viscosities at the surface conditions.

3. Prediction of bubble points and oil formation volume factors at different gas oil ratios using the oil and gas gravities.
4. Measurements of bubble points and oil formation volume factors at different gas oil ratios.

6.3.1 Compositional Analyses

Oil samples from three wells 10-35, 8-35 and 12-35 were analyzed by simulated distillation (SIMDIS) on a capillary gas chromatographic column. A Hewlett-Packard Model 5890 Series II Gas Chromatograph with on-column injection was used for these analyses. A flame ionization detector was used to detect the material that eluted from the column with the detector signal stored on a microcomputer. The carbon number distribution of the samples were determined using two SIMDIS computer programs; one that utilized the inverse lever-arm rule and another described by Worman and Green (1965). The mathematical equivalence between the two techniques was also established (Neer and Deo, 1994). The determination of compositions of oils that display a wide carbon number distribution is challenging, particularly if the oils are waxy and difficult to inject, like the oils from the Monument Butte Unit. The compositional analysis became a special part of this project and resulted in a paper that has been accepted for publication in the *Journal of Chromatographic Science*.

The compositional measurements for carbon numbers up to C₄₄ were obtained using a J and W Scientific DB-1, 30 m × 0.25 mm ID glass capillary column, with a 0.25 μM film thickness. The initial oven temperature was 40°C and was held at this value for 4.5 minutes. The temperature was then increased to of 350°C at a constant rate of 12°C/minute. The temperature was held at this final value for 20 minutes. The injector temperature was programmed to track the column temperature, while the injector pressure was held at 139 kPa.

The carbon number distributions of the three samples are presented in Figure 6.1¹. It should be observed that there is little variation in the compositions of the three samples suggesting that the oils belong to the same reservoir source. In all of the samples approximately 70% of the material elutes from the column indicating that about 30% of the oil consists of fractions boiling above 1000°F. The oil produced from 10-35 is slightly heavier than the oil produced from 12-35. Well 10-35 is producing oil from both the D- and the B-sands while only oil from D-sands is being produced from 12-35. This suggests that the oil from the B-sands is heavier than the oil from the D-sands. Well 8-35 is open in four sands and is in the middle of the curves.

Chromatograms of the oil samples from the three wells (a sample chromatogram is presented in the report, *Near Wellbore Effects*) obtained using on-column capillary chromatography clearly showed the peaks of significant alkanes. The paraffin content of the oil is defined as the concentration of C₁₈+ alkanes, even though it should be recognized that the concentration of compounds that do precipitate in the near wellbore region necessarily differs from this definition. The definition is useful as an index to assess the susceptibility of compound precipitation from the oil. Based on this definition, the paraffin content of the oil

¹Tables and Figures are at the end of the Chapter

was determined to be 9.63%. The implications of the presence of paraffins in oil is discussed in Chapter 8, *Near Wellbore Effects*.

Gas analyses were performed using a Hewlett Packard 5890 Series II gas chromatograph. A Supelco MR 26837, 6 ft long, 0.125 in OD packed column was used for the analyses. The injector temperature was 150°C and the detector temperature was kept at 250°C. The oven initial temperature was 40°C. The oven was held at the initial temperature for 0.5 minutes and was programmed at a rate of 15°C/min to a final temperature of 200°C. The compositions of gases from different wells did not have significant variations. The compositions of gases from wells 10-35 and 12-35 are presented in Table 6.1. The gases appear to have compositions typical of gases from an undersaturated reservoirs.

6.3.2 Measurement of Bulk Properties

For reproducible measurements of API gravities and viscosities the oils were filtered using cloth filters. Small amounts of water and particulates in the oils make significant difference in measured values of API gravities and viscosities.

The API gravities of the oils at room temperature were measured using a pycnometer. The waxy nature of the crudes created special difficulties in accurate and reliable measurements of API gravities. The pycnometer used was a nominal 25 cc volumetric container. The actual volume of the pycnometer was determined at 22°C. The pycnometer was weighed, filled carefully with oil and allowed to equilibrate at room temperature after carefully removing air bubbles. The vessel was then reweighed and the specific gravity calculated. The API gravities of all of the three oils from the Monument Butte unit were about 34 °API (specific gravity 0.86).

The oil viscosities at the reservoir temperature of 140°F were measured using a Brookfield cone and plate viscometer, model LVT. Spindle CP-41 (3° cone) requiring 2 ml of sample was employed. The RPM of the apparatus was adjusted to obtain a torque in the appropriate range. For most measurements, the RPM was 12. The viscosity of the oil from well 10-35 was found to be 13.6 cp. Viscosities at a few other temperatures are tabulated in Table 6.2. The temperature at which the slope of the viscosity versus temperature curve changes is interpreted as the cloud point. The cloud point of the sample based on the data in Table 6.2 was 122°F. Pour points of the oils from the three wells were also determined. The pour points were considerably lower than the cloud point and were in the 95-100°F range. The oil viscosities under reservoir conditions were adjusted for the presence of solution gas using established correlations (McCain, 1989). The bulk properties of the fluids from the Monument Butte Unit are summarized in Table 6.3.

6.3.3 Prediction of Thermodynamic Properties

API gravities, gas gravities and gas oil ratios can be used to calculate the oil bubble points and formation volume factors. General correlations developed by Glaso (1980) were employed for this purpose.

The oil bubble point at the reservoir conditions was calculated using the following two correlations:

$$\log p_b = 1.7669 + 1.7447 \times \log p_b^* - 0.30218 \times (\log p_b^*)^2$$

where,

$$p_b^* = \left(\frac{R}{\gamma_g} \right)^{0.816} \times \frac{T^{0.172}}{\gamma_{API}^{0.989}}$$

In the above equations, p_b is the bubble point (saturation) pressure in psia, R is the producing gas oil ratio in scf/stb, γ_g is the average specific gravity of the total surface gases, T is the reservoir temperature in °F and γ_{API} is the stock tank API gravity of the oil. The term p_b^* is a mathematical intermediate used in the calculations.

The formation volume factor is also calculated using similar correlations.

$$\log (B_{ob} - 1) = -6.58511 + 2.991329 \times \log B_{ob}^* - 0.27683 \times (\log B_{ob}^*)^2$$

where,

$$B_{ob}^* = R \left(\frac{\gamma_g}{\gamma_o} \right)^{0.526} + 0.968 \times T$$

In addition to the symbols described for the previous equations, γ_o is the specific gravity of the stock tank oil, B_{ob} is the oil formation volume factor in RB/stb, and B_{ob}^* is a mathematical intermediate.

The oil bubble points and formation volume factors at increasing gas oil ratios are presented in Figures 6.2 and 6.3 as functions of oil and gas gravities. It is believed that the initial GOR for the Monument Butte field was about 500 scf/stb. At this GOR, for the measured API gravity of 35 and a gas gravity of 0.75, the bubble point at the reservoir temperature is predicted to be 2250 psia and the oil formation volume factor is calculated to be 1.27 RB/stb.

6.3.4 Measurement of Thermodynamic Properties

The thermodynamic property measurements were undertaken in the newly constructed mercury-free PVT system. A detailed schematic of the PVT system is presented in Figure 6.4. For safety and environmental considerations, the system was designed not to use mercury. This made the thermodynamic experiments more involved. Measurement of a single bubble point and an oil formation volume factor consisted of a series of complicated procedures.

All the experiments were conducted at the reservoir temperature of 140°F. The experiments were conducted at a series of GOR's. In order to attain a given GOR, the volume of gas required for a fixed amount of dead oil was calculated. Applying nitrogen pressure at 200 psig, the pistons in the three moving piston vessels (MPVs) were lowered. The PVT cell and the rest of the system was then evacuated and the MPVs were filled with the reservoir gas. Using the real gas law, the amount of gas required at the reservoir temperature and the choice of charging pressure (for a desired GOR) was determined and charged to the PVT cell. The excess gas in the MPVs was transferred back to the original gas container. The PVT cell was then isolated from the system and the MPVs were once again lowered and evacuated for the loading of oil. The required amount of dead oil, plus an additional 20 cc was placed into one of the MPVs. The excess oil was transferred to another MPV as a

backup for any oil that might be needed during the experiment. The required amount of dead oil was transferred to the PVT cell by a high-pressure positive-displacement pump. The mixture of oil and gas was compressed to a pressure well above the expected bubble point. A high-pressure, heated circulating pump was used to thoroughly mix the oil and the gas for the attainment of thermodynamic equilibrium.

The P-V measurements were recorded by lowering the pressure in the PVT cell by small amounts. Below the bubble point, the oil level in the PVT cell at various pressures was also measured. The measured volumes were corrected for the system and hydraulic oil compressibilities. Pressure was plotted against the corrected volume and the inflection point on this plot shows the oil bubble point pressure at that value of GOR. Pressure - volume plots for two different GOR values are presented in Figures 6.5 and 6.6. Essentially the same type of experiments were repeated for several GOR values. The bubble point pressures are indicated in the plot. The volume of dead oil remaining in the PVT cell after each experiment was measured. This volume along with the oil level data in the PVT cell and the P-V data were used to calculate B_{os} (oil formation volume factor).

The experimental thermodynamic measurements were in close agreement with the predictions from Glaso's correlations. The reservoir fluid property information is compiled into an integrated tabular form in Table 6.4. These reservoir fluid property data are used in the given form by the reservoir simulator.

6.3.5 Rock-fluid Properties

Relative permeabilities shown in Figure 6.7 were used for the field history match. The relative permeabilities used were similar to the oil-water relative permeabilities measured in preliminary unsteady state coreflooding experiments. The general purpose PVT/core flooding system shown in Figure 6.4 was used for these experiments. The residual oil saturation used for the history match (0.22) was lower than the value observed experimentally (≈ 0.3). Previous studies have also found lower residual oil saturations, when water flooding is performed in the presence of free gas (Kyte, et al., 1959). The lower value was used to match the quick response to the water flood which was observed in Monument Butte. Despite the use of these relative permeabilities the response to the water flood lagged the field response by a few months. This is discussed in the next section. Over most of the saturation range, the relative permeability to water in the Monument Butte reservoir remains low. In fact, an end-point water relative permeability of 0.07 was used. The relative permeability to oil remained high over most of the operating saturation range.

6.4 Simulation Results

The initial oil saturation in the reservoir, both in the D- and the B-sands was assumed to be 0.76. The initial reservoir pressure in the field was estimated to be between 2200 to 2300 psia. The initial field pressures were not measured and were thus unavailable. The bubble point of the reservoir crude at the initial GOR of about 450-500 scf/stb is around 2250 psia - very close to the initial reservoir pressure. As the first well was placed on production, the reservoir pressure dropped below the bubble point, resulting in the formation of free gas in

the reservoir. Gas being less viscous than oil, was preferentially produced and the production GOR increased. In fact, at the end of primary production, the average gas saturation in the reservoir had increased to about 10%. The average reservoir pressure at the end of the primary was about 1200 psia. This reservoir pressure is not sufficient in sustaining economically viable oil flow rates. It should also be recognized that for an effective water flood, it is necessary to drive the free gas back into solution. The pressure profile in the reservoir at the end of primary production in D-sands is shown in Figure 6.8. The profile shows a more or less uniform depletion over the entire reservoir. The oil saturation contours in D-sands are shown in Figure 6.9. The average saturation in the field at the end of primary had declined to 0.66. The middle of the reservoir showed marked depletion and the oil saturation contours appeared to correspond well with the pressure contours. The most productive wells in primary production were, 5-35, 4-35, 3-35 and 2-35. The cumulative oil production plots comparing the field production with the simulation results for these four wells are presented in Figures 6.10, 6.11, 6.12 and 6.13. The simulations predict the field results within $\pm 15\%$.

The picture gradually changed as water was injected into the reservoir. The water injection profile is shown in Figure 6.14. The simulation matches the actual water injection profile fairly well. By December 1992, 2 MM stb of water had been injected into the reservoir. As the reservoir was pressurized, the production GOR declined to the current values of about 350 scf/stb. The reservoir pressure was well above the bubble point pressure for the producing GOR. Even though there are pockets of free gas at a few locations in the reservoir, the free gas saturation in the reservoir at the current time is negligible. The oil saturation contours in D-sands at the end of the simulation period (December 1992) is presented in Figure 6.15. The average oil saturation at the end of this period had declined to about 60%. As expected, the reservoir shows a wide variation in oil saturation, ranging from 25% in the vicinity of the injectors to 70% in regions away from the injectors. The contours show oil being effectively displaced toward the producers. The effect of the injection in 5-35, the biggest injector is also evident in the figure. Some of the most productive wells in the secondary production phase were 10-35, 12-35, 6-35 and 1-34. The cumulative oil production curves for these wells are presented in Figures 6.16, 6.17, 6.18 and 6.19. The agreement between the simulation results and the field results is reasonably good.

Figure 6.20 shows the comparison of the field cumulative oil production and that predicted by the reservoir simulator. It should be noted that the oil production had leveled off at the end of the primary (Aug. 87). The water flood rejuvenated the oil production. The cumulative oil production at the end of primary was 420,000 stb and about the same amount of oil has been produced since, by water flooding. The simulator does not do a very good job of predicting the quick response to the water flood observed in the field. Selected high-permeability paths or fractures in the vicinity of the injectors maybe responsible for the quick response to the water flood. It is seen that the simulator tracks the field oil production very closely.

The mechanism of water flooding can be clearly understood by examining the instantaneous GOR as a function of time (Figure 6.21). In primary production, we start at a GOR of between 400 to 500 scf/stb. As was observed previously, the reservoir pressure falls below the bubble point pressure within a few days of operation and the instantaneous GOR increases rapidly. As more and more free gas is formed in the reservoir and this gas is preferentially

produced, the production GOR continues to increase, reaching a peak value of about 10,000 scf/stb. As the water injection is begun (Aug. 87), the reservoir is slowly pressurized, gas is driven back into solution and the production GOR declines. Once again, the simulator lags behind the field response to the water flood. It takes more time in the simulation for the GOR's to decline than in the field. This decline continues to the current value of about 350 scf/stb. Since the average reservoir pressure at this time is expected to be higher than the current bubble point, this corresponds almost exclusively to the solution GOR and is not expected to decline further. Matching instantaneous GOR by reservoir simulation is complex since the value depends not only on the thermodynamics of oil and gas but also on the three-phase flow aspects of oil, water and gas. The fact that this is closely matched by simulations indicates that the thermodynamic and three-phase representations adopted in our reservoir simulation have been reasonably accurate.

Figure 6.22 shows that the the cumulative gas production is also closely tracked by the reservoir simulation. The simulator does a poor job of matching the initial increase in gas production, as the reservoir initially declines below the bubble point. It is seen that at the end of primary production, about 1.6 MMM scf of gas is produced at an average production GOR of about 4000 scf/stb. Since the initiation of the water flood, only 0.6 MMM scf of gas is produced at an average GOR of 1400 scf/stb. This is a dramatic illustration of how water injection pressurizes the reservoir, drives the gas back into solution and reduces production GOR's.

The simulator predicts oil rates of around 400 stb/day for injection rates of about 1200 bbl/day by December 1992. The production rates in the field, however, have been around 300 stb/day. The primary reason for this discrepancy is the fact that the fluvial reservoir modeled in this work is a subsystem which is a part of a much larger geologic system. The injected water maybe leaving the boundaries of the unit through sands channeling out of the unit. Other possible reasons for lower than expected oil production rates are:

1. Paraffin deposition in the vicinity of injection and production wells. This is not accounted for in the model.
2. Anisotropy of hydraulic fractures around wells.

Thus, even though the simulator does a reasonably good job of matching the reservoir performance to date, it should be used with caution for future predictions.

Monument Butte reservoir performance in both the primary and secondary stages is a classic illustration of primary depletion and water flooding in an undersaturated reservoir whose initial reservoir pressure is very close to the bubble point of the reservoir.

6.4.1 Extended Predictions

The simulations were extended to the end of year 2000 using the same reservoir representation. Results are tabulated in Table 6.5. The simulations predict that by the end of year 2000, 1.86 MMstb of oil would have been produced from the unit. This amounts to a recovery of 19.2% of the OOIP. Water injection rates currently being used in the unit were continued in these extended simulations. Complications such as wax precipitation in production wells could not specifically be addressed in these simulations. The simulations project that the

water cut would have increased to 72% by the year 2000. If good vertical sweep is realized in this field (if there are no significant higher permeability zones), it is expected that the water flood would recover a total of between 25% - 30% of the OOIP before the unit waters out.

6.5 References

- Glaso, O., 1980, Generalized Pressure-Volume-Temperature Correlations, *J. Pet. Tech.*, Vol. 32, No. 5, 785-795.
- Kyte, J. R., Stanclift, R. J., Jr., Stephen, S.C., Jr. and Rapoport, L. A., 1959, Mechanism of Water Flooding in the presence of Free Gas, Petroleum Transaction Reprint Series, No. 2, *Water Flooding*, Printed by the SPE of AIME, Dallas, Tx, 135-143.
- McCain, W. D. Jr., 1989, The Properties of Petroleum Fluids, Second Edition, Pennwell Books, PennWell Publishing Company, Tulsa, Oklahoma.
- Neer, L. A. and Deo, M. D., 1994, Simulated Distillation of Oils with Wide Carbon Number Distributions, *Journal of Chromatographic Science*, In Press.
- Saleri, N.G., 1993, Reservoir Performance Forecasting: Acceleration by Parallel Planning, *J. Pet. Tech.*, Vol. 45, No. 7, 652-657.
- Worman, J. C. and Green, L. E., 1965: Simulated Distillation of High-Boiling Petroleum Fractions, *Analytical Chemistry*, Vol. 37, No. 12, 1620-21.

Table 6.1: Results of Gas Analyses

Component	Well 10-35	Well 12-35
Methane	71.763	73.437
Ethane	14.951	13.507
Propane	9.967	9.105
Butanes	2.691	2.701
Pentanes	0.379	0.820
Hexanes	0.249	0.430

Table 6.2: Viscosities of Monument Butte Oils

Temperature (°F)	Viscosity (cp)
105	25.1
120	18.0
140	13.6
160	11.5

Table 6.3: Bulk Properties of Monument Butte Fluids

Property	Value
API Gravity	34° API
Gas Gravity	0.77
Residue (fraction) (C ₄₄₊)	0.3
C ₉₀₊ (fraction)	0.08
Paraffin Content	9.6%
Pour point	95°F
Cloud point	122°F

Table 6.4: Reservoir Fluid Thermodynamic Properties Monument Butte Unit

P	R_s	B_o	E_g	μ_o	μ_g
15	0.0	1.000	4.7	14.10	0.0101
500	115	1.063	168.8	12.25	0.0103
1000	230	1.125	350.8	7.25	0.0109
1200	276	1.150	426.6	6.21	0.0112
1500	345	1.188	541.8	5.35	0.0118
2000	450	1.250	851.0	4.14	0.0129
2500	575	1.313	950.0	3.45	0.0139
3000	690	1.375	1140.0	3.11	0.0152
4000	921	1.500	1500.0	2.42	0.0164

P	Pressure, psia
R_s	Solution gas oil ratio, scf/stb
B_o	Oil formation volume factor, rb/stb
E_g	Gas expansion factor, scf/rb
μ_o	Oil viscosity, cp
μ_g	Gas viscosity, cp

Table 6.5: Extended Simulation Predictions

Year (End of)	Cumulative Oil Production (Mstb)	Recovery % OOIP
1993	926	9.56
1994	1060	10.94
1995	1196	12.34
1996	1334	13.77
1997	1471	15.18
1998	1606	16.57
1999	1737	17.93
2000	1861	19.21

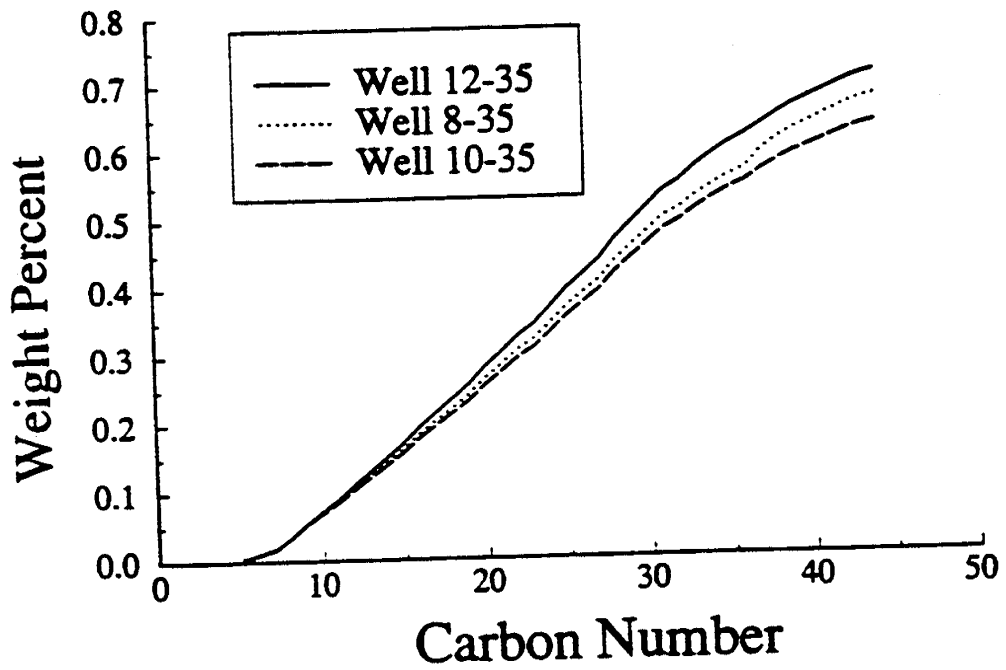


Figure 6.1: Carbon number distributions of oils from three wells in the Monument Butte Unit.

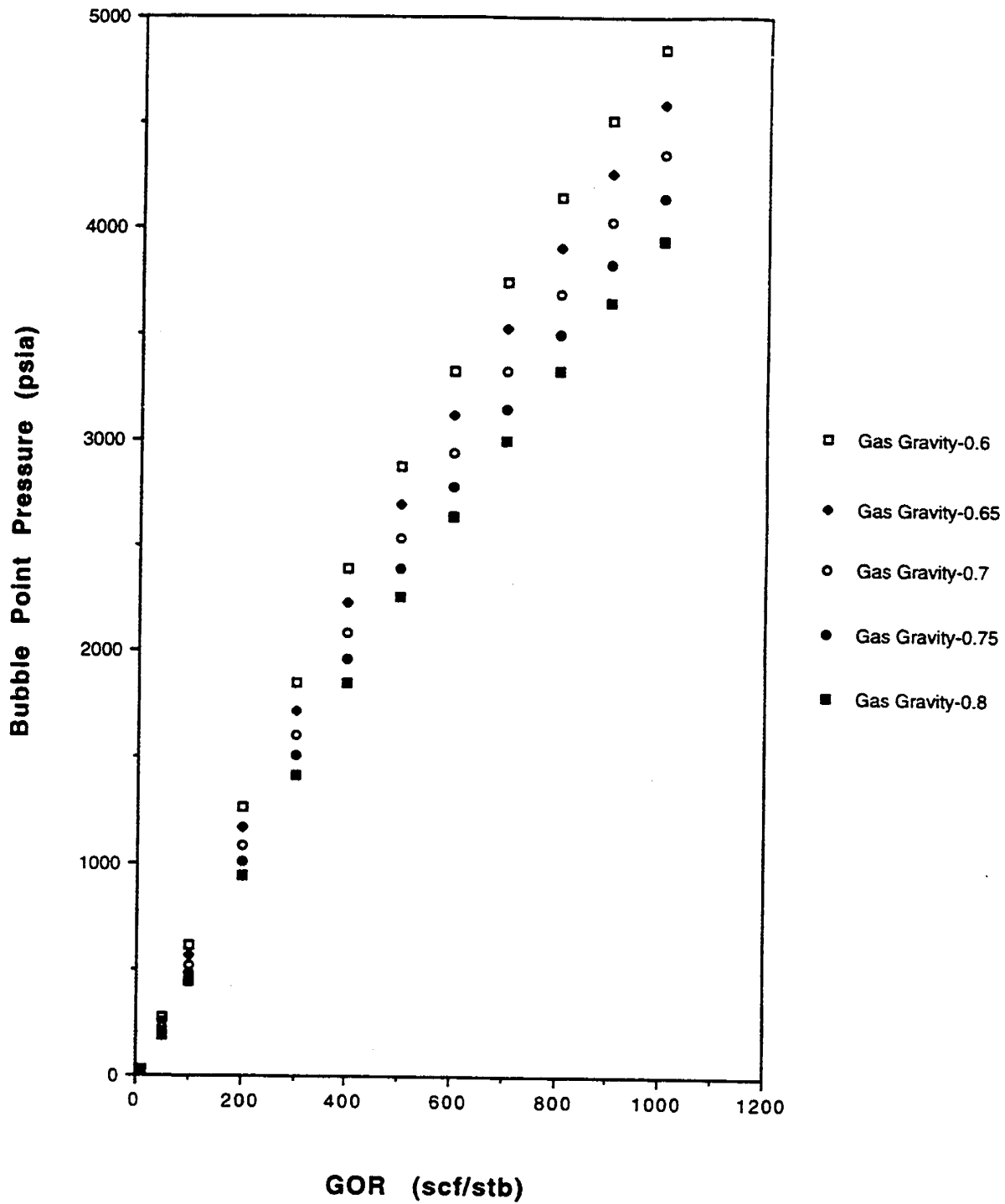


Figure 6.2: Predictions of bubble point versus gas-oil-ratio (GOR) for a 35° API oil at different gas gravities.

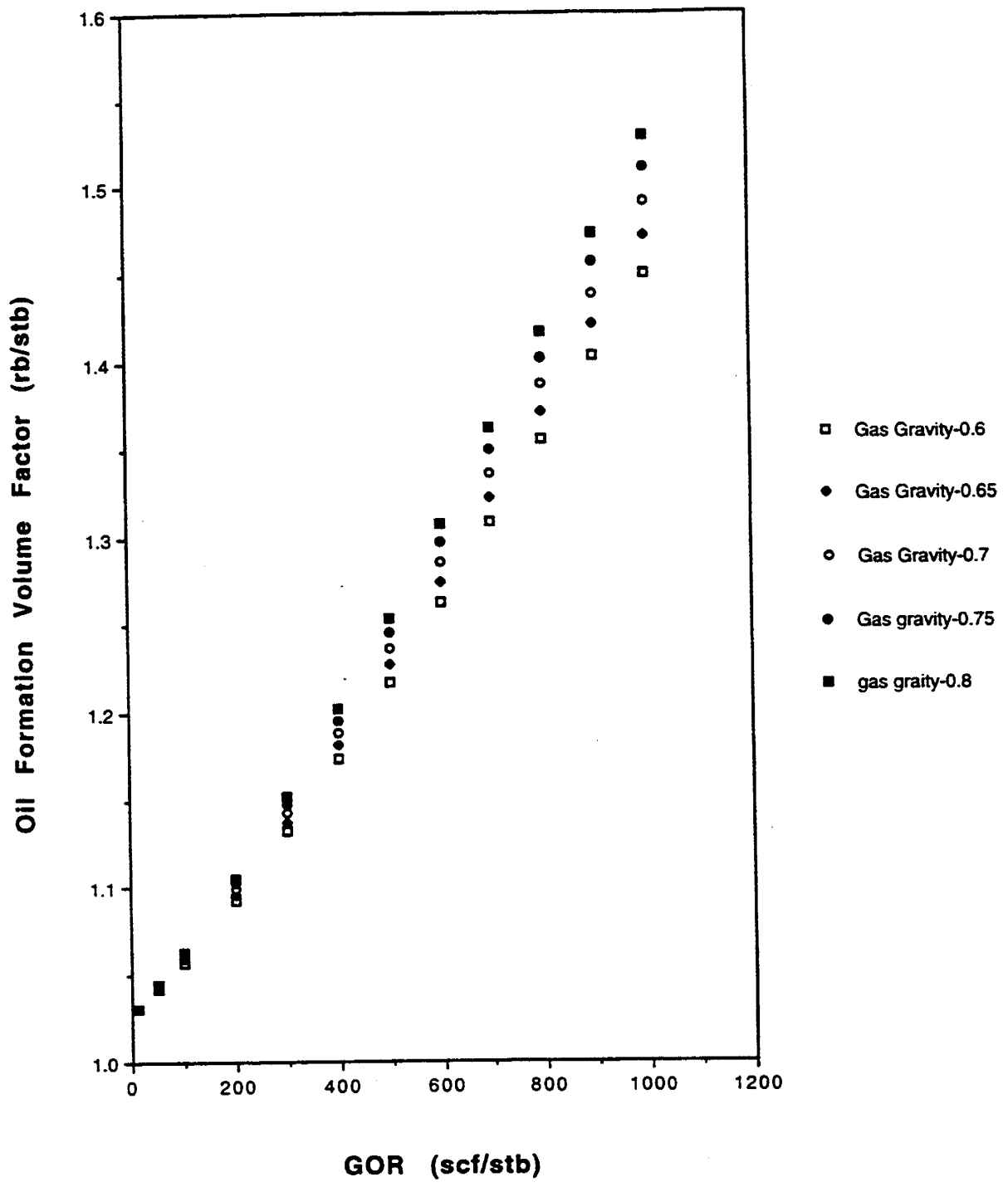


Figure 6.3: Predictions of oil formation volume factor versus gas-oil-ratio (GOR) for a 35° API oil at different gas gravities.

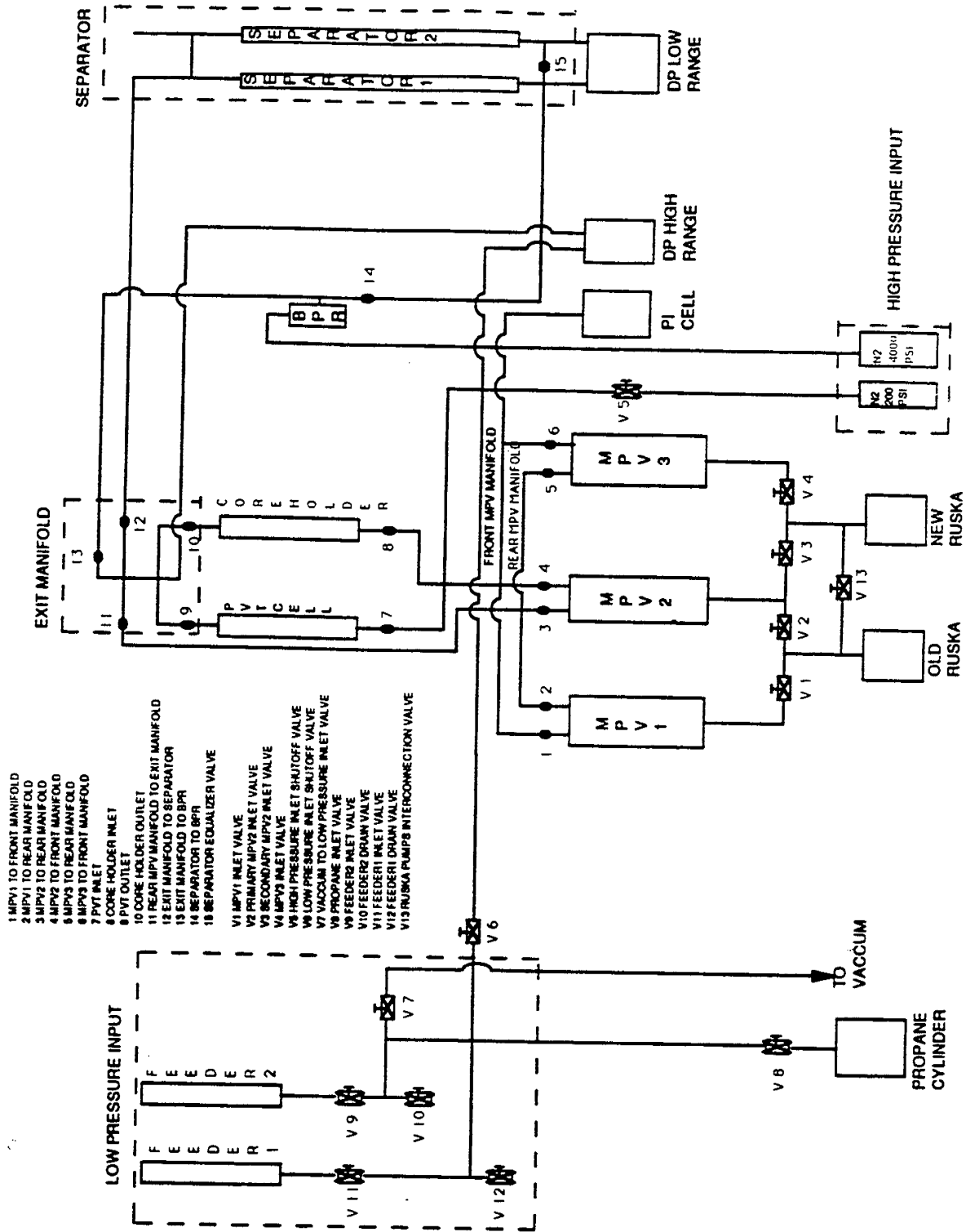


Figure 6.4: Schematic of the pressure-volume-temperature apparatus used for the measurement of thermodynamic properties of reservoir fluids.

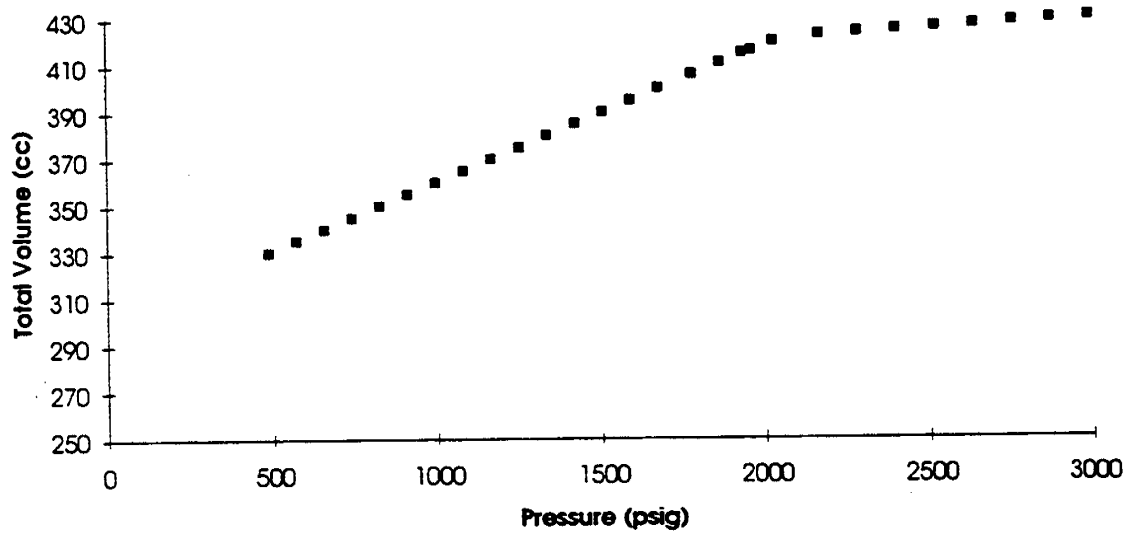


Figure 6.5: Experimental pressure versus volume measurements for the Monument Butte crude with a gas-oil-ratio (GOR) of 418 SCF/STB; the inflection point in the curve at 2120 psia indicates the bubble point.

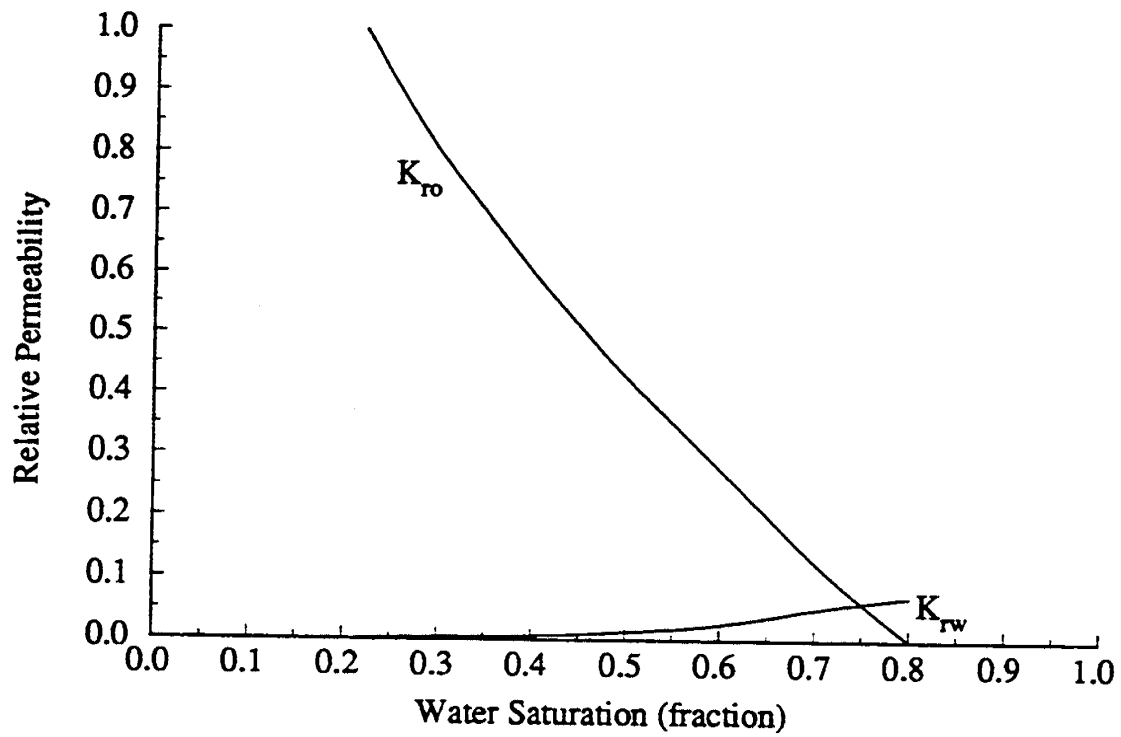


Figure 6.6: Relative permeability curves employed in this simulation study to obtain a satisfactory match with the field results

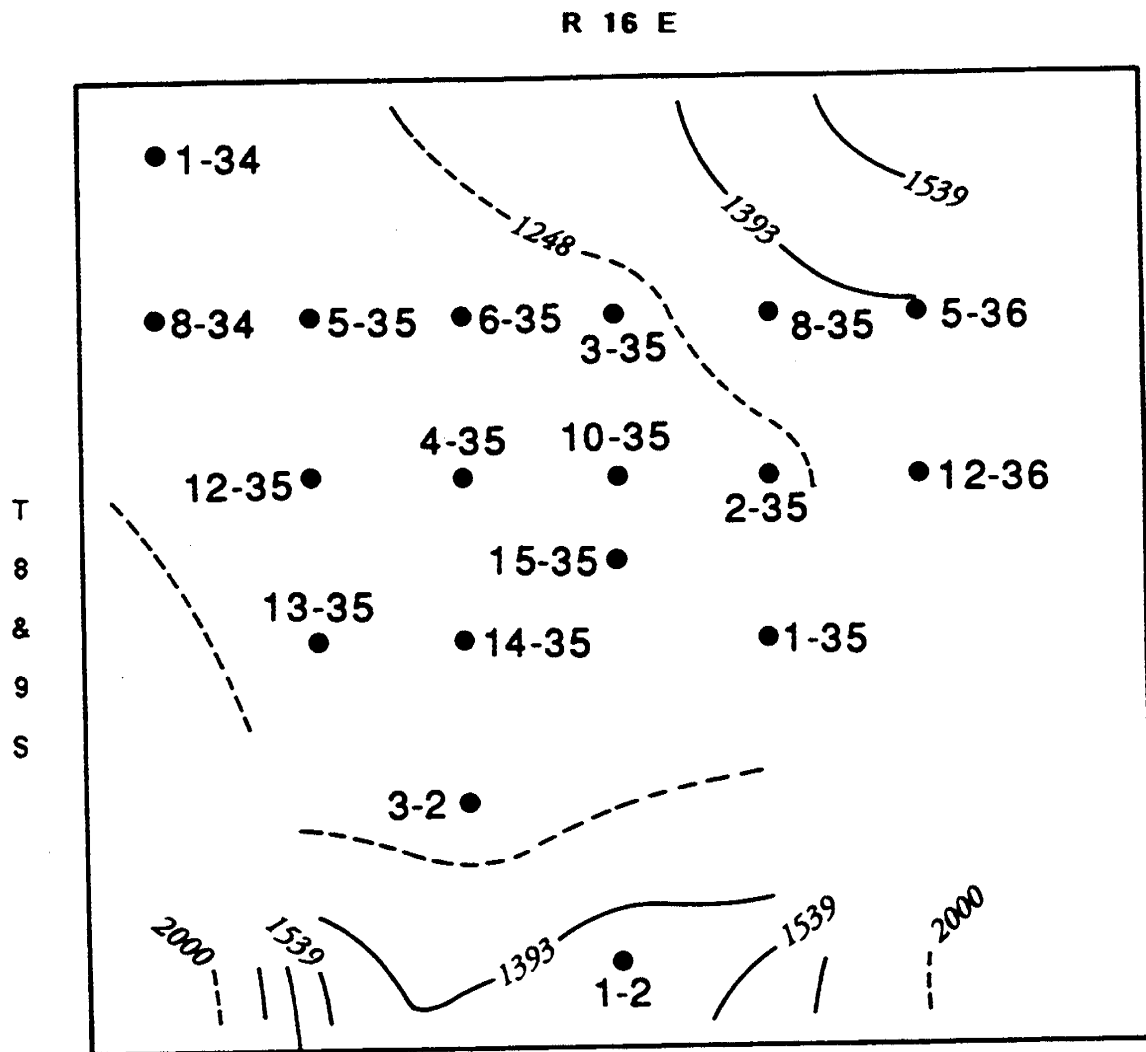


Figure 6.7: Pressure contours in D-sands at the end of primary production (August 1987).

R 16 E

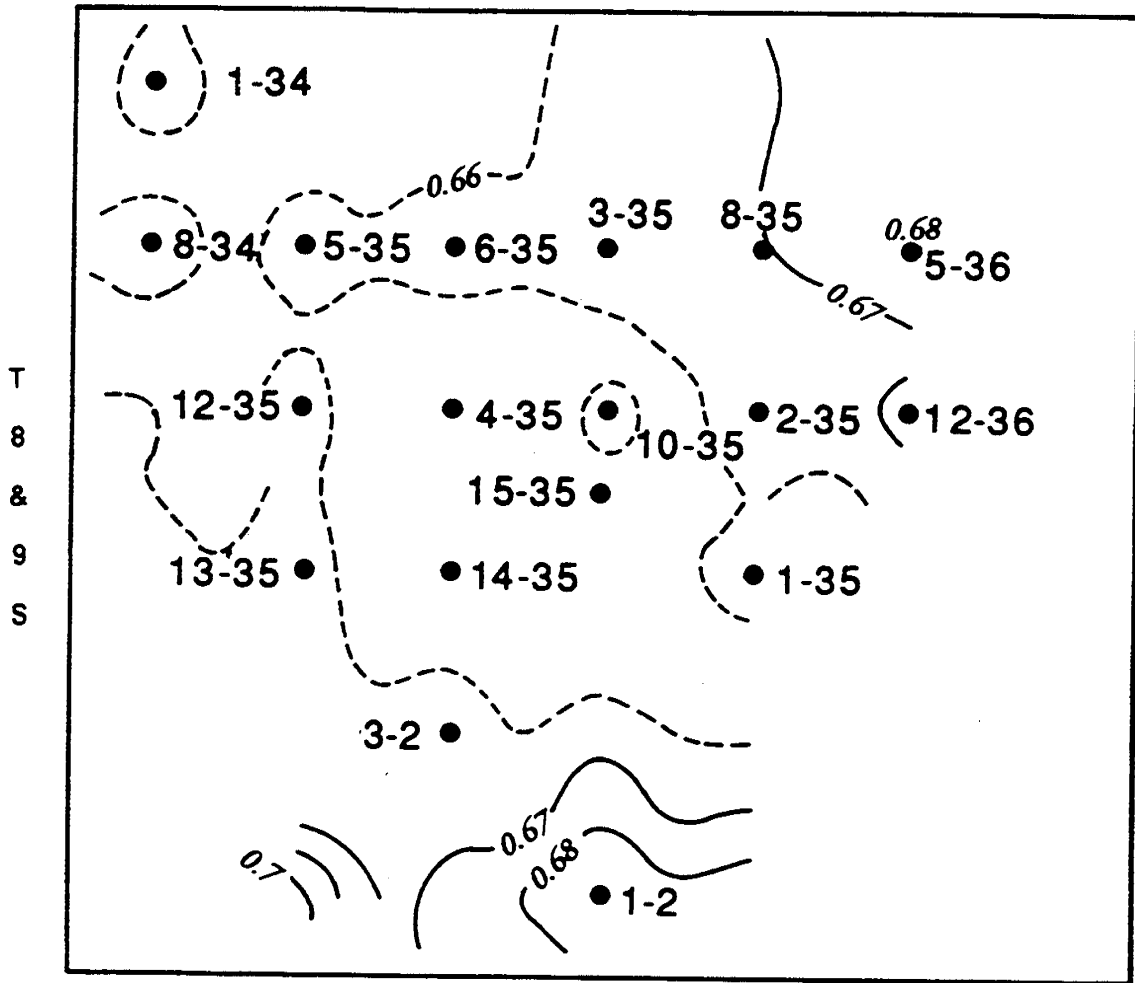


Figure 6.8: Saturation contours in D-sands at the end of primary production (August 1987).

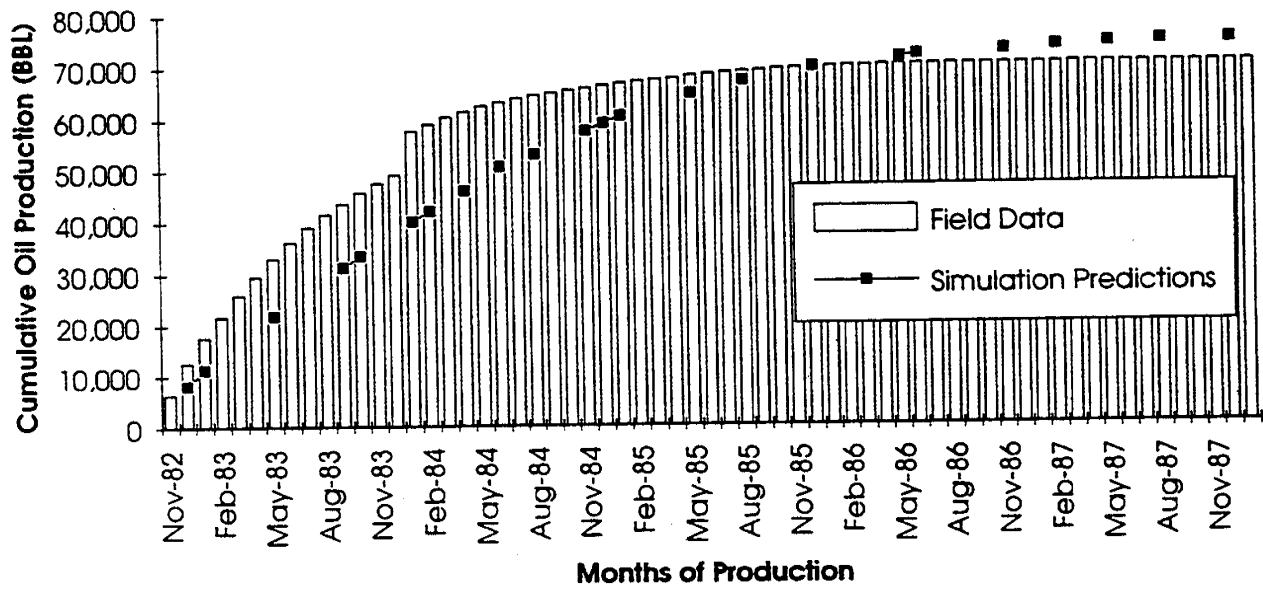


Figure 6.9: Cumulative oil production from Monument Butte well 5-35; comparison of field production with the simulation results.

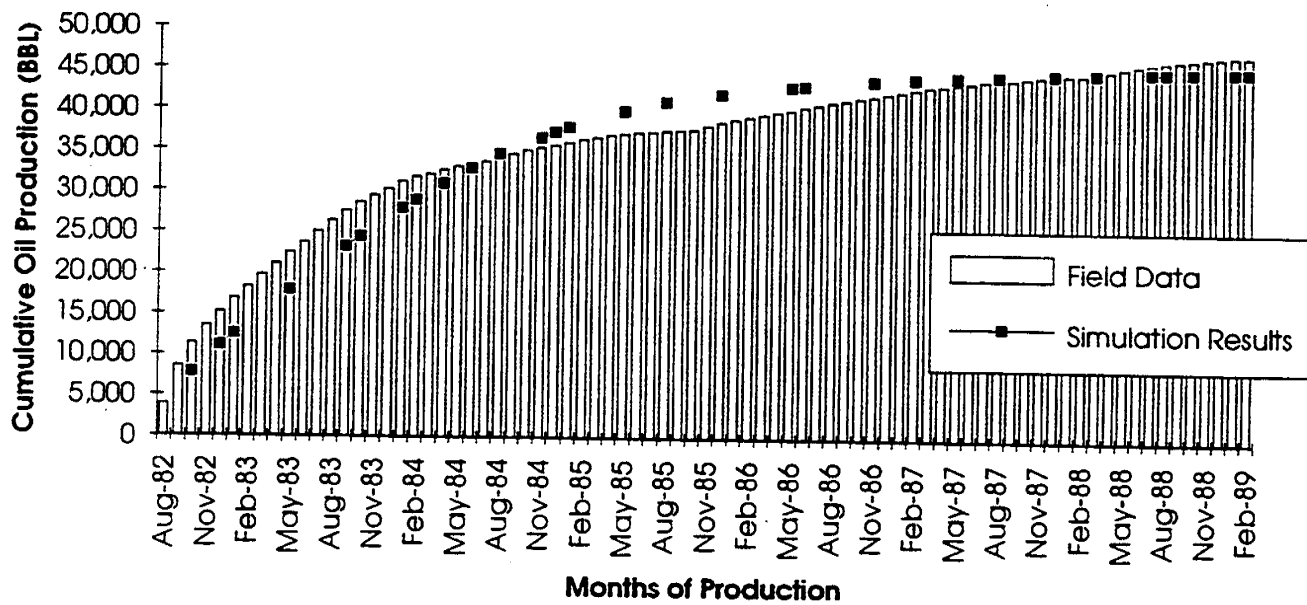


Figure 6.10: Cumulative oil production from Monument Butte well 4-35; comparison of field production with the simulation results.

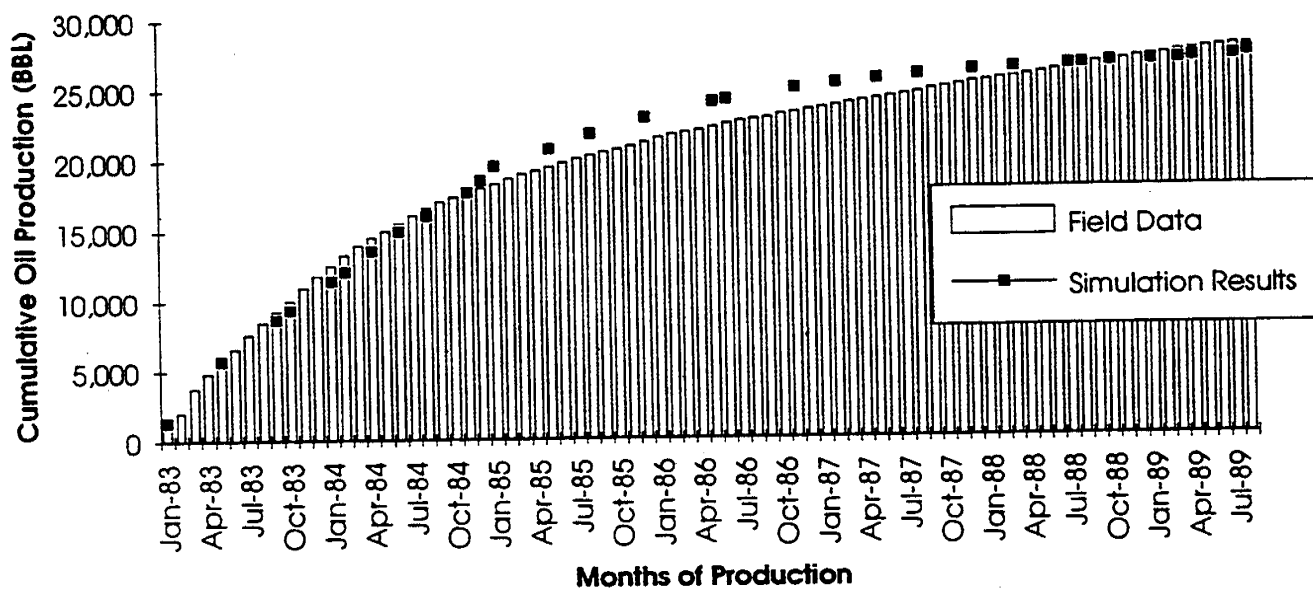


Figure 6.11: Cumulative oil production from Monument Butte well 3-35; comparison of field production with the simulation results.

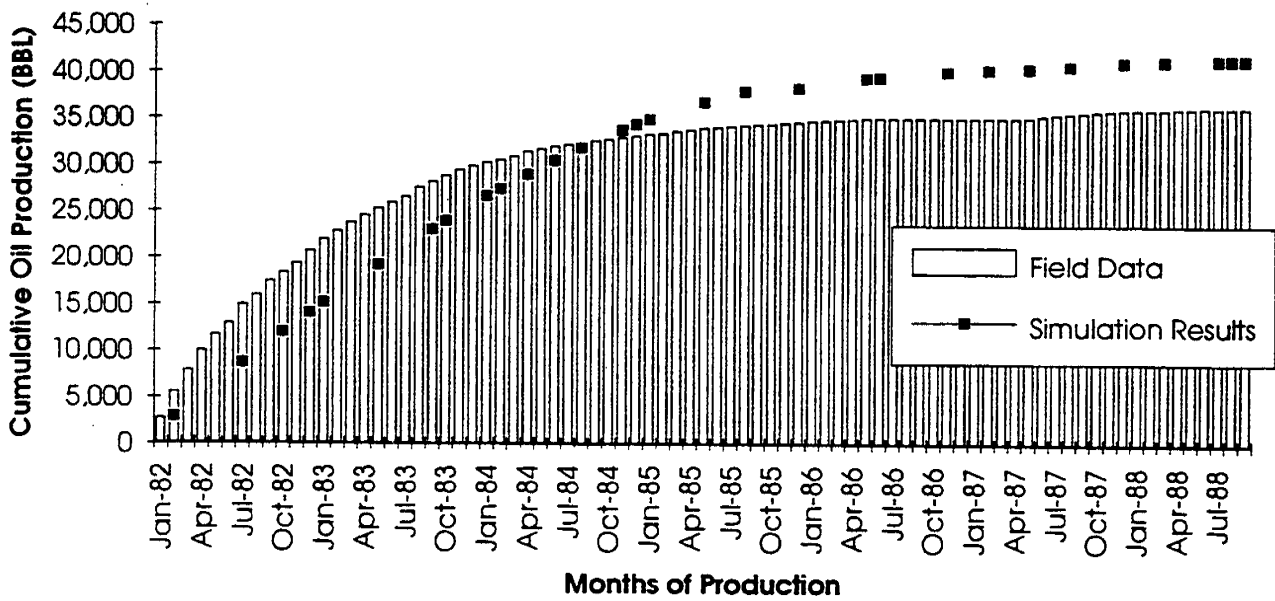


Figure 6.12: Cumulative oil production from Monument Butte well 2-35; comparison of field production with the simulation results.

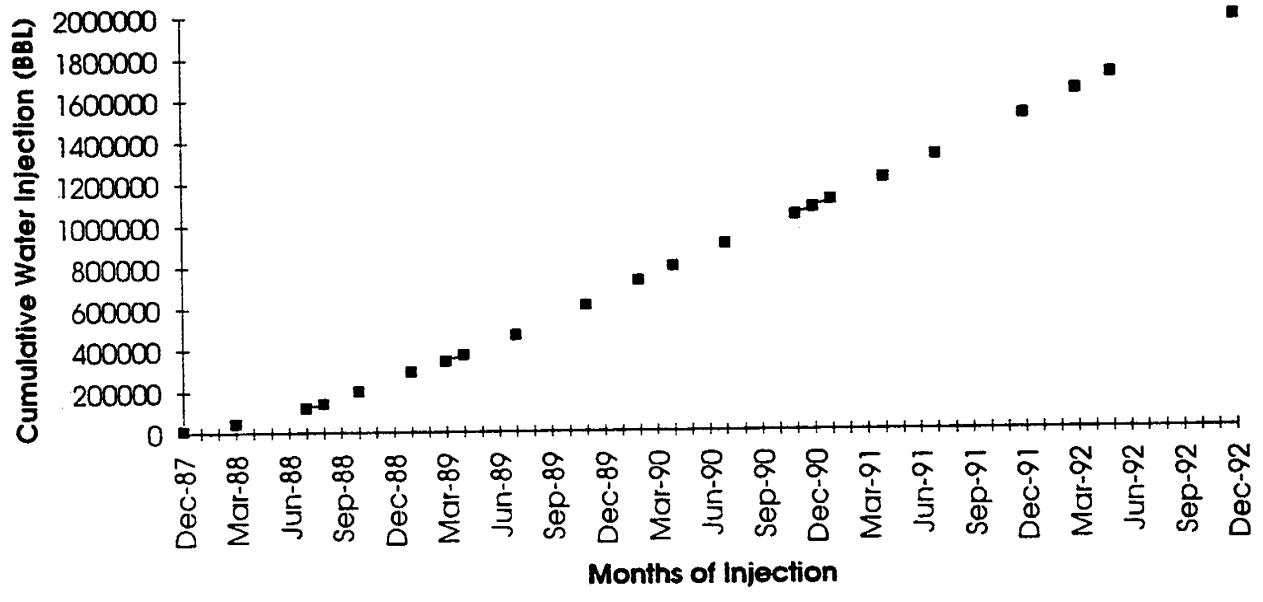


Figure 6.13: Cumulative water injection profile used in the simulation results.

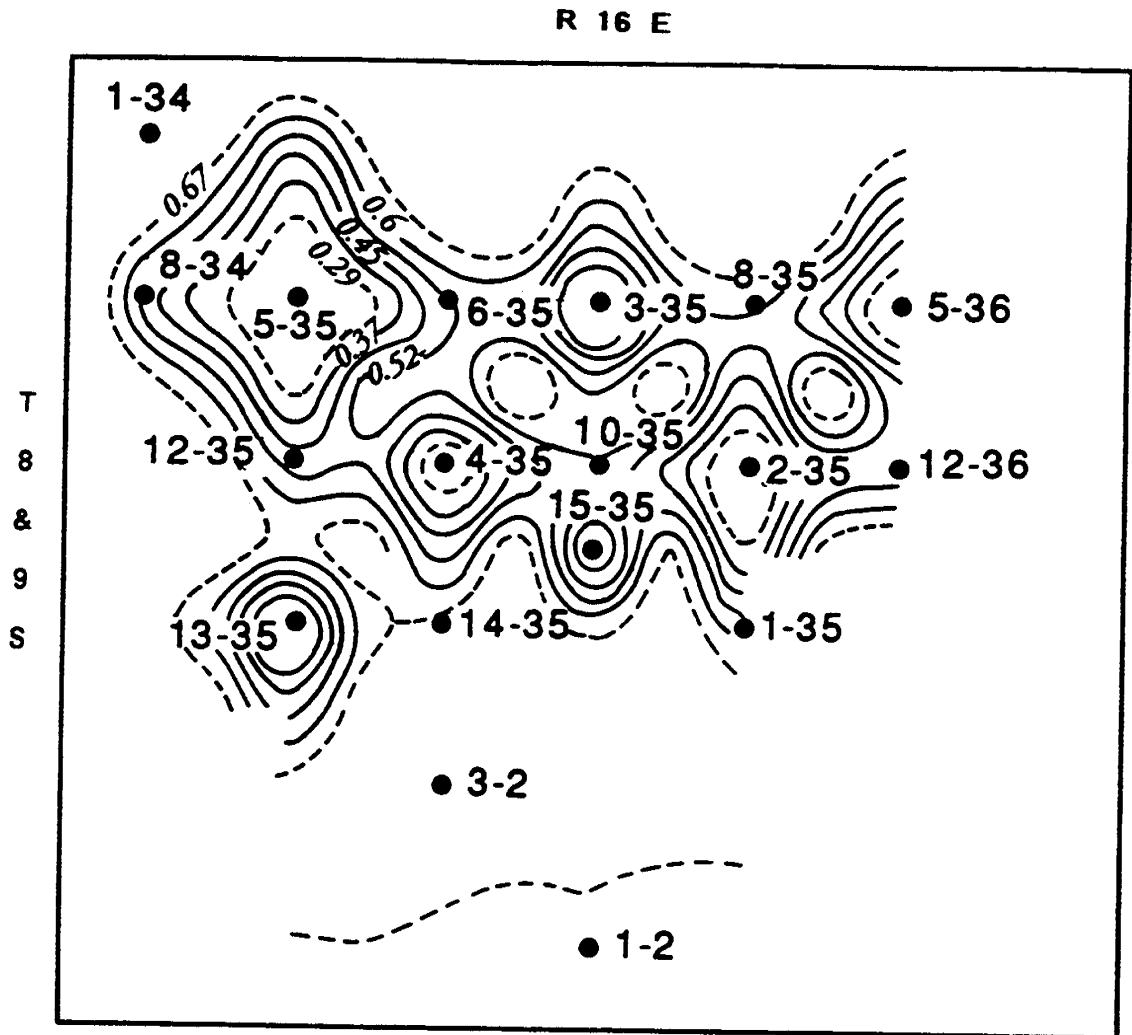


Figure 6.14: Oil saturation contours in D-sands at the end of the simulation period (December 1992).

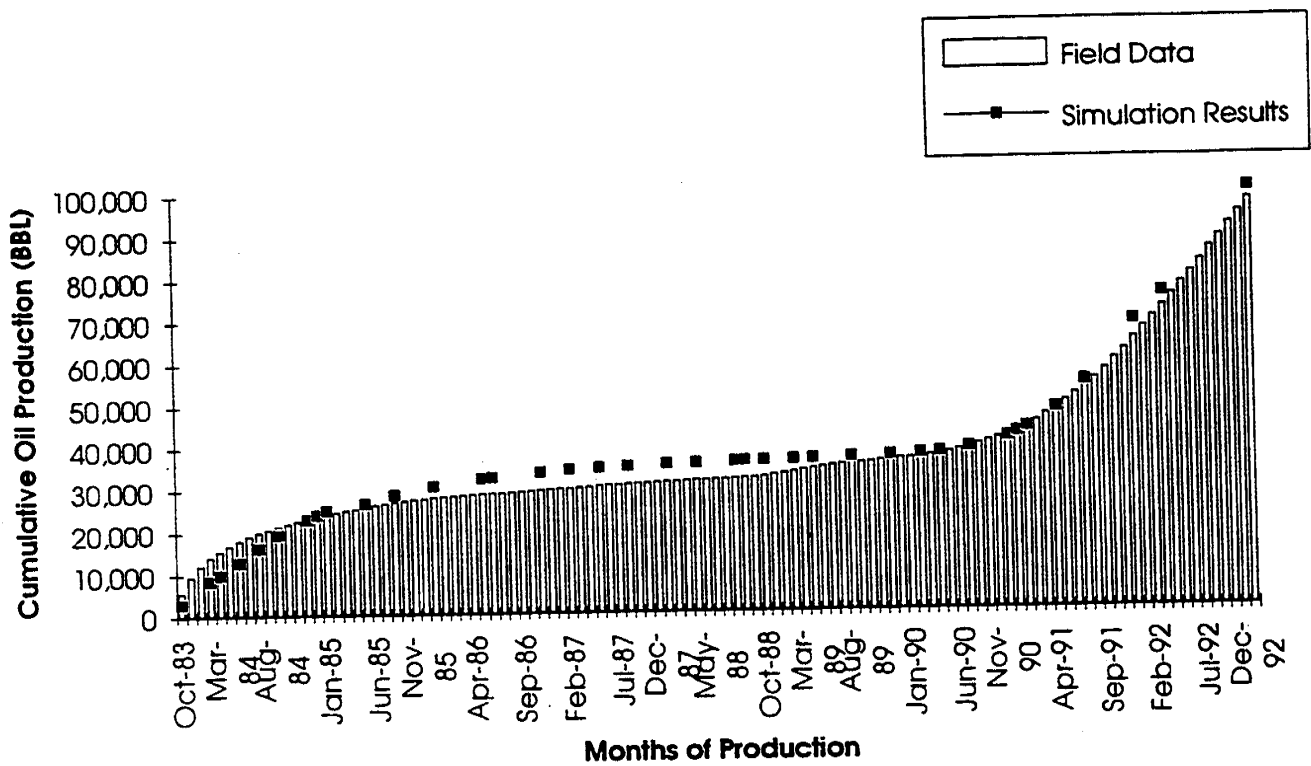


Figure 6.15: Cumulative oil production from Monument Butte well 10-35; comparison of field production with the simulation results.

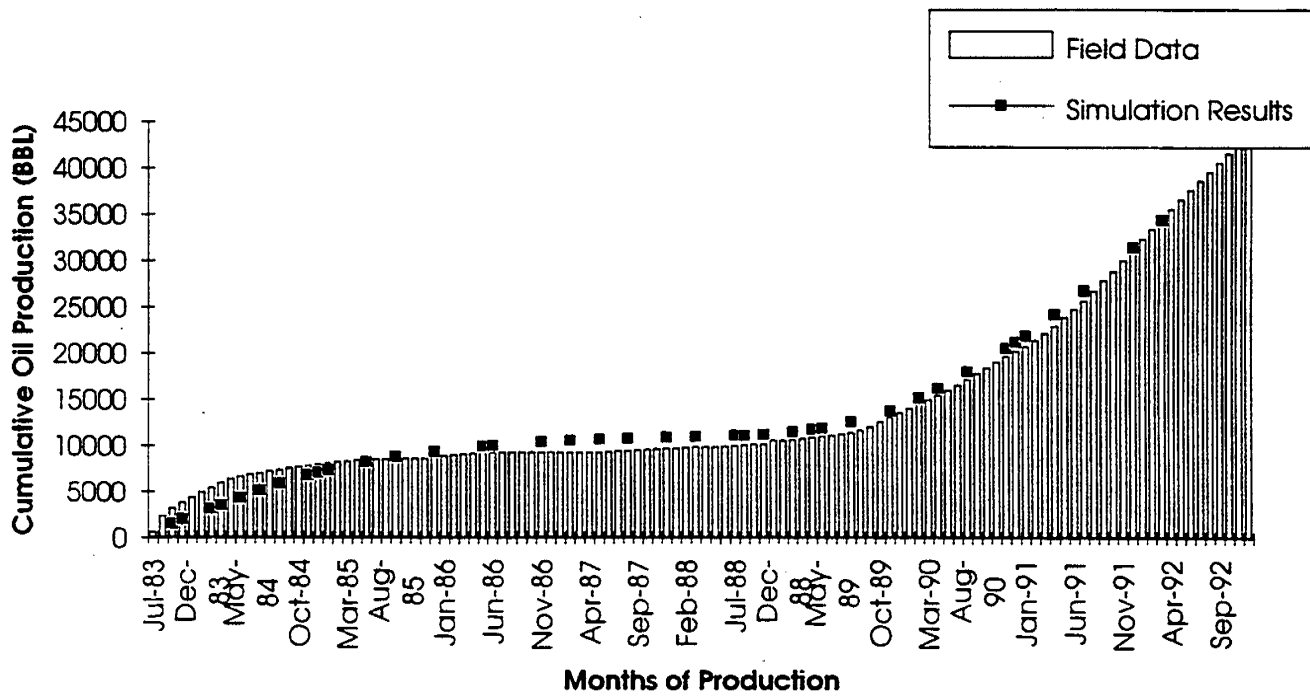


Figure 6.16: Cumulative oil production from Monument Butte well 12-35; comparison of field production with the simulation results.

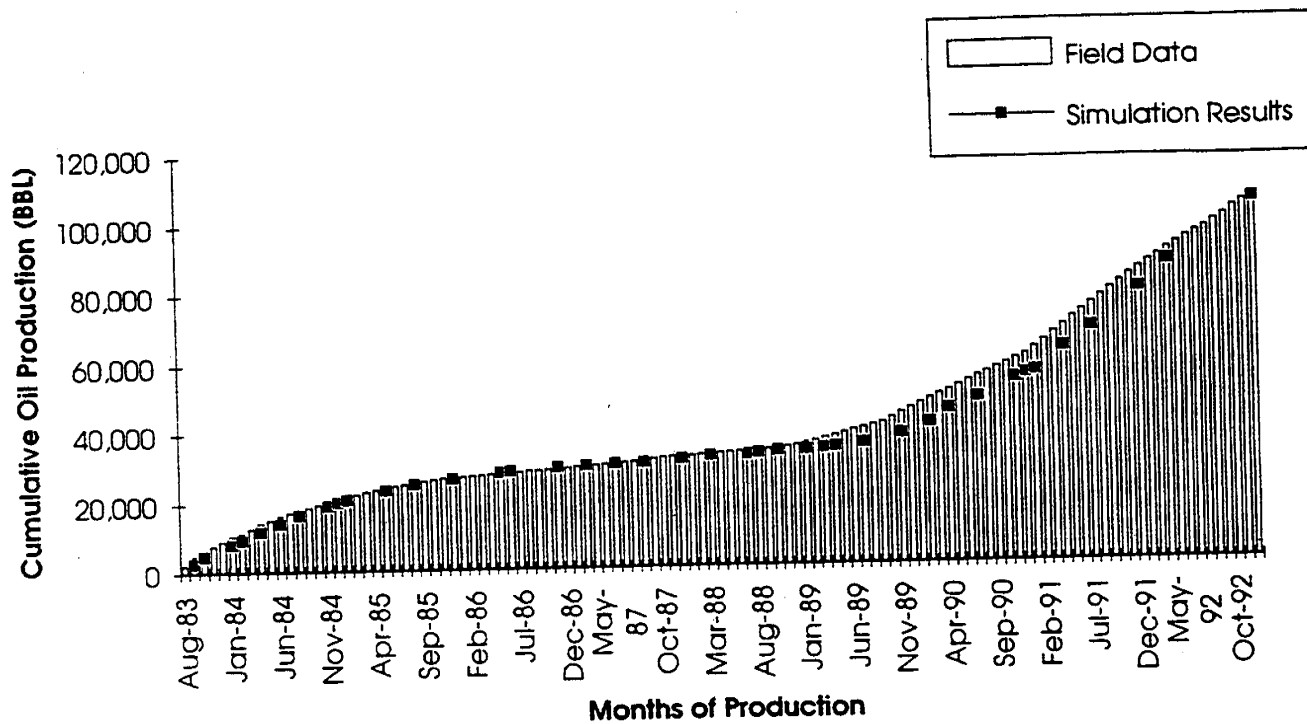


Figure 6.17: Cumulative oil production from Monument Butte well 6-35; comparison of field production with the simulation results.

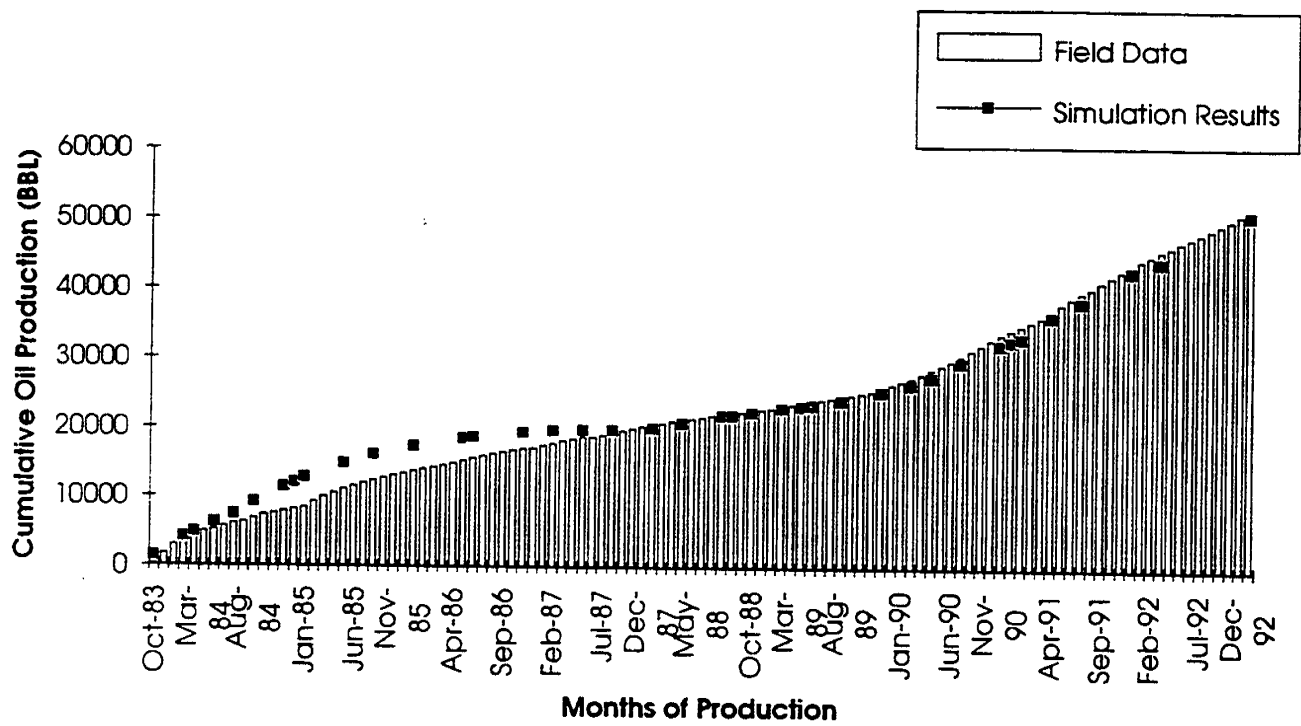


Figure 6.18: Cumulative oil production from Monument Butte well 1-34; comparison of field production with the simulation results.

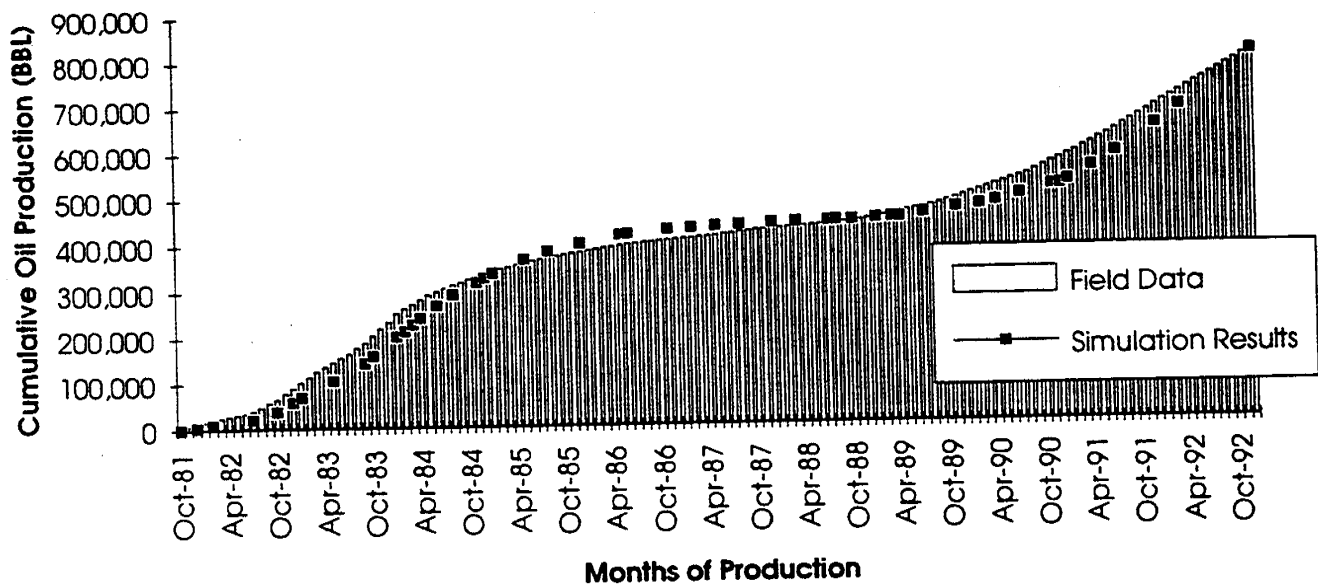


Figure 6.19: Cumulative oil production from the entire Monument Butte Unit; comparison of field production with the simulation results.

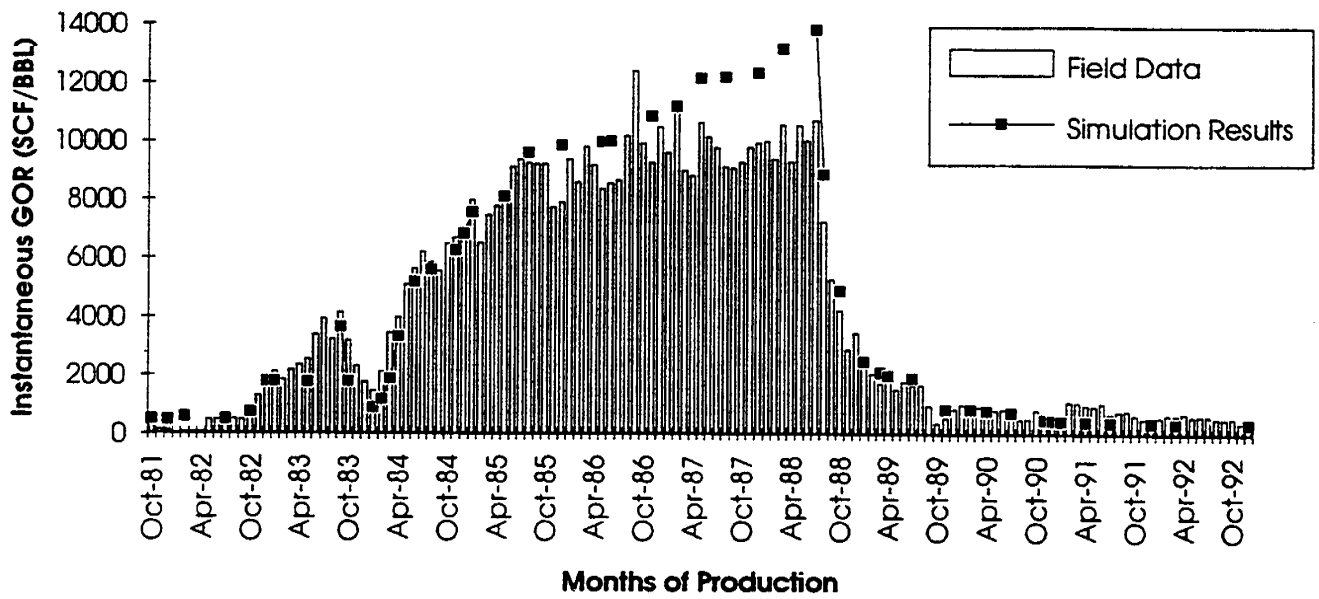


Figure 6.20: Comparison of the field production GOR values with those predicted by simulations.

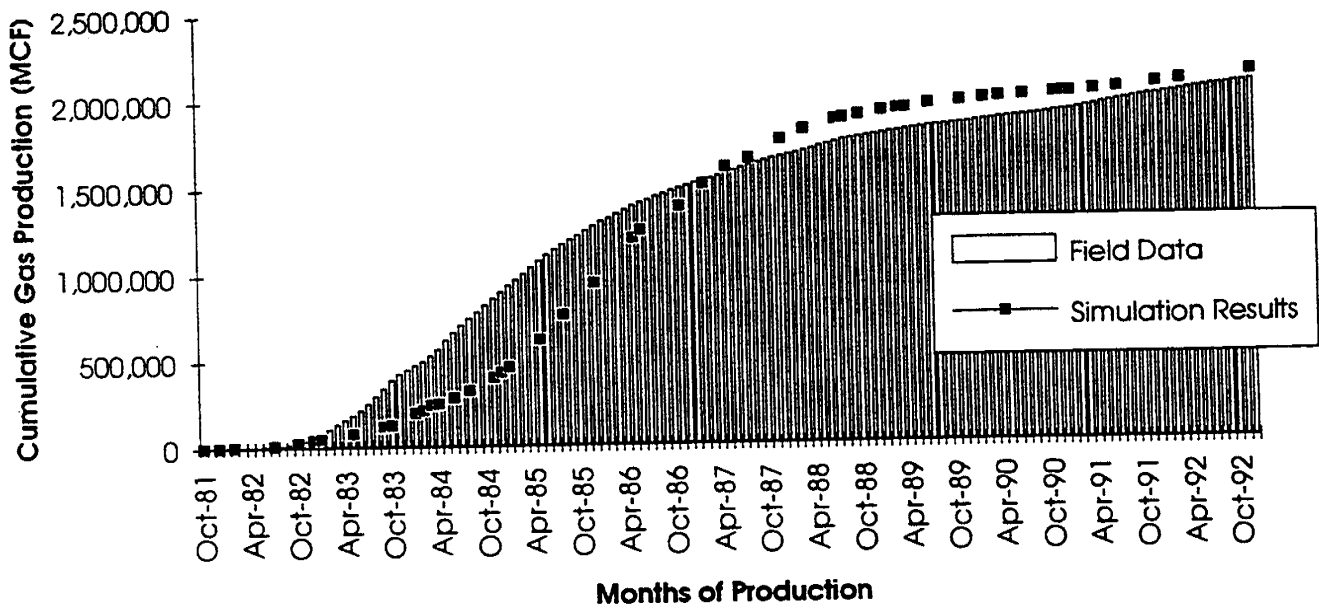


Figure 6.21: Cumulative gas production from the entire Monument Butte Unit; comparison of field production with the simulation results.

Chapter 7

Travis Case Study

7.1 Reservoir Description

A preliminary model of the Travis Field has been developed at the University of Utah. Simulations carried out with the model match overall field gas and oil production within 5%, and simulated production from individual wells was matched within 15-20% of actual production. The model makes use of isopach data (Lomax Exploration) for reservoir zone thickness estimation. At this point in time, the model representation is preliminary and the model will be tuned to incorporate a more accurate geologic description later. The model also does not account for permeability improvements due to occasional hot oil treatments that have been applied. All of the Travis reservoir simulations were performed with a black oil simulator, IMEX, developed by Computer Modeling Group (CMG). The FMI logs on the new well drilled, 14a-28 suggested extensive reservoir fracturing and after consultation with UURI personnel and Lomax Exploration, decision was made to use a fractured model representation for the Travis Unit. It should be noted that the primary production history of Travis does not suggest extensive fracturing. The overall GOR in fractured reservoirs is significantly less than in conventional reservoirs. The overall GOR for the Travis unit was about 4400 scf/stb, with an initial GOR of 550 scf/stb. The daily GOR curve from the field resembles the one for nonfractured undersaturated reservoirs. However, the water channeling observed once the water injection program was begun suggested the presence of an active fracture network. Hence a dual-porosity fracture model was used. These studies made use of the dual porosity, dual permeability option of the IMEX simulator to describe the fractured reservoir. The use of this option requires separate sets of descriptive reservoir data for the reservoir matrix and for the fracture system.

The Travis Unit consists of moderately fractured sands, vertically separated by shale strata and by layers of unproductive sand. Seven wells now operate in the unit, five producers, and two injectors. The wells have been perforated in numerous sands, but the three main sands account for the great majority of production from the unit. The model description of the reservoir consists of a 5x7x8 Cartesian coordinate grid, with total areal dimensions of 3300 feet x 4620 feet. The variable thickness of the productive sands of the reservoir was modeled by variable grid block thickness. The top two layers of the model correspond to the D sands, the next to an impermeable separation zone, the following two to the Lower Douglas Creek Sands, the next to another separation zone, and the bottom two layers to

the Castle Peak Sands. Zone thicknesses were assigned based on isopach information and perforated interval data from individual wells. A constant matrix permeability of 1.0 mD and a fracture permeability of 18.75 mD in the horizontal direction and 36.50 mD in the vertical direction were assumed. The matrix permeability, as determined from core data, is typically 1-5 mD. It is not possible to characterize the fracture properties using core data. This is because it is almost impossible to obtain representative core samples that contain appropriate fractures. The fracture thicknesses, the materials present in the fractures, etc. are variables that are not easily measured or characterized. A base porosity of 0.132 was used over the entire reservoir, this being the average of the measured values from cores. A uniform oil saturation of 0.78 was assumed for the entire field. There was no free gas present in the reservoir initially, therefore initial water saturation was set to a value of 0.22 which represents the difference between unity and the oil saturation. The reservoir description of the Travis Unit is summarized in Table 7.1¹.

7.2 Reservoir Fluid Properties

Oil and gas samples were collected from several producing wells in the Travis unit. The characterization of reservoir fluid properties consisted of the following measurements and calculations: 1) Measurement of the bulk properties of the oils (API gravities and viscosities). 2) Determination of thermodynamic properties. In order to achieve reproducible measurements of API gravities and viscosities, the oils were filtered through a cloth to remove small amounts of water and particulates. The three oils from the Travis Unit that were tested had API gravities of about 33°API (specific gravity 0.90). Oil viscosities were measured at selected temperatures, with a Brookfield cone and plate viscometer, model LVT, equipped with a spindle CP-41 (3° cone). The viscosity of oil from well 10-28 was found to be 31.7 cp at 140°ircF and 23 cp at 150°F. The initial reservoir temperature was not known accurately. However, the field temperature measurements indicated that the reservoir temperature was between 150°F to 155°F. The viscosities at reservoir conditions were adjusted for the presence of solution gas using established correlations (McCain, 1989). The bulk reservoir fluid properties are summarized in Table 7.2.

The thermodynamic properties of the Travis reservoir fluids were determined in a manner analogous to the Monument Butte fluid properties (please see the section on Monument Butte Case Study, Chapter 6). These thermodynamic properties were employed in reservoir simulation and are summarized in Table 7.3. Relative permeabilities and capillary pressures, typical of water-wet sands were employed in all the simulations.

7.3 Simulation Results

Figure 7.1 is a comparison of the field cumulative oil production and that predicted by simulations. Both the oil production trend and the overall oil production are represented fairly well by the simulations. Comparison of the simulated and actual cumulative gas production is shown in Figure 7.2. The initial field gas production is higher than the simulated result;

¹Tables and Illustrations are at the end of the Chapter

however, the simulated production catches up to the field production and the final cumulative production predicted by the simulations is in reasonably close agreement with the field data.

The water injection into 15-28 resulted in a steady increase in reservoir pressures. The simulator predicts nominal increases in oil production rates in wells 10-28 and 2-33. The field production rate at the end of simulation period, December 1992, as predicted by the simulator was about 15 stb/day. The predicted water cut is 70%. Injection of 300 stb/day of water into 15-28 and 3-33, steadily increases reservoir pressures and the model predicts oil production rates of about 95 stb/day for the field, with a water cut of about 80% by the end of 1994. The reservoir appears to be behaving differently in response to the water flood. Possible reasons for this are:

1. Inadequate geologic characterization.
2. Domination of the reservoir performance by local fracture jobs. Each of the wells in Travis is fractured prior to production. These singular fractures around the well bore may be dominating the reservoir performance.

Better geologic models which may be capable of predicting the water flood response are now under development.

7.4 References

McCain, W. D. Jr., 1989, *The Properties of Petroleum Fluids*, Second Edition, Pennwell Books, PennWell Publishing Company, Tulsa, Oklahoma.

Table 7.1: Reservoir Description of the Travis Unit Employed for Reservoir Simulations

Reservoir type	Dual porosity, dual permeability
Reservoir extent	3300 ft × 4620 ft
Sand bodies	LDC, D-sands and Castle Peak
Average depth	6000 ft
Matrix porosity	13.2%
Fracture porosity	4×10^{-5}
Matrix permeability	1 mD
Fracture permeability (x and y)	18.75 mD
Fracture permeability (z)	37.5 mD
Fracture spacing	10 ft
Initial reservoir temperature	152°F

Table 7.2: Bulk Properties of Travis Fluids

Property	Value
API Gravity	33° API
Gas Gravity	0.77
Residue (fraction) (C ₄₄₊)	0.31
C ₉₀₊ (fraction)	0.103
Paraffin Content	9.8%
Pour point	98°F

Table 7.3: Reservoir Fluid Properties for the Travis Unit

P	R_s	B_o	B_g	μ_o	μ_g
14.7	3	1.00	0.2043	22.0	0.0107
500.0	108	1.05	0.0056	13.0	0.0127
1000.0	218	1.09	0.0026	8.15	0.0134
1500.0	325	1.15	0.0017	6.02	0.0145
2000.0	440	1.21	0.0015	4.22	0.0159
2500.0	543	1.26	0.0012	3.49	0.0177
3000.0	650	1.30	0.0010	3.15	0.0195
3500.0	760	1.37	0.0009	2.67	0.0214

P	Pressure, psia
R_s	Solution gas oil ratio, scf/stb
B_o	Oil formation volume factor, rb/stb
B_g	Gas formation volume factor, rb/scf
μ_o	Oil viscosity, cp
μ_g	Gas viscosity, cp

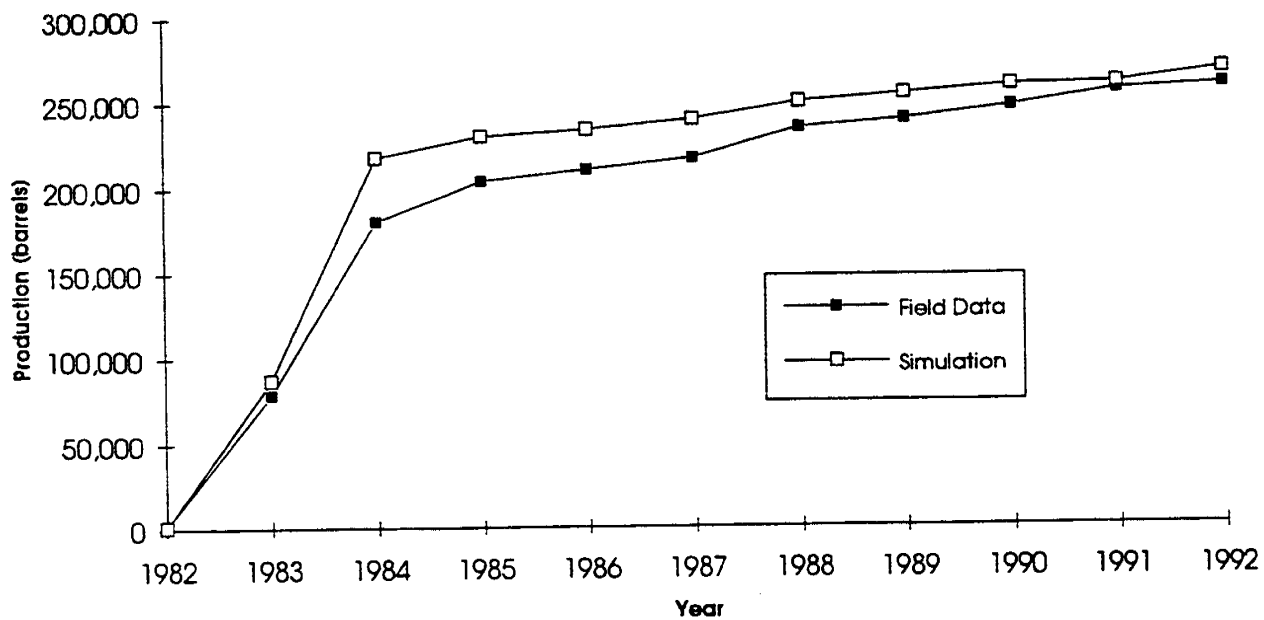


Figure 7.1: Cumulative oil production from the Travis Unit; comparison of field production with the simulation results.

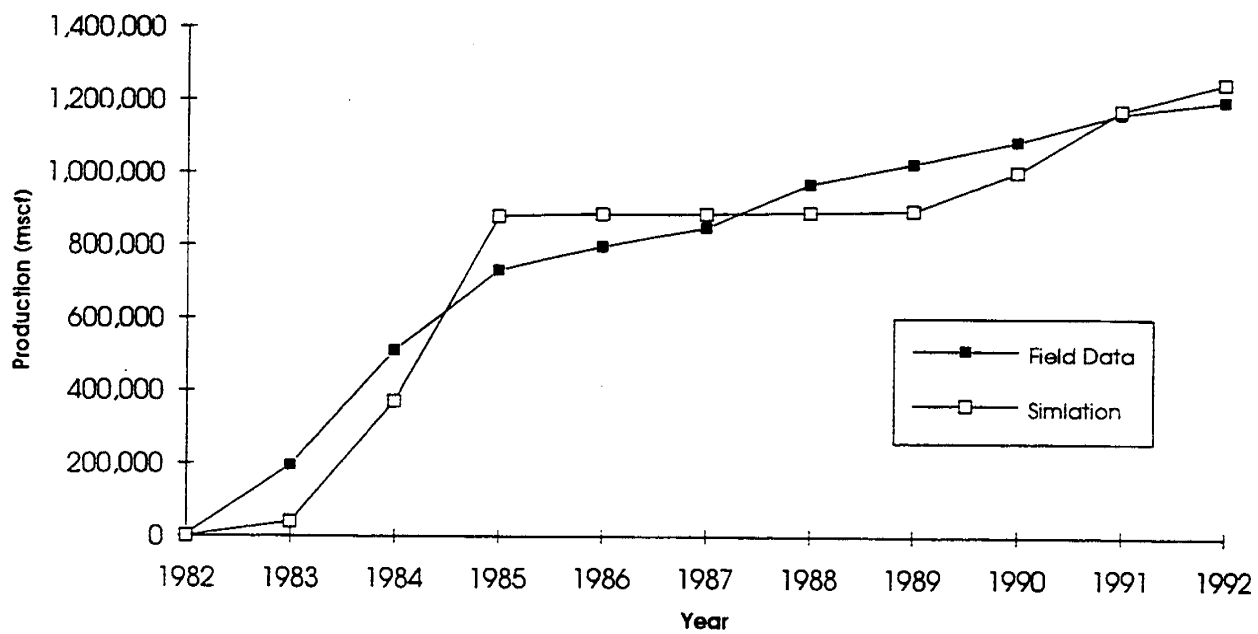


Figure 7.2: Cumulative gas production from the Travis Unit; comparison of field production with the simulation results.

Chapter 8

Near Wellbore Effects

8.1 Synopsis

Numerous studies have established the formation cooling in oil reservoirs on continued cold water injection. This could have serious consequences, particularly, for light oil reservoirs containing significant amounts of paraffins in the oil. The formation cooling reduces water flood oil recoveries by, 1) adversely affecting the oil-water fractional flow behavior and by 2) causing paraffin precipitation in the vicinity of the well bore, thereby reducing injectivities and eventually the reservoir sweep. These adverse effects of cold-water injection in paraffinic crude reservoirs has not been examined to date. In this report heat transfer calculations have been performed that establish the distinct possibility of paraffin wax formation in the vicinity of the wellbore. In the case of Monument Butte, field and geologic data, and extensive reservoir simulations have shown that the production from the unit is limited by the injectivity of the injectors and that the reservoir sands are not being swept uniformly. The reservoir contains light (Gravity = 35° API), but highly paraffinic oil (with a pour point of about 100°F) at a reservoir temperature of 140°F. About 2.5 million barrels of cold water at around 55-60°F have been injected into the formation to date. It is believed that continued injection of cold water into the reservoir has cooled the wellbore and the formation around the wellbore and has precipitated high-molecular paraffins from the oil in the immediate vicinity of the wellbore. The effect of continued cold water injection on wax formation in the vicinity of the wellbore and its impact on oil recoveries in paraffinic crude reservoirs has been explored in this report.

8.2 Technical Discussion

The compositions of the oils produced from the D and the B-sands are very similar (Lomax et al., 1992). A chromatogram of the oil from well 12-35, obtained via capillary gas chromatography is shown in Figure 8.1¹. The distinct peaks on the chromatogram correspond to normal paraffins present in the crude. The presence of high molecular weight normal paraffins results in the oils having high pour points. The pour point of the sample shown in Figure 8.1 was 95°F. The cloud point of the oil was not determined; however for these type

¹Illustrations and Tables are at the end of the Chapter

of crude oils, it has been observed that the cloud point temperature is significantly higher than the pour point temperature (Matloch and Newberry, 1983). Conventional simulated distillation analysis revealed that the oil samples from the unit were comprised of about 30% of material boiling above 538°C (C₄₄₊), and high-temperature simulated distillation analyses of the oils (Neer and Deo, 1994) showed that about 10% of the oils were in the C₉₀₊ carbon number range. The paraffin content of the oils, as defined by the concentration of C₂₀₊ normal alkanes was between 8-13%. The presence of high-molecular weight paraffinic constituents makes these oils susceptible to precipitation with changes in temperature and pressure.

The problem of paraffin deposition in petroleum reservoirs has been difficult to define and hence alleviate. The paraffin content of oil provides an index as to the susceptibility of precipitation. However, the actual composition of the precipitate will depend on the overall oil composition and the conditions in the vicinity of the wellbore. Noll (1992) provided a comprehensive review of paraffin deposition problems encountered and possible solutions. This review to the most part was limited to wax deposition on oil production. Noll (1992) reported that cloud point and paraffin content were the most important factors dictating the deposition potential. Based on the data available so far, the cloud point of the Monument Butte reservoir crude is between 95°F and 140°F.

A complete review of paraffin deposition research is beyond the scope of this report. A comprehensive study of hot oiling practices (a commonly practiced technique for alleviating paraffin problems in producing wells) resulted in guidelines for maximizing the efficiency of the hot oil treatment (Mansure and Barker, 1993). Mansure (1994) also compiled a computer program that incorporated heat loss calculations in the wellbore to enable operators to estimate temperatures at various depths. The general principles of wellbore heat loss have been well established (Moss and White, 1959; Ramey, 1962; Wooley, 1980, Pratt 1982). The potential of significantly cooler fluids reaching the formation has been established in these investigations. Moss and White (1959) determined temperature profiles for injected water as a function of depth and time by considering the oil well as a cylinder of infinite length in an infinite medium. While considering a 5000 ft deep well, injecting 300 barrels per day of water at 50°F into a formation at 145°F (linear geothermal gradient), they found that after one year, the water was entering the formation at about 108°F. The parameters used by Moss and White (1959) in their calculations are very similar to the ones for Monument Butte. Ramey (1962) used a more sophisticated heat transmission model and found, for a specific cold water injection into casing that the injected fluid reached the formation about 50°F cooler than the formation. In this specific field, significant formation cooling was also observed in observation wells several hundred feet away from the injector. Both of the above approaches did not consider the thermal resistance of the cement and of the fluids in the annulus. Thus they overpredicted the temperatures of the water entering the formation and the actual temperatures would be lower. These investigations do establish that the temperatures of the injected water entering the formation in Monument Butte would be around 100°F, a temperature at which paraffin deposition becomes a distinct possibility.

Ring and Wattenbarger (1992) developed a simulator for studying the paraffin deposition problem. They considered a paraffin solubility model to predict paraffin precipitation, a deposition model to estimate the amount of paraffin deposited and a permeability reduction model to determine the loss in porous media permeability. It should be pointed out, however,

that there have been few studies on deposition problems related to cold water injection into paraffinic crude reservoirs. Bedrikovetski and Klyakhandler (1991) report their findings on the effect of precipitated paraffin on non-isothermal displacement of oil. In this paper, a Buckley-Leverett type analysis of the cold water injection problem has been undertaken. It has been concluded that the paraffin deposition has a strong negative effect on oil recovery from low-permeability finely porous reservoirs and that this effect is felt only in the later stages of the water flood. Thus cold water injection has two distinct effects on the recovery efficiency in paraffinic crude reservoirs:

1. The obvious reduction in permeability in the vicinity of the wellbore due to paraffin deposition.
2. A more subtle alteration of the water-oil fractional flow curve resulting in higher water saturations on breakthrough and lower overall recoveries. It is this effect that manifests itself in the later stages of the water flood.

The Monument Butte Unit had produced about 5% of the oil in place at the end of primary production and was producing at a rate of 40 stb/day oil, when the water flood was initiated. The water flood has been extremely successful and the unit has produced over 300 stb/day of oil for over three years. Reservoir simulation of the unit based on the available reservoir description, fluid thermodynamic properties and rock-fluid interactions has provided a good match of the primary recovery and water flooding history (Deo, et al., 1994) (The details of the history match have been provided in the Monument Butte Case Study). A good match of reservoir performance suggests that good mechanistic understanding of physical processes underway has been established. The Monument Butte unit has eight injectors. Injection profile for well 2-35 is shown in Figure 8.2. The profile shows a steady decline in injection rates over about three years of injection. This decline could possibly be attributed to paraffin deposition in the vicinity of the wellbore. Injection rates in Monument Butte are in the range of 100-500 barrels/day. About 2.5 MMstb of cold water (at about 55°F) has already been injected into the Monument Butte unit. It would take about 1.79×10^{10} kcals to raise the temperature of this water to the reservoir temperature of about 140°F and this heat has been extracted from the reservoir fluids and from the reservoir rock. The effect is highly skewed however, as most of this heat loss occurs in the vicinity of the wellbore. In order to assess the effect of hot water injection on well injectivities, Lomax Exploration has begun injecting heated water into one of their smaller injectors, well 3-35. The hot water injection was begun approximately a month ago using a simple on-line heater. The injection rates have increased slightly and appear to be more stable than during cold water injection; however, it is too early to evaluate the results on well injectivity and far too early to assess the impact on the water flood effectiveness.

Hot-water drives have not been popular (Pratt, 1982). However, most applications have been for recovering viscous crudes. The Schoonebeek hot water flood was considered successful (Spillette and Nielson, 1968), but even in this case, the oil viscosity at the initial reservoir condition was 175 cp, considerably higher than the Monument Butte oil, which has a viscosity of 4.5 cp at the initial reservoir conditions. A tertiary hot water flood study (Martin, et al., 1968) did find 200-400% enhancements in water injectivities. Hot water injection could be effective in Monument Butte by preventing paraffin deposition in the vicinity of the

wellbore and by enhancing injectivities. Hot water injection should not be contemplated for the conventional purpose of reservoir heating/viscosity reduction.

A comprehensive evaluation of the effect of cold water injection in paraffinic crude reservoirs would consist first of examination of temperatures of injected water in the wellbore as function of injection rate, time and depth.

8.2.1 The Wellbore Model

The temperature of injected fluids in the wellbore as a function of depth and time is given by:

$$T(z, t) = az + b - aA + (T_0 + aA - b)e^{z/A}$$

where,

$$A = \frac{Wc[k + r_1 U f(t)]}{2\pi r_1 U k}$$

The terms in the above equations are explained in Nomenclature. U is the overall heat transfer coefficient and considers the net resistance to heat flow offered by the fluid inside the tubing, the tubing wall, fluids in the annulus, the casing wall and the cement. A schematic of the resistances to heat flow are given in Figure 8.3. The time function $f(t)$ is estimated from solutions for radial heat conduction from an infinitely long cylinder. The general form of the overall heat transfer coefficient, U , is given by the following equation.

$$\frac{1}{U} = \frac{1}{h_t} + \frac{r_1 \ln(r_2/r_1)}{k_i} + \frac{r_1}{r_3 h_c} + \frac{r_1 \ln(r_4/r_3)}{k_o} + \frac{r_1 \ln(r_5/r_4)}{k_c}$$

All the terms in the above equation are explained in the nomenclature. The function $f(t)$, for large values of time is calculated using the following approximation.

$$f(t) = 0.403 + 0.5 \ln(t_D)$$

The argument t_D is given by:

$$t_D = \frac{\alpha t}{r_5^2}$$

8.3 Results and Discussion

The above procedure was used in calculating the temperature profiles in the Monument Butte injectors. A sample temperature profile is shown in Figure 8.4. The parameters used in the calculation are tabulated in Table 8.1. The sample calculation was performed with an injection rate of 300 stb/d, which can be considered a middle of the range for the Monument Butte Unit. Figure 8.4 shows that the temperature of the water entering the perforations after about 1 year of injection is 83.8°F for the parameters employed in this calculation. For smaller injectors (100 stb/d) the injected water reaches the perforations at 109°F, while for

the larger injectors (500 stb/day), the injected water reaches the formation at 76°F. The effect of injection rate on the temperature of the injected water at 5000 ft is summarized in Figure 8.5.

Continued injection of cold water does not change the above results significantly. For example, after ten years of injection, the temperature of the injected water for the base case (300 stb/day) at the perforations was 82.3°F. It should be noted that the thermal resistance of cement dominates these calculations. The effect of surface injection temperatures on temperatures at the perforations for the base case (after one year, 300 stb/day injection) is shown in Figure 8.6. It would be desirable to maintain the temperatures of the injected water (entering the formation) at or above the cloud point of the oil (approximately 125°F). For the base case calculations, it is clear that the surface injection temperatures would have to be around 150°F to achieve this goal. Finally, Figure 8.7 shows the surface temperatures required to assure effective injection temperatures of 125°F for various injection rates. For an injection rate of 500 stb/day, a surface injection temperature of 138°F was found to be adequate. For smaller injectors, it is more efficient to let the geothermal gradient heat the injected fluids.

In Travis, about 1000 stb/day of water was injected into well 15-28. The predicted temperature profile of the injected fluid in this well after one year of injection is shown in Figure 8.8. As can be seen from this figure, the injected water reaches the perforations at a temperature of 71.9°F. Other temperature effects are expected to be analogous to those observed and discussed for the Monument Butte unit.

8.4 Summary

In summary, the near wellbore calculations have established formation cooling due to continued injection of cold water into the formation in Monument Butte and Travis units. The bottom-hole injection temperatures predicted by the model raise the distinct possibility of paraffin precipitation in the vicinity of the wellbore. The model was also used to calculate surface injection temperatures necessary to alleviate the paraffin deposition problem for various injection rates.

8.5 References

- Bedrikovetski, P.G. and Klyakhandler, I.L., 1991, The Effect of Precipitated Paraffin on Non-Isothermal Displacement of Oil, Unverified English Translation from Neftyanoe Khzyaistvo, No. 8.
- Deo, M. D., Sarkar, A., Nielson, D.L. and Lomax, J.D., 1994, Monument Butte Case Study, Demonstration of a Successful Waterflood in a Fluvial Deltaic Reservoir, SPE 27729, Paper presented at the Improved Oil Recovery Symposium of the SPE and the U.S. DOE to be held in Tulsa, Oklahoma, April 17-20.
- Lomax, J.D., Deo, M. D. and Nielson, D. L., 1992, "The Development of New Reserves in the Uinta Basin", Paper presented to the Interstate Oil and Gas Compact Commission, Salt Lake City, Utah, Utah, 8 pp.

- Lomax, J. D., Deo, M. D., Nielson, D. N., 1993, The Green River Formation Water Flood Demonstration Project Showing the Development of New Reserves in the Uinta Basin, Paper presented to the Department of Energy, BPO Contractor Review Conference, Bartlesville, Oklahoma, 10 pp.
- Mansure, A.J, 1994, Personal Communications Regarding the Hot Oiling Spreadsheet with Milind D. Deo, University of Utah, Salt Lake City, Utah, January, 1994.
- Mansure, A.J. and Barker, K. M, 1993, Insights into Good Hot Oiling Practices, SPE 25484, presented at the Production Operations Symposium of the Society of Petroleum Engineers, in Oklahoma City, OK, March 21-23.
- Martin, W. L., Dew, J.N., Powers, M.L. and Stevers, H.B., 1968, Results of a Tertiary Hot Waterflood in a Thin Sand Reservoir, *J. Pet. Tech.*, Vol. 20, No. 7, 739-750.
- Matloch, W.J. and Newberry, M.E., 1983, Paraffin Deposition and Rheological Evaluation of High Wax Content Altamont Crude Oils, SPE 11851, Presented at the Rocky Mountain Regional Meeting, Salt Lake City, UT, May 23-25.
- Marx, J.W. and Langenheim, R.H., 1959, Reservoir Heating by Hot Fluid Injection., *Trans. AIME*, Vol. 216, 312-315.
- Moss, J.T. and White, P.D., 1959, How to Calculate Temperature Profiles in a Water Injection Well, *Oil and Gas J.*, March 9, Vol 57, No 11, 174.
- Neer, L. A. and Deo, M. D., 1994, Simulated Distillation of Oils with a Wide Carbon Number Distribution, *J. Chromatographic Science*, In Press.
- Noll, Leo, 1992, Treating Paraffin Deposits in Producing Oil Wells, Topical Report, Performed Under Co-operative Agreement No. FC22-83FE60149, IIT Research Institute, NIPER, Bartlesville, Oklahoma, January.
- Pratt, M., 1982, Thermal Recovery, Monograph Volume 7, Society of Petroleum Engineers, Henry L. Doherty Series.
- Ramey, H.J. Jr., 1962, Wellbore Heat Transmission, *J. Pet. Tech.*, Vol. 14, No. 4, 427-440.
- Ring, J.N. and Wattenbarger, R.A., 1992, Simulation of Paraffin Deposition in Reservoirs, SPE 24069, presented at the Western Regional Meeting of the Society of Petroleum Engineers, in Bakersfield, CA, March 30-April 1.
- Spillette, A.G. and Nielsen, R. L., 1968, Two-Dimensional Method for Predicting Hot Waterflood Recovery Behavior, *J. Pet. Tech.*, Vol. 20, No. 6, 627.
- Wooley, G.R., 1980, Computing Downhole Temperatures in Circulation, Injection, and Production Wells, *J. Pet. Tech.*, Vol. 32, No. 9, 1509.

8.6 Nomenclature

- A** Factor used in temperature profile calculations, defined in the text, ft
- a** Geothermal gradient, °F/ft
- b** Surface temperature, °F
- c** Specific heat of injected fluid, Btu/lb-°F
- f(t)** Transient heat conduction time function for earth, dimensionless
- h_t** Heat transfer coefficient for the fluid inside the tubing, Btu/day-sq ft-°F
- h_c** Heat transfer coefficient for the fluid inside the casing, Btu/day-sq ft-°F
- k** Thermal conductivity of the earth, Btu/day-ft-°F
- k_i** Thermal conductivity of the tubing material, Btu/day-ft-°F
- k_o** Thermal conductivity of the casing material, Btu/day-ft-°F
- r_1** Inside radius of the tubing, ft
- r_2** Outside radius of the tubing, ft
- r_3** Inside radius of the casing, ft
- r_4** Outside radius of the casing, ft
- r_5** Outside wellbore radius inclusive of cement, ft
- $T(z,t)$** Temperature of the injected fluid in the wellbore, °F
- T_0** Surface injection temperature, °F
- t** Time from start of injection, days
- t_D** Dimensionless time defined in the text
- U** Overall heat transfer coefficient based on the inside tubing diameter, Btu/day-sq ft-°F
- W** Mass injection rate, lb/day
- z** Depth, ft
- α** Thermal diffusivity of the earth, sq ft/day

Table 8.1: Parameters used in Calculating the Temperature Profiles in Injection Wells

Surface Temperature	60°F
Geothermal Gradient	0.016°F/ft
Reservoir Temperature at 5000 ft	140°F
Water Injection Temperature	60°F
Tubing, Outside Diameter	2.875 in
Tubing, Inside Diameter	2.441 in
Casing, Outside Diameter	5.5 in
Casing, Inside Diameter	4.892 in
Cement, thickness	0.5 in
Thermal Conductivity, Steel	600 Btu/day-ft-°F
Thermal Conductivity, Earth	34 Btu/day-ft-°F
Thermal Conductivity, Cement	12 Btu/day-ft-°F
Thermal Diffusivity, Earth	1 sq ft/day

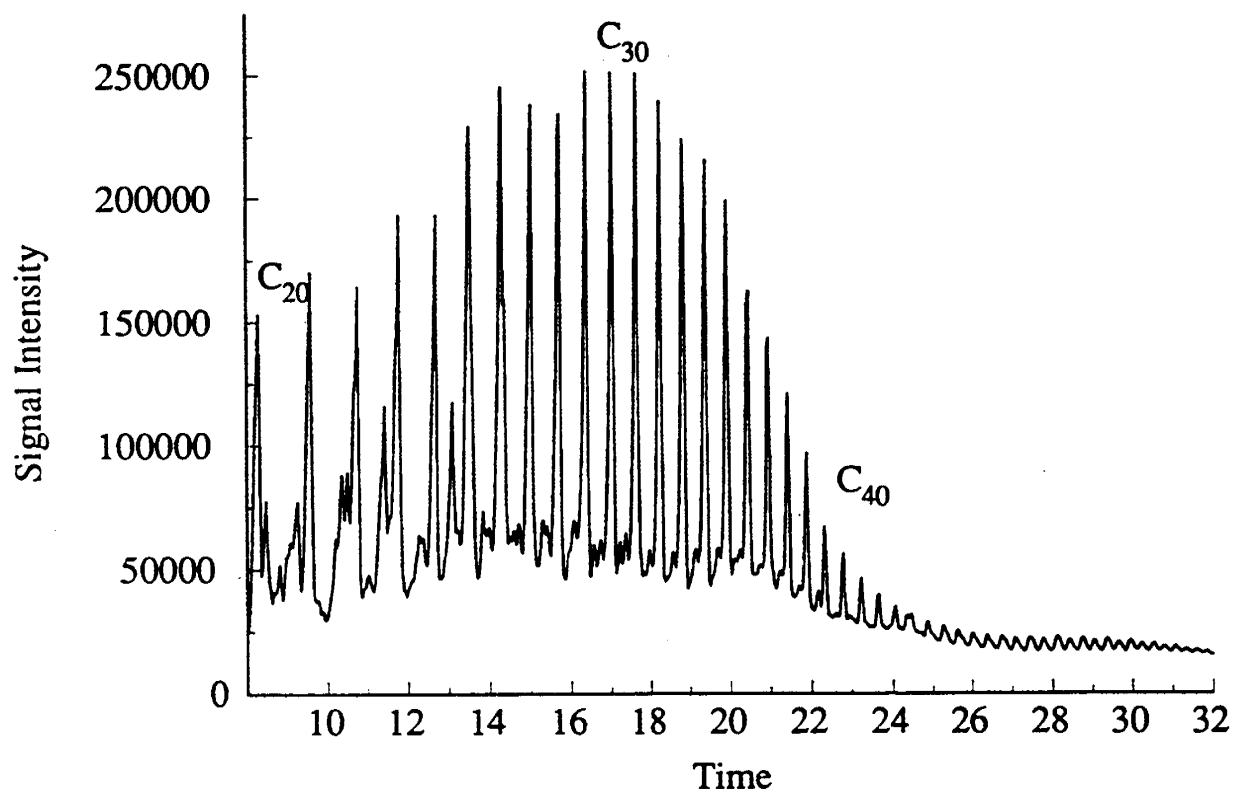


Figure 8.1: Chromatogram of an oil sample from the Monument Butte Unit showing the significant presence of high-molecular weight paraffins.

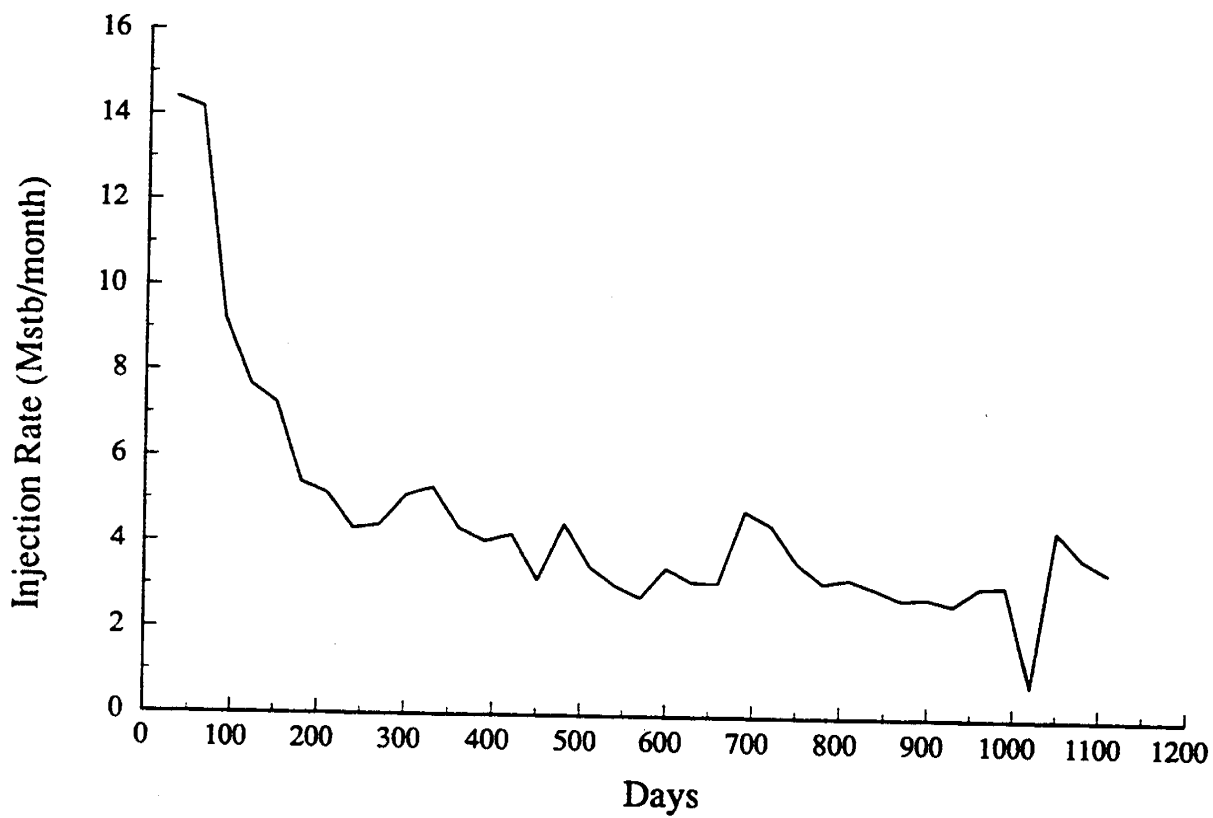


Figure 8.2: Typical injection profile for an injection well in the Monument Butte unit (well 2-35).

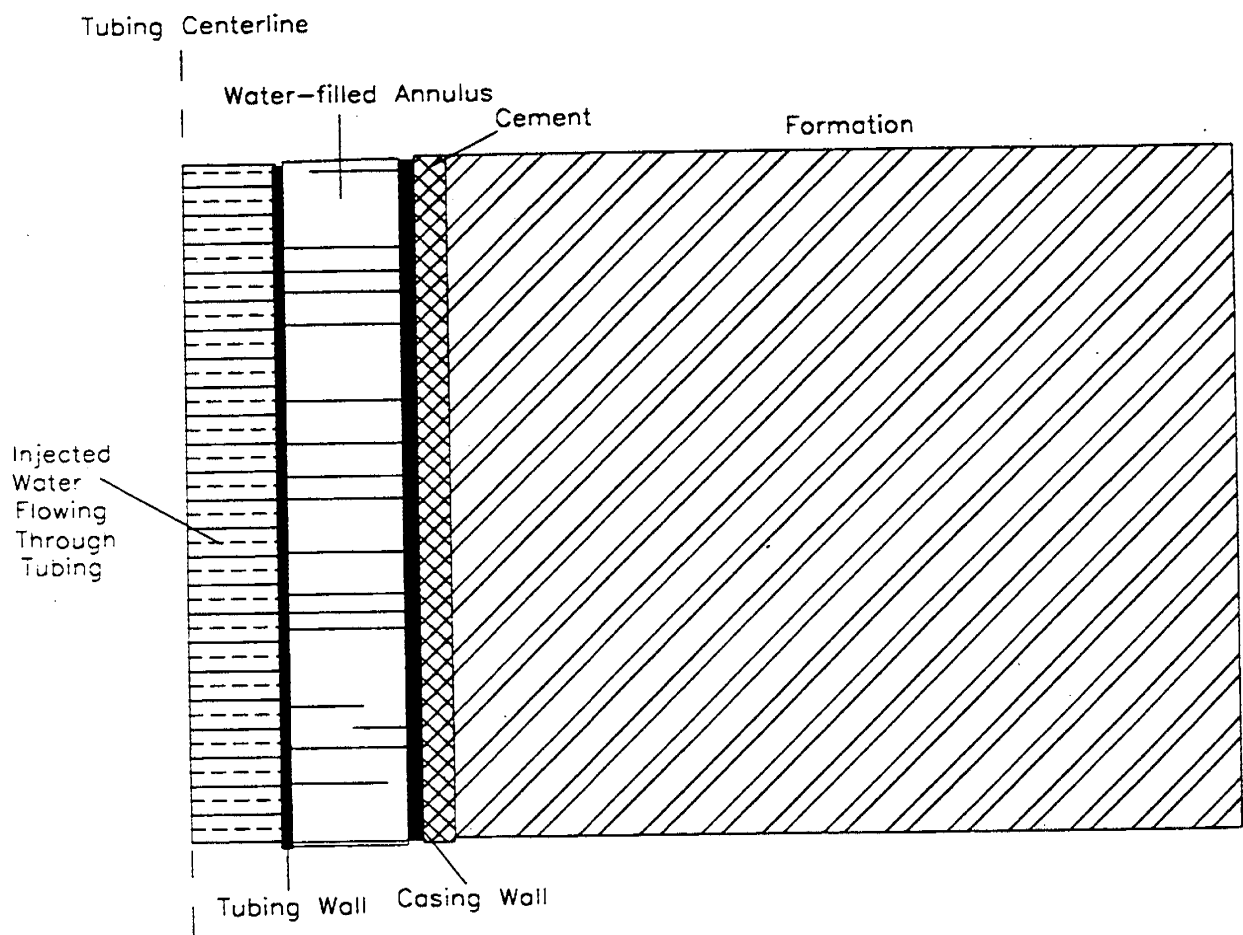


Figure 8.3: Schematic of the wellbore showing the sequence of resistances which are considered in the wellbore heat loss calculations.

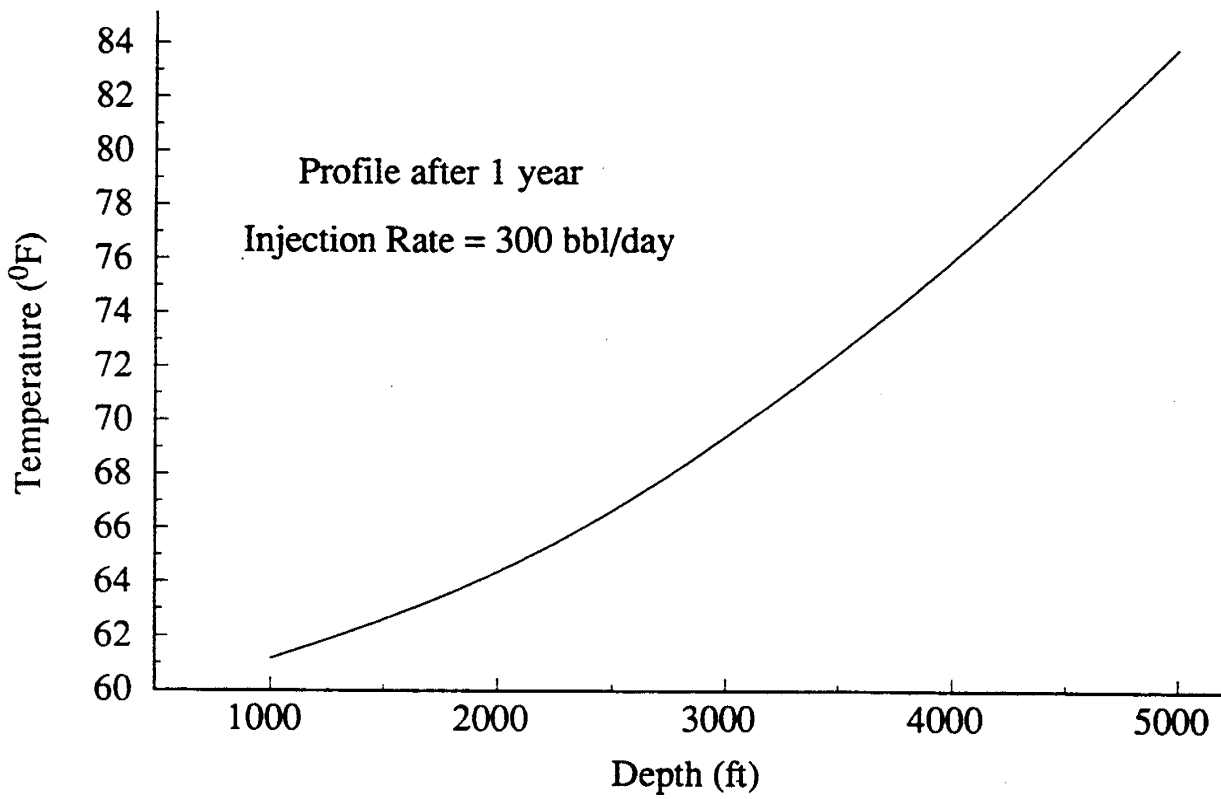


Figure 8.4: Temperatures of injected fluid as a function of depth for a typical Monument Butte injector.

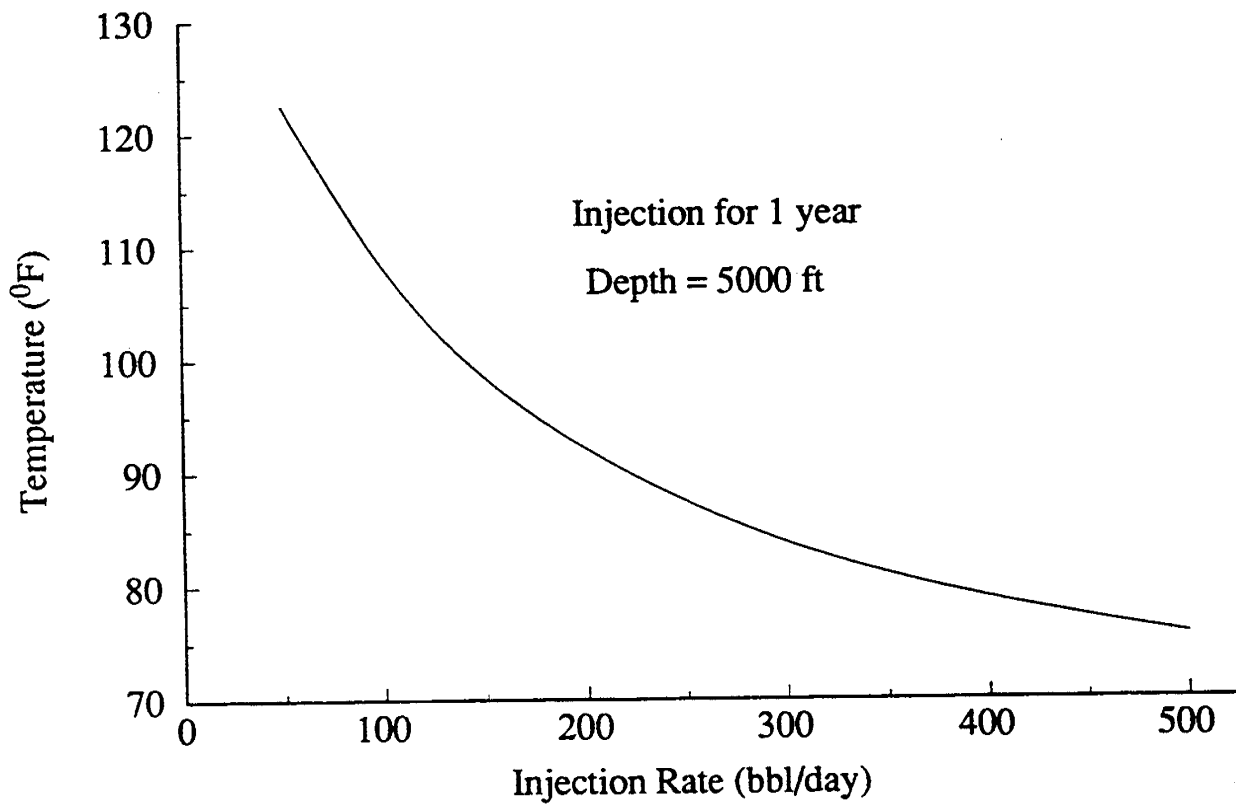


Figure 8.5: Effect of injection rates on bottom hole temperatures of injected fluids for the Monument Butte injectors.

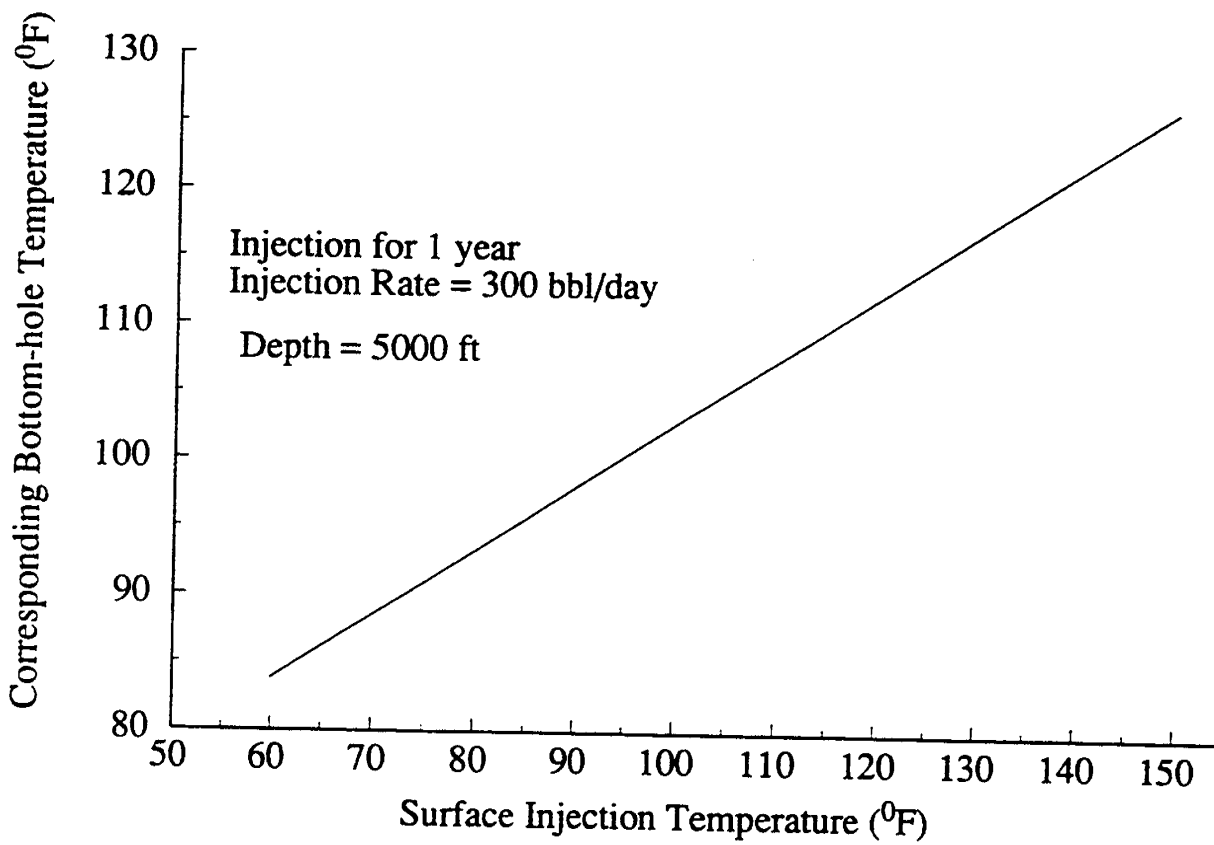


Figure 8.6: Effect of surface injection temperatures on bottom hole temperatures of injected fluids for the Monument Butte injectors.

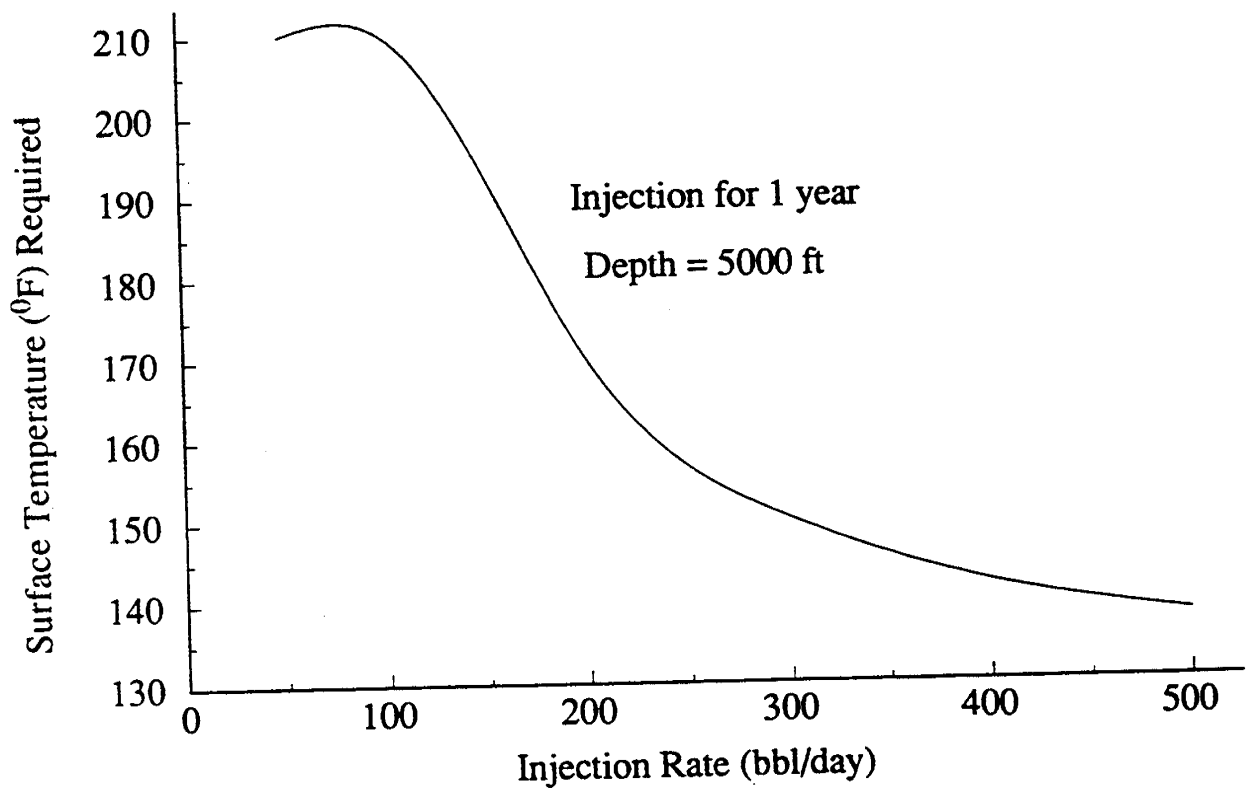


Figure 8.7: Surface temperatures required to keep the bottom hole injection temperatures above the oil cloud point for Monument Butte injectors as a function of injection rate.

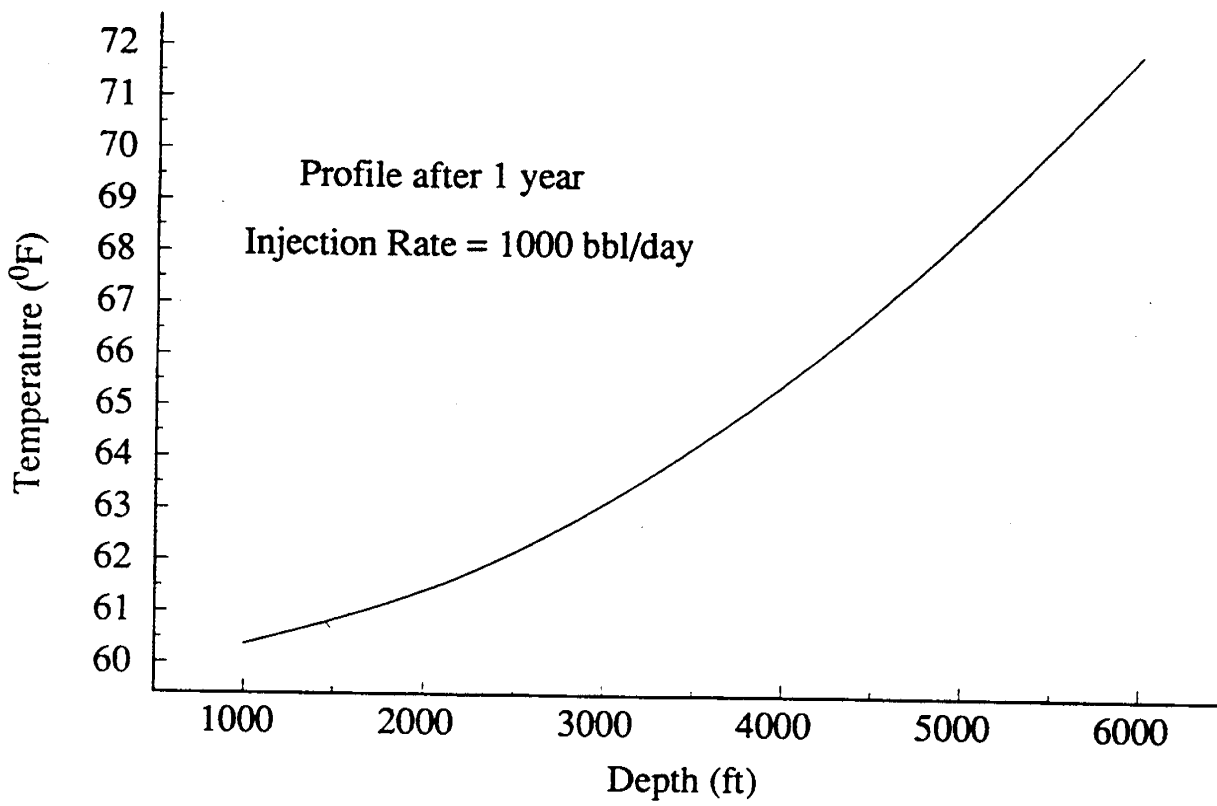


Figure 8.8: Temperatures of injected fluid as a function of depth for a well 15-28 in Travis.

